QUANTUM SYSTEM BEHAVIOUR OF JAYNES-CUMMINGS

MODEL WITH KERR-LIKE MEDIUM

CHAN YEEN CHIA

MASTER OF SCIENCE (MATHEMATICS)
UNIVERSITI UTARA MALAYSIA

2016

Permission to Use

In presenting this thesis in fulfilment of the requirements for a postgraduate degree from Universiti Utara Malaysia, I agree that the Universiti Library may make it freely available for inspection. I further agree that permission for the copying of this thesis in any manner, in whole or in part, for scholarly purpose may be granted by my supervisor(s) or, in their absence, by the Dean of Awang Had Salleh Graduate School of Arts and Sciences. It is understood that any copying or publication or use of this thesis or parts thereof for financial gain shall not be allowed without my written permission. It is also understood that due recognition shall be given to me and to Universiti Utara Malaysia for any scholarly use which may be made of any material from my thesis.

Requests for permission to copy or to make other use of materials in this thesis, in whole or in part, should be addressed to :

Dean of Awang Had Salleh Graduate School of Arts and Sciences
UUM College of Arts and Sciences
Universiti Utara Malaysia
06010 UUM Sintok

Abstrak

Model Jaynes-Cummings digunakan secara meluas dalam sistem kuantum kerana kemampuannya untuk menerangkan telatah kuantum dengan lebih tepat dan mudah. Terkini, kajian tentang model Jaynes-Cummings tidak melibatkan peralihan multi-foton dan keterlibatan kuantum tri-*qubit* yang kedua-duanya digandingkan bersama medium Kerr-like. Oleh itu, tujuan utama kajian ini adalah mencari telatah baharu untuk sistem kuantum dengan kedua-dua syarat tersebut digandingkan bersama medium Kerr-like. Bagi mencapai objektif ini, model Jaynes-Cummings diubahsuai dengan menambah peralihan multi-foton dan sistem kuantum tri-*qubit* digandingkan bersama medium Kerr-like. Berdasarkan syarat peralihan multi-foton, keformalan Pegg-Barnett digunakan untuk mengukur telatah sistem kuantum dalam model Jaynes-Cummings terubah suai. Hasil kajian menunjukkan apabila kekuatan gandingan meningkat, telatah sistem kuantum menjadi lebih aktif. Walau bagaimanapun, peningkatan dalam bilangan peralihan foton akan mengurangkan pengaruh medium Kerr-like terhadap telatah sistem kuantum. Seterusnya, berdasarkan syarat sistem kuantum tri-*qubit* bersama peralihan foton-tunggal, keadaan tri-*qubit* kuantum berinteraksi dengan persekitaran Markovan dan tak-Markovan, yang keduanya diwakili oleh ketumpatan spektrum Lorenztian. Keserentakan batas bawah digunakan untuk mengukur keteguhan keterlibatan kuantum. Hasil kajian menunjukan apabila kekuatan gandingan Kerr-like ditingkatkan untuk kedua-dua persekitaran Markovan dan tak-Markovan, keterlibatan kuantum bertambah teguh. Pada masa yang sama, pengaruh keteguhan keterlibatan kuantum berkurang apabila interaksi dwikutub-dwikutub semakin kuat. Kesimpulannya, kajian ini telah menemui telatah baharu bagi sistem kuantum dengan pengaruh medium Kerr-like yang mempunyai potensi dalam aplikasi pemprosesan maklumat kuantum.

Kata kunci: Model Jaynes-Cummings, Keadaan kuantum tri-*qubit*, Peralihan multi-foton, Medium Kerr-like.

ii

Abstract

Jaynes-Cummings model is widely used to represent a quantum system as it is able to explain quantum behaviour in a more accurate and simple way. To date, the study of Jaynes-Cummings model does not involve multi-photon transitions and also three-qubit quantum entanglement, both coupled with Kerr-like medium. Thus the main objective of this study is to discover new behaviour for quantum system under these two conditions coupled with Kerr-like medium. In achieving this objective, Jaynes-Cummings model is modified to include multi-photon transition and three-qubit quantum system coupling with Kerr-like medium. Under the multi-photon transition condition, Pegg-Barnett formalism is used to measure the quantum system behaviour in the modified Jaynes-Cummings model. The result shows that as the strength of the coupling increases, the quantum system behaviour becomes more active. However, as the number of photons transition increases, the influence from Kerr-like medium towards quantum system behaviour decreases. Next, under the three-qubit quantum system with one-photon transition condition, the three-qubit state interacts with Markovian and non-Markovian environments, both represented by Lorenztian spectral density. The lower bound concurrence is used to measure quantum entanglement robustness. Result shows that when Kerr-like medium coupling strength is increased for both Markovian and non-Markovian environments, the quantum entanglement are more robust. Concurrently, the influence of quantum entanglement robustness is reduced when dipole-dipole interaction is getting stronger. As a conclusion, this study discovered new quantum system behaviour under the influence of Kerr-like medium with potential application in quantum information processing.

Keywords: Jaynes-Cummings model, Three-qubit quantum state, Multi-photon transition, Kerr-like medium.

Acknowledgement

I would like to thanks Associate Prof. Dr Haslinda Ibrahim for the guidance completing this thesis. Associate Prof. Dr Haslinda Ibrahim provide me a clear and precise guidance on how to complete this thesis. Thanks to her patience in guiding and providing me knowledges that necessary in completing this thesis.

I would also like to thanks Prof. Dr. Mahmoud Abdel-Aty for his guidance in quantum physics theory. Prof. Dr. Mahmoud Abdel-Aty provide me understanding of quantum physics theory in more simplify way.

Lastly, I would also thanks for everyone which supported me in pursue postgraduate study ecspecially my family members.

Table of Content

List of Tables

List of Figures

List of Appendices

List of Symbols

$\left|GHZ\right\rangle$ GHZ state for three-qubit

$\left|W\right\rangle$ W State for three-qubit

$$\left|W\right\rangle = \frac{1}{\sqrt{3}}\left(\left|001\right\rangle + \left|010\right\rangle + \left|001\right\rangle\right)$$

$\left|001\right\rangle, \left|010\right\rangle, \left|100\right\rangle$ and $\left|111\right\rangle$ Different three-qubit state

$\left|1\right\rangle$ Excited state

$\left|0\right\rangle$ Ground state

Δx Change of particle's vector

Δp Change of particle's momentum

$\hbar$ Planck constant

H Hamiltonian of total system

V Potential energy

T Kinetic energy

n Number of particles or photon

r Position vector

p Momentum of the particle

t Time

m Mass of the particle

ω_0 Atomic transition frequency

ω Cavity field frequency

σ_z Atomic pseudo spin inversion

σ^+ Raising operator

σ^- Lowering Operator

g Atom field coupling constant

χ Kerr-like medium coupling strength

a^t Annihilation operator

a Creation operator

H_0 Free Hamiltonian and

H_1 Atom-cavity field interaction

i Complex number $\sqrt{-1}$

$\left|\Psi(t)\right\rangle$ Quantum state after t

$\left|\Psi(0)\right\rangle$ Quantum state at $t=0$

$\exp, \ell$ Exponential

$\left|\alpha\right\rangle$ Cavity field state

φ Phase angle

$\bar{n}$ Average photon number

α Amplitude of the cavity field

$\left|n\right\rangle$ Energy eigenvector of Hamiltonian

G Markovian or non-Markovian environment

R Qubit and cavity field coupling strength

Γ Half-width at half-height of field spectrum profile

α_n Dimentionless real constant

T_q Relaxation time

T_c Cavity correlation time

E Quantity of entanglement

ρ Density operator

U Unitary Operator

$S_v(\rho)$ Von Neumann entropy

p Probabilities outcome of measurement

ρ_{Q1} Reduce density operator of quantum state

$\left|\Phi^+\right\rangle$ Bell state of two-qubit quantum system with $\left|\Phi^+\right\rangle = \dfrac{\left|00\right\rangle + \left|11\right\rangle}{\sqrt{2}}$

ρ_A Reduce density operator of quantum state A

ρ_B Reduce density operator of quantum state B

$\left|\Psi^+\right\rangle$ Bell state of two-qubit quantum system with $\left|\Psi^+\right\rangle = \dfrac{\left|01\right\rangle + \left|10\right\rangle}{\sqrt{2}}$

$\left|\Psi^-\right\rangle$ Bell state of two-qubit quantum system with $\left|\Psi^-\right\rangle = \dfrac{\left|00\right\rangle - \left|11\right\rangle}{\sqrt{2}}$

$H1$ Hilbert space

$\left|\Phi\right\rangle$ Quantum state

$C(\rho)$ Concurrence

λ Square root of eigenvalue of quantum system

E_f Entanglement of formation

$\langle \ |$ adjoint of quantum state, $| \ \rangle$

d dipole-dipole interaction

K Kerr-like medium coupling strength

CHAPTER ONE

INTRODUCTION

1.1 Introduction

Quantum physics has gained a considerable interest for its potential impact on technology. One of the uses of quantum physics is quantum information processing. Quantum information processing can be divided into quantum cryptography, computation, and teleportation (Atteberry, n.d.). Quantum information processing needs a robust quantum entanglement. The behaviour of a quantum system is described by its quantum state as a function of time. A quantum state is a vector in a vector space, which can also be called a state vector that describes the quantum system. A state vector contains the position and momentum of a particle, which describe the quantum state. This study mainly focuses on quantum entanglement and quantum system behaviour, which are useful in quantum information processing application.

1.2 Qubit in Quantum System

In quantum information processing, a quantum system is used. Data is stored, processed, and transmitted digitally in terms of qubit. The term qubit is used to represent a quantum system, which has two dimensions. For a quantum system consisting of two qubits, it will be represented by a density matrix with the symbol ρ.

1

Quantum systems of different qubits will provide different entanglement properties whereby a three-qubit quantum system produces higher robustness than a two-qubit quantum system (Abdel et al., 2010). It has also been found that an entanglement of a three-qubit quantum system is more complex than that of a two-qubit quantum system, which also tells us that the entanglement of a higher qubit system will display a more complex behaviour. For example, a study found a three-qubit quantum system entanglement of two different types of entanglement which acted differently and led to different entanglement properties (Dur et al., 2000). A three-qubit quantum state also opens up an opportunity to study higher level qubits. That is, we are able to explore and understand the entanglement of the three-qubit quantum behaviour which might prove beneficial towards its application in quantum information processing. Further explanation on the three-qubit quantum system entanglement will be explained in section 2.5.

1.3 Quantum System and State

In choosing a good quantum system, the system should be able to propagate well and be able to hold a quantum entanglement for a longer time where it needs to be in a discrete basis. Furthermore, the quantum system must be able to interact in a specified manner while maintaining the quantum entanglement of the whole coupled system. The main five quantum systems include photons, atoms/ions, quantum dots, magnetic moments or spins, and superconducting rings (Spiller, 1996). In this study atoms are chosen as the quantum system and known as qubit. This is because an atom is more stable and able to maintain a longer time of quantum entanglement (Langer et al., 2005).

A quantum system behaviour is represented by the direction and momentum. In understanding the quantum system, a model is used to represent the quantum system behaviour. Hilbert space is widely used to represent the quantum state based on the position of the state, while Hamiltonian uses the total energy of the quantum system to determine the quantum behaviour. These are the two major representations being used and there are more models or formulation to represent a quantum state. Based on these formulations, a representation for a quantum system such as the Jaynes-Cummings model is used to represent the quantum state and model is explained below. Under the influence of time, a quantum system will start to interact with the environment or act differently, so a Schrodinger equation will come into play to represent the quantum system state dependent on time, which is explained further in section 2.3.2.

The Jaynes-Cummings model is one of the models that can represent a quantum system of a two-level atom interacting with a cavity field. In a recent study, a single, two and three-qubit quantum system were used to couple to a nanomechanical resonator which generated a cavity field. It was found that its entanglement properties are varied with different numbers of qubit (Abdel et al., 2010). The three-qubit quantum state showed a significance change in the quantum entanglement behaviour compared to the lower number of qubit where the quantum entanglement is more robust. Besides that, the quantum entanglement of the three-qubit quantum state is more complex and this may be generalized to a higher qubit quantum state (Dür et al., 2000).

Atoms in the Jaynes-Cummings model are also called quantum state. This study uses a three-qubit quantum state which consists of three types. The first type is GHZ state and W state, shown in equation (1.1) and (1.2), respectively.

$$|GHZ\rangle = \frac{1}{\sqrt{2}}\left(|000\rangle + |111\rangle\right)$$

(1.1)

$$|W\rangle = \frac{1}{\sqrt{3}}\left(|001\rangle + |010\rangle + |100\rangle\right)$$

(1.2)

Both of these states consist of three states of entanglement where the first state is three-qubit quantum system is entangled to each other directly. The second state is a bipartite entanglement, where a two-qubit quantum system is entangled to each other, so that the two-qubit state will act as a single qubit state to form another entanglement with the other single qubit state (Chen et al., 2012). Figure 1.1 shows the visualization of the bipartite entanglement. The bipartite entanglement will be considered a two-qubit entanglement where the concurrence will be used as the entanglement measure.
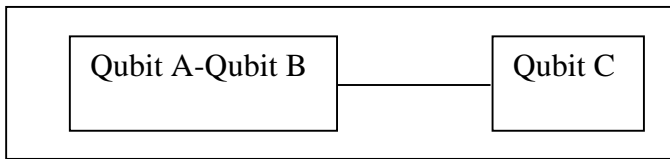
Figure 1.1. Bipartite entanglement for three-qubit quantum system

The last state of a three-qubit quantum state is the separable state where no entanglement exists among the qubit.

1.4 Quantum Entanglement

A quantum entanglement plays an important role in quantum information processing, such as in quantum computation and quantum teleportation (Heo et al., 2015). It also plays a role in quantum cryptography. A quantum entanglement is used to reconstruct quantum states by measuring the correlation between each state. A quantum entanglement produces a nonlocal correlation when a collective unitary transformation is applied to a quantum state (Plenio et al., 2014). Hence, the quantum information processing utilizes the quantum entanglement for faster results in terms of solving problems and sending messages.

A quantum entanglement involves particles, such as photons and atoms, which are separated after interacting with each other. After being separated, there will be a correlation between the particles where a change in one particle would also cause the other particle to change as well. In other words, each particle will be dependent on each other.

The particles can also be called a quantum state and they can be divided into pure and mixed where the mixed state of a quantum system consists of several pure states. This leads to a quantum entanglement, which is divided into pure and mixed, if the quantum state is pure and mixed, respectively.

5

1.4.1 Influence towards Quantum System Behaviour

The robustness of a quantum entanglement and quantum behaviour can be influenced by a difference factors, such as the number of photon transition for two level atoms, the existence of Kerr-like medium coupling, the cavity field environment (Abdalla et al., 2015), the detuning frequency, and the dipole-dipole interaction. A dipole-dipole interaction represents a quantum state where a three-qubit quantum state means there are three dipoles. These dipoles will interact with each other and form a quantum entanglement. An increase in the dipole-dipole interaction will be able to improve the quantum entanglement robustness (An et al., 2011).

In reality, more than one factor will influence how a quantum system is going to behave. With a combination of different factors, different parameters or values of the factor lead to different quantum behaviours and then subsequently different quantum entanglement strength (Yu et al., 2013). It is thus interesting to identify which parameter will be able to optimize the quantum entanglement.

Numerous studies have been done to understand the behaviour of a quantum system in terms of model formulation and identification of variables that affect the behaviour of a quantum system. A quantum behaviour can be influenced by numerous factors and one of them is a Kerr-Like medium coupling (Gantsog et al., 1996). The Kerr-like medium coupling influences the quantum state behaviour for different coupling strengths. In turn, the quantum state properties increase in collapse and revival as the Kerr-like medium

coupling strength increases. The Kerr-like medium coupling is also able to influence the quantum entanglement robustness (Yu et al., 2010), which motivates this study to observe the influence of the quantum state behaviour and quantum entanglement.

In observing quantum behaviour and in representing the real world quantum system, the number of photon transitions is considered as it is one of the factors to influence the behaviour of a quantum system. The quantum system becomes more active when there is an increase in the number of photon transitions, and with a combination of a Kerr-like medium the quantum system activity is likely to increase (Gantsog et al., 1996). This study formulates a quantum system involving a multi photon transition coupling with the Kerr-like medium.

1.4.2 Measurement Quantum Behaviour

A suitable measurement needs to be selected to quantify and measure quantum behaviour and quantum entanglement base on formulated model. A better picture is needed to show the robustness of the quantum entanglement and quantum behaviour. Currently, there are a few theoretical methods widely used to measure quantum entanglement, such as entanglement formation (Li et al., 2006), concurrence (Li et al., 2008), negativity (Verstraete et al., 2001) and entanglement witness (Behrman et al., 2013). Different measurement techniques reveal different entanglement behaviours depending on the focus area. This study uses lower bound concurrence to measure the entanglement properties. Lower bound concurrence (LBC) is suitable in measuring a multi-partite entanglement

because this type of entanglement is more complex and LBC is able to differentiate and provide accurate quantification towards the quantum entanglement robustness (Li et al., 2009). In this study a three-qubit quantum state is used.

To observe the quantum state properties of quantum behaviour, the Pegg-Barnett Formalism is a suitable method to measure the quantum state properties in the Jaynes-Cummings model when the qubit interacts with the cavity field. Section 2.5.3 explains further the method.

1.4.3 Loss of Quantum Entanglement

In the real world, quantum information processing will inevitably be affected by decoherence that destroys quantum superposition and quantum entanglement. Quantum decoherence can occur when the quantum system interacts with the environment or when it is disturbed, such as when conducting measurement (Paz et al., 2001). When a quantum state interacts with the environment, it will cause the quantum state to resemble a classical system. Hence, the quantum entanglement is destroyed. A classical system is a system where the state is known with certainty. The environment-induced decoherence of superconducting charge qubits has been extensively studied both theoretically (Makhlin et al., 2001; Mooij et al., 1999) and experimentally (Nakamura et al., 2002) in the absence of ac driving fields (free decay). Therefore, it is necessary to reduce the impact of decoherence, on one hand, and to guarantee coherent interactions in order to create strongly entangled states, on the other hand. Numerous studies have also been done to improve the

robustness of a quantum entanglement, such as by adding a correction term to a thermodynamic equilibrium for a better formulation of quantum behaviour (Wigner, 1932). A study on quantum behaviour by focusing on the effect of coupling strength in an open quantum system in the pure state has helped in the understanding of quantum decoherence.

Moreover, in superconducting-qubit-based quantum computation, ac fields (e.g., microwave fields) are usually used to manipulate the quantum state. A recent experiment (Ithier et al., 2005) showed that decoherence time of a superconducting qubit was significantly increased in the presence of a resonant ac driving field. Thus a comprehensive understanding of decoherence of a realistic superconducting qubit needs to include the influence of driving fields (Buchleitner et al., 2008).

1.5 Problem Statement

The Jaynes-Cummings model is represented by two level atoms where each level is called the excited and the ground state. Each time the atoms move from the excited to the ground state, a single photon transition will occur. A study on the Jaynes-Cummings model showed an increase in activity of the quantum behaviour when a number of photon transitions increased (Zhang et al., 1991). Another study on the Jaynes-Cummings model coupling with a Kerr-like medium also showed an interesting behaviour of the quantum system (Chia et al., 2014). To the best of our knowledge, a study on the Jaynes-Cummings model coupled with a Kerr-like medium has not been conducted in-depth; rather studies have looked into a four-photon transition (Qing et al., 2010). Different numbers of photon transition show

different results (Trung et al., 1990). For example, a two-photon transition showed that the quantum behaviour is more active than one photon transition (Gantsog et al., 1996). Besides, an increase in the Kerr-like medium coupling strength causes quantum behaviour to be more active for both a single and a two-photon transition. Further increase in the number of photon transition to four has led to unexpected results showing that the quantum behaviour is more active with the presence of the Kerr-like medium (Qing et al., 2010). Hence, a study of a multi-photon transition coupling with a Kerr-like medium is an opportunity to discover a new feature of quantum behaviour.

Besides, Jaynes-Cummings model can be extended to a three-qubit quantum state. This is because a study of a three-qubit quantum system is the beginning for a multi-partite quantum system. The system has showed a more complex interaction than a bipartite quantum system, which is the first step towards a multi-partite quantum system. A three-qubit quantum system is more robust than a bipartite quantum system (Abdel et al., 2010), so this is an opportunity to further study a three-qubit quantum system and understand the quantum entanglement properties for three-qubit quantum system. A study on a three-qubit quantum system will allow us to generalize to a higher qubit quantum system, which benefits future studies. Besides, an integration of a Kerr-like medium is able to change the quantum entanglement behaviour as it is able to increase the entanglement robustness. This is because the Kerr-like medium plays an important role in providing a strong quantum state (Tanaś et al., 1983). However, to the best of our knowledge, a vast span of literature on three-qubit quantum systems using the Jaynes-Cummings model does not include a Kerr-like medium coupling. Therefore, further studies on three-qubit quantum systems

10

coupling with a Kerr-like medium could lead to new improvements in the application of quantum information processing, provide new features to quantum entanglement robustness, and are useful future research on multi-qubit systems. In this study also, quantum system behaviour will be examined which include a multi-photon transition for the Jaynes-Cummings model coupling with a Kerr-like medium.

1.6 Scope of Study

This study is discovered the new features of quantum behaviours in the Jaynes-Cumings model under two circumstances. The first one is when the Jaynes-Cummings model is coupled with a Kerr-like medium for a multi-photons transition. This study will be based on the change of two parameters of a Kerr-like medium and the number of photon transition measured by the Pegg-Barnett formalism. This study also identified the number of photon transition up to six photons as one of the influence towards quantum behaviour. When the transition reaches this numbers, the behaviour shows a similar pattern with a five-photon transition.

The second circumstance is the investigation of new features of quantum entanglement using the Jaynes-Cummings model for a three-qubit quantum system coupled with a Kerr-like medium. In the second circumstance, the Markovian and non-Markovian environment represented by Lorenztian spectral density are included. A three-qubit quantum state is represented by the dipole-dipole interaction. The measurement used in this study is lower bound concurrence to observe the quantum entanglement. The factors

11

that influence quantum entanglement considered are Kerr-like medium coupling strength, dipole-dipole interaction, Markovian or non-Markovian environment, and detuning frequency. The combination of each parameter will be simulated and the quantum entanglement is studied.

1.7 Research Objectives

The primary objective of this study is to model a quantum system behaviour of the Jaynes-Cummings model under the influence of a Kerr-like medium. The objective is divided into sub-objectives, as shown below:

- To discover the new features of quantum state properties under a multi-photon transition with the influence of Kerr-like medium coupling.
- To identify the major variables that bring about the robustness of the quantum entanglement.
- To investigate the new features that emerge when a three-qubit quantum system coupled with a Kerr-like medium is used.

1.8 Framework of Study

Figure 1.2 outlines the process of this study from input to output. The Hamiltonian rotating wave approximation will be the base model used to represent the Jaynes-Cummings model. Then the Schrondinger equation will be included into the Hamiltonian rotating wave approximation to transform the Hamiltonian rotation wave approximation into a time

dependent model. This study has two models which use a multi-photon transition Jaynes-Cummings model and a single photon transition Jaynes-Cummings model for a three-qubit quantum state. Both of these models will be coupled with a Kerr-like medium. Then to measure the quantum behaviour (phase properties) and quantum entanglement, the Pegg-Barnett formalism and lower bound concurrence are used, respectively. Different parameters will be observed to study the phase properties and quantum entanglement. For the phase properties the parameters are the Kerr-like medium coupling strength and the number of photon transition are observed. Then for quantum entanglement, the parameters considered are the Kerr-like medium, the type of environment, the dipole-dipole coupling strength, and the detuning frequency.
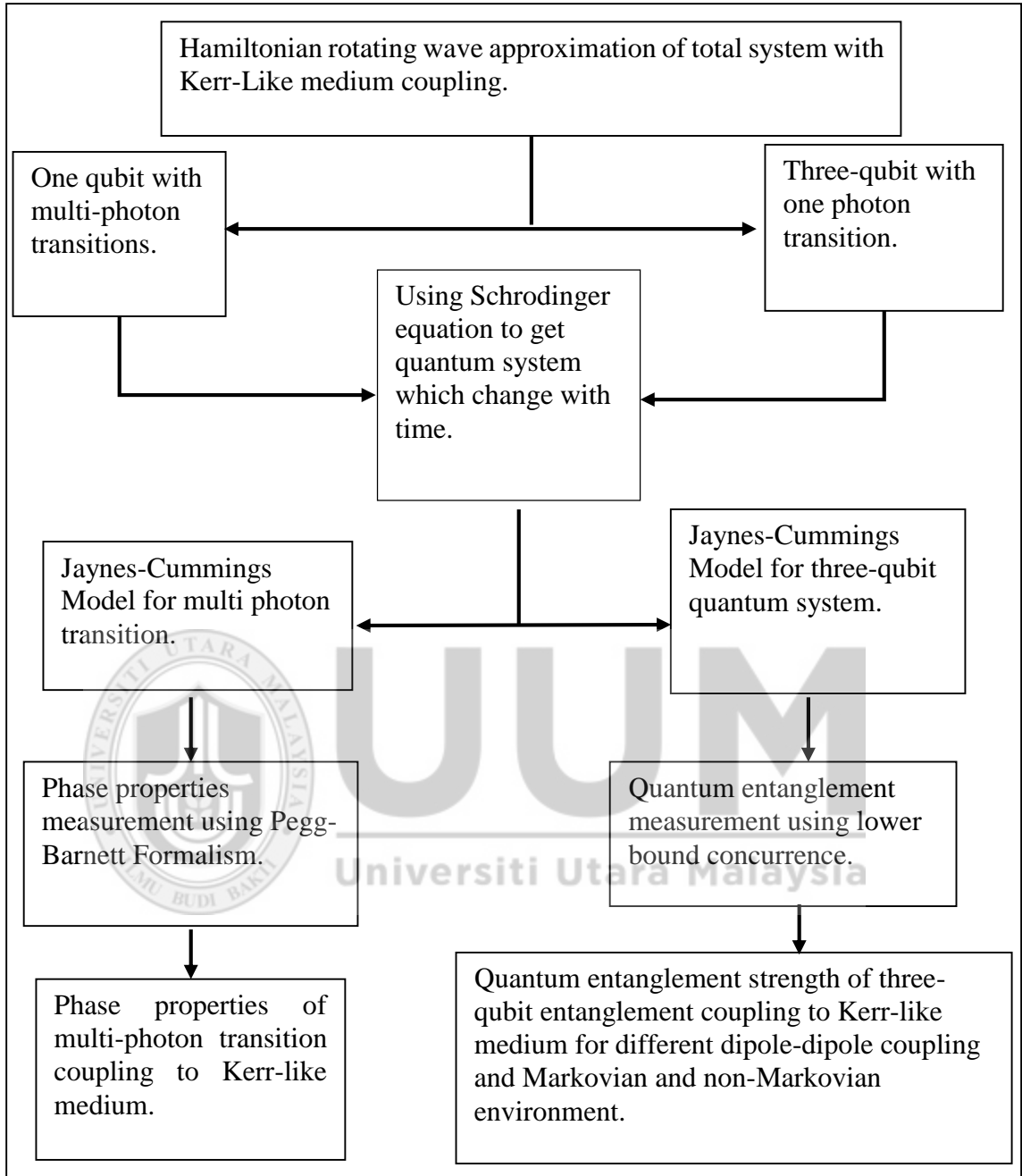
Figure 1.2. Framework of study on multi-photon Jaynes Cummings model coupled with

Kerr-like medium and a three-qubit quantum state coupled with Kerr-like medium

14

1.9 Thesis Outline

Improving quantum entanglement will provide better quantum information processing that will increase the effectiveness of its application. Applications of quantum information processing occur widely in many sectors, such as banking and finance, medicine, and communication. This study is primarily focused on quantum system behaviour of a multi photon transition Jaynes-Cummings model coupling with a Kerr-like medium and a three-qubit quantum entanglement in the Jaynes-Cummings model coupling with a Kerr-like medium.

In this thesis consist of five Chapter with Chapter One provides the overview of this study which includes the introduction of quantum physics, purpose and flow of this study. Then, Chapter Two discusses in detail each quantum behaviour, entanglement measurement methods, and the models to be used. The models discussed include the Jaynes-Cummings model, the Hamiltonian and a three-qubit quantum system. Chapter Three discusses the model formulation and the results observed of multi-photon transitions of the Jaynes-Cummings model with a Kerr-like medium. Next, Chapter Four discussed the integration of a three-qubit quantum state with the Jaynes-Cummings model with the Kerr-like medium. The quantum entanglement robustness when the quantum system begins to interact is discussed in this chapter as well. Lastly, this study is completed with some concluding remarks in Chapter Five.

CHAPTER TWO

QUANTUM BEHAVIOUR WITH KERR-LIKE MEDIUM

2.1 Introduction

In this chapter, the discussion will focus on previous studies and how they can contribute to the current study.

This chapter is divided into three sections based on the objectives stated in Section 1.7. Section 2.2 explains the behaviour of coupling, Section 2.3 model of quantum system, Section 2.4 characteristics of a three-qubit quantum system, and Section 2.5 entanglement measurement and phase properties.

2.2 Behaviour of Coupling

A quantum state does not only interact among the qubits only; it also interacts with the environment near them. For example, a cavity field entangling with a quantum state will interact which each other and influence the quantum state behaviour. It was found that the decay rate of a cavity field and the coupling strength between a qubit and the cavity field were able to affect the entanglement robustness (Abdel et al., 2009; Tahir & MacKinnon, 2010). Increases in both the coupling strength and the decay reduce the entanglement robustness. This section discusses a Kerr-like medium coupling and a number of photon transition.

16

2.2.1 Kerr-Like Medium Coupling

Studied on two-level atoms coupling to cavity field Kerr-like medium become one of the factor in influencing the phase properties which will change the quantum entanglement strength as well. Kerr-like medium has provided a lot of features of quantum system such as formation of Schrodinger cats which explain the superposition of quantum system and squeezing which able to improve the measurement of quantum behaviour (Ruiz et al., 2013; Baghshahi et al.,2014).

In actual cavity field will be influenced by environment and become non-linear medium (Rui et al., 2013). Kerr-like medium coupling with qubit will be able to stimulate well on the actual case. Kerr-like medium coupling will change the refractive index of the cavity field.

Kerr-like medium coupling changed the quantum behaviour significantly which is represent by phase properties. Without coupling of Kerr-like medium exist, the phase properties consist of a pattern with a peak at the phase equal to zero as shown in Figure 2.1a. Once Kerr-like medium increased, it had impact the phase properties a lot and cause the phase properties uncertainty with more collapse and revival in the phase properties, Figure 2.1b.
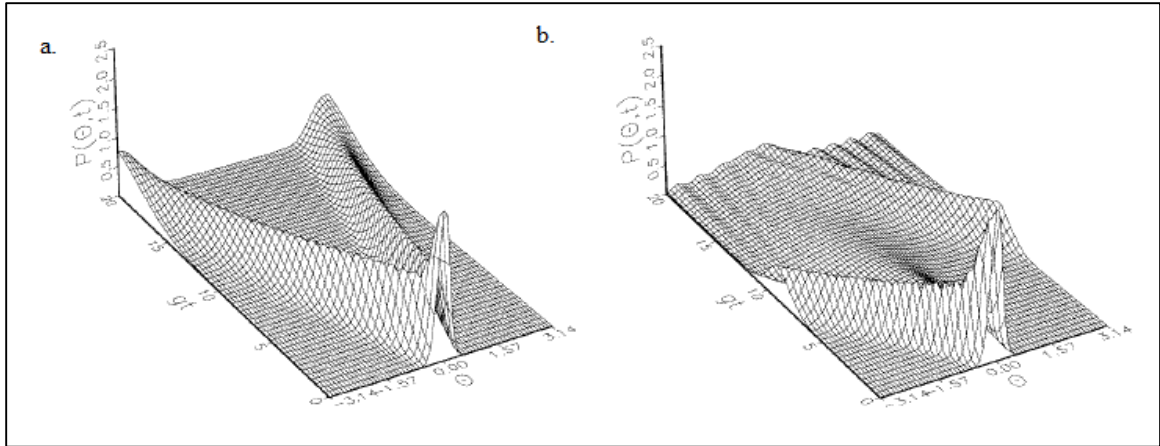
Figure 2.1. Phase properties for (a) non-Kerr-like medium coupling (b) 0.01 of a Kerr-like medium coupling strength

2.2.2 Photon Transition

A multi-photon transition also causes a quantum behaviour to behave differently, which has become an interesting topic to study. A quantum system behaves differently for a single photon transition and a two-photon transition. Figure 2.2 shows that there is an increase in collapse and revival in a two-photon transition compared to a single photon transition (Gantsog et al., 1996). Figure 2.2 shows that a two-photon transition has a higher peak and more increases in collapse and revival than a single photon transition. Besides, the amplitude fluctuation also increases in a two-photon transition compared to a single photon transition. This shows that the two-photon transition influences the atom to be more excited and subsequently increase in fluctuation, which is the collapse and revival of the atoms.

18
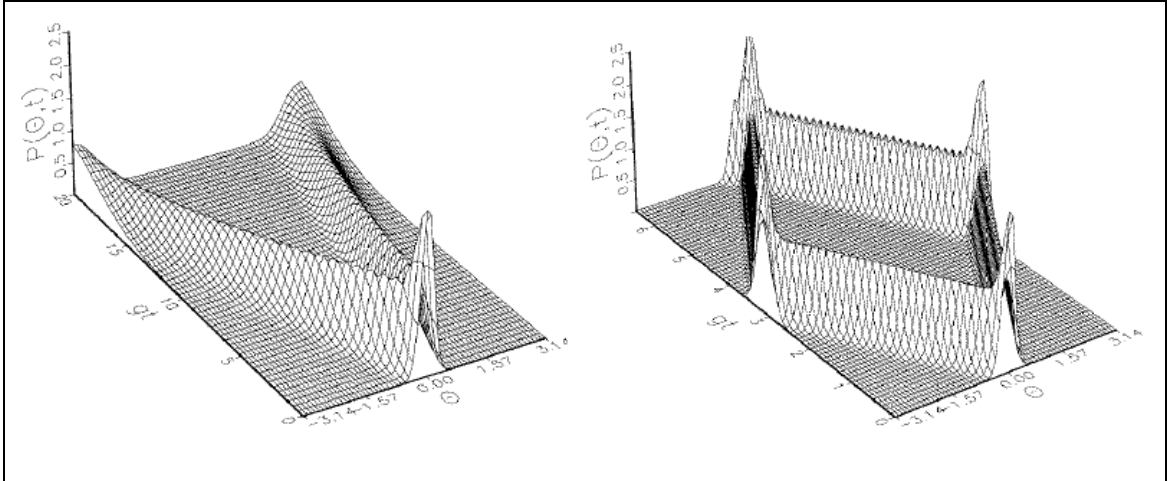
Figure 2.2. Left is the phase distribution for a single photon transition while right is the phase distribution for a two-photon transition in Jaynes-Cummings model in terms of phase and time

A study on a multi-photon transition showed that the quantum behaviour acted differently when the number of photon transition was different in terms of quantum field squeezing (Zhang et al., 1991), which is useful for further study in quantum field theory. Quantum field squeezing is where the product of change of position, Δx and change of momentum, Δp is the minimum, $\Delta x \Delta p = \dfrac{\hbar}{2}$ and this is where the uncertainty of quantum system behaviour approaches to a constant.

2.3 Model of Quantum System

Numerous models have been used in past research to explain quantum behaviour. Table 2.1 shows the different models to represent a quantum system.

Table 2.1

Type of models used to represent quantum system

Type of Model	Authors
Hamiltonian Rotating Wave Approximation	Gantsog et. al, 1996
Jaynes-Cummings model	Obada et al., 1998
Bosonic field in Heisenberg equation	Liu et al., 2005
Bloch Sphere model	Li et al. 2008
Markovian and non-Markovian	Breuer et. al, 2009
Non-equilibrium Green function model	Tahir and MacKinnon, 2010
N-qubit Hamiltonian model	Abdel et al., 2010

One model is not able to represent a quantum system. For instance, Hamiltonian was used in a simple quantum system and applied to a non-equilibrium Green function to model the quantum system (Tahir & MacKinnon, 2010).

This section discusses the model used in this study. In Section 2.3.1, the Hamiltonian rotating wave approximation, which is the base model to derive the Jaynes-Cummings model due to its simplicity to represent a quantum system coupling with a Kerr-like medium, is discussed. Then Section 2.3.2 discusses the Jaynes-Cummings model of a quantum state, cavity field and the quantum system as whole. The cavity field is divided into two different phases. In the first cavity field involving the phase properties of a multi-photon Jaynes-Cummings model, a coherent field is used as a cavity field because we are

20

able to replicate the classical harmonic oscillator which is close to reality. Then to simulate the situation of a non-Markovian and Markovian environment, Lorentzian spectral density is applied.

2.3.1 Hamiltonian Rotating Wave Approximation

This study uses the Jaynes-Cummings model which consists of a two-level atom interacting with a cavity field. The Hamiltonian rotating wave approximation is introduced to the model to assess the interaction between the atom and the cavity field.

The Hamiltonian rotating wave approximation is the fundamental model used to further develop the Jaynes-Cummings model. Hamiltonian is an operator which represents the energy of a total quantum system which includes kinetic energy and potential energy of particles. Kinetic energy is the ability of the particles to move around, while potential energy is the energy stored by the particles at a certain position. Equations (2.1) and (2.2) represent the total energy system for one particle and n-particles.

$$H = T + V \qquad (2.1)$$

$$H = \sum_{n=1}^{N} T_n + V \qquad (2.2)$$

where

$$V = V(r_1, r_2, r_3, ..., r_N, t)$$
$$T_n = \frac{p_n \cdot p_n}{2m_n} \qquad (2.3)$$

Equation (2.3) tells us that potential energy is a function of vector and time of the particles and kinetic energy is the function of dot product of the momentum divided by mass. Hence, Hamiltonian as a total system depends on the vector position and momentum of particles, as shown in equation (2.4) for a single particle, and (2.5) for n-particles.

$$H = \frac{p \cdot p}{2m} + V(r,t) \tag{2.4}$$

$$
\begin{aligned}
H &= \sum_{n=1}^{N} \frac{p_n \cdot p_n}{2m_n} + V(r_1, r_2, r_3, ..., r_N, t) \\
&= \sum_{n=1}^{N} \frac{p_n \cdot p_n}{2m_n} + V(r_1, t) + V(r_2, t) + V(r_3, t) + ... + V(r_N, t) \\
&= \sum_{n=1}^{N} H_n
\end{aligned}
\tag{2.5}
$$

Under the Hamiltonian rotation wave approximation, the model is shown in equation (2.6). The rotating wave approximation is where one of the Hamiltonian fast oscillating factors is taken out, leaving only the slow oscillating factor. This model describes the interaction between the two-level atom and the cavity field with the effect of a Kerr-like medium in a multi-photon transition which is the focus of this study.

$$H = \omega a^{t} a + \omega_0 \sigma_z + g(\sigma^+ a + \sigma^- a^t) + \chi a^{t2} a^2 \tag{2.6}$$

The lowering and raising operator is a pseudo spin operator used to represent the state of the atom or the quantum state for $\sigma^+ = |1\rangle\langle 0|$ and $\sigma^- = |0\rangle\langle 1|$ which $|1\rangle$ and $|0\rangle$ represent the excited and ground states, respectively. The inversion operator $\sigma_z = |1\rangle\langle 1| - |0\rangle\langle 0|$ is the difference of the population between the excited and ground state.

The pseudo spin operator represents the spin of the particles and will be changed in the quantum state either to be in the excited state or the ground state. The ground state and the excited state in a matrix representation are shown in equation (2.7) and the pseudo spin operators in the matrices are shown in equation (2.8), (2.9), and (2.10).

$$|1\rangle = \begin{pmatrix} 1 \\ 0 \end{pmatrix}, \ |0\rangle = \begin{pmatrix} 0 \\ 1 \end{pmatrix} \tag{2.7}$$

$$\sigma^+ = \begin{pmatrix} 1 \\ 0 \end{pmatrix} \begin{pmatrix} 0 & 1 \end{pmatrix} = \begin{pmatrix} 0 & 1 \\ 0 & 0 \end{pmatrix} \tag{2.8}$$

$$\sigma^- = \begin{pmatrix} 0 \\ 1 \end{pmatrix} \begin{pmatrix} 1 & 0 \end{pmatrix} = \begin{pmatrix} 0 & 0 \\ 1 & 0 \end{pmatrix} \tag{2.9}$$

$$\sigma_z = \begin{pmatrix} 1 \\ 0 \end{pmatrix} \begin{pmatrix} 1 & 0 \end{pmatrix} - \begin{pmatrix} 0 \\ 1 \end{pmatrix} \begin{pmatrix} 0 & 1 \end{pmatrix} = \begin{pmatrix} 1 & 0 \\ 0 & -1 \end{pmatrix} \tag{2.10}$$

Two frequencies are also included in the Hamiltonian rotation wave approximation in equation (2.6), which are ω and ω_0. The two frequencies are equal to each other to produce resonance for the excitation of the quantum state as shown in equation (2.11).

$$\Delta = \omega - \omega_0 = 0 \tag{2.11}$$

In equation (2.6) there is another operator, i.e. annihilation and creation operator, which plays an important role. The annihilation and creation operator is a mathematical operator used to lower and increase the number of photons. In this study, it is used to change the two-level quantum state from either the ground state and the excited state to the excited stated and the ground state, respectively. The creation operator is adjoining the annihilation operator and the mathematical representation is shown in equation (2.12).

23

$$a^t = \frac{\omega r - ip}{\sqrt{2\hbar\omega}}$$

$$a = \frac{\omega r + ip}{\sqrt{2\hbar\omega}}$$

(2.12)

$$a|n\rangle = \sqrt{n}|n-1\rangle$$

$$a^t|n\rangle = \sqrt{n+1}|n+1\rangle$$

(2.13)

Equation (2.13) represents the change in the quantum state for the annihilation and creation operator. It is shown that the annihilation operator will reduce the number of particles, while the creation operator will increase the particle number.

The Hamiltonian rotating wave approximation model consists of two parts, which are:

$$H = H_0 + H_1, [H_0, H_1] = 0$$

(2.14)

where

$$H_0 = \omega_0\left(a^t a + \sigma_z\right)$$

$$H_1 = \Delta\sigma_z + g\left(\sigma^+ a + \sigma^- a^t\right) + \chi a^{t2} a^2$$

$$H = \omega_0\left(a^t a + \sigma_z\right) + \Delta\sigma_z + g\left(\sigma^+ a^m + \sigma^- a^{tm}\right) + \chi a^{t2} a^2$$

$$= \omega_0 a^t a + \omega_0\sigma_z - \omega_0\sigma_z + \omega\sigma_z + g\left(\sigma^+ a^m + \sigma^- a^{tm}\right) + \chi a^{t2} a^2$$

(2.15)

$$= \omega_0 a^t a + \omega\sigma_z + g\left(\sigma^+ a^m + \sigma^- a^{tm}\right) + \chi a^{t2} a^2$$

24

The Hamiltonian rotating wave approximation is the sum of free Hamiltonian and Hamiltonian interaction, shown in equation (2.14) (Gantsog et al., 1996). A free Hamiltonian consists of an annihilation and a creation operator, and also the inversion operator of a pseudo spin. A free Hamiltonian represents the quantum state that does not interact with a cavity field. A Hamiltonian interaction is the evolution of the quantum state when the interaction between the quantum state, the cavity field and a Kerr-like medium occurs.

2.3.2 Jaynes-Cummings Model

A commonly used model in representing a quantum system is the Jaynes-Cummings model. The Jaynes-Cummings model is a model that represents a two-level atom interacting with a cavity field. In this study a quantum state will be the two-level atom which consists of a ground state and an excited state.

This model has been used by many studies that looked at the phase properties under the effect of a Stark shift and a Kerr-like medium (Obada et al., 1998) and studies that examined the properties of the field in the Jaynes-Cummings model (Dung et al., 1990). The Jaynes-Cummings model is widely used because it is commensurable to Rabi frequencies and its behaviour in this model is periodic. Rabi frequencies are used to represent the strength of the coupling between light which acts as a cavity field and an atomic transition, which is an oscillation for the atomic transition which is proportionate to the Jaynes-Cummings model (Obada et al., 1998). This model was further developed

and applied to more levels atom such as a fix-level atom (Li et al., 2006). Besides that, the Jaynes-Cummings model has also been used to study the quantum entanglement properties when coupling between cavity fields or coupling among qubit, such as a three-qubit entanglement (An et al., 2011).

Section 2.3.2.1 and Section 2.3.2.2 explain respectively in detail the Jaynes-Cummings model, which is divided into a quantum state and a cavity field. Finally, Section 2.3.2.3 discusses a quantum system when both the quantum state and the cavity field interact with each other.

2.3.2.1 Quantum State

A quantum state and a cavity field interact with each other as time goes, so a Schrodinger equation is introduced to explain the evolution of the quantum state when it interacts with the cavity field. Equation (2.16) is the Schrodinger equation for the time dependent Hamiltonian, while equation (2.17) is for the time independent Hamiltonian. Both equations show similarities where the Hamiltonian interaction is used to evolve the quantum state. A free Hamiltonian, $e^{-iH_0 t}$ is neglected because this study focuses on the quantum behaviour that interacts with a cavity field with a Kerr-like medium coupling. $e^{-iH_I t}$ is also called a unitary operator that represents the time evolution of the quantum state (Gantsog et al., 1996).

26

$$H_1|\Psi(t)\rangle = i\frac{\delta}{\delta t}|\Psi(t)\rangle \tag{2.16}$$

$$|\Psi(t)\rangle = e^{-iH_1t}|\Psi(0)\rangle \tag{2.17}$$

$$H = g\left(a\sigma^- e^{-i(\omega_0+\omega)t} + a^t\sigma^+ e^{-i(\omega_0+\omega)t} + a\sigma^+ e^{-i(-\omega_0+\omega)t} + a^t\sigma^- e^{-i(-\omega_0+\omega)t}\right) \tag{2.18}$$

Equation is the interaction picture of a quantum system where it shows the Hamiltonian rotating wave approximation in the form of time dependent (Negele et al., 1988). Equation (2.18) shows that the Hamiltonian rotating wave approximation contains two oscillating components, which are the fast oscillation $(\omega_0 + \omega)$ and the slow oscillation $(-\omega_0 + \omega)$ where the $(\omega_0 + \omega) \gg |-\omega_0 + \omega|$. The fast oscillating component is neglected in the Hamiltonian rotating wave approximation as the approximation is only valid for a low intensity cavity field and near resonance. Hence, only the slow oscillating component is maintained in this study.

2.3.2.2 Cavity Field State

Coherent state and Lorentzian spectral density will be used to represent the cavity field state of this study. The details discussion regarding these two fields are shown below:-

27

- **Coherent State**

A cavity field for the Jaynes-Cummings model used in this study is a coherent state. The cavity field was initially in the coherent state. A coherent state is a quantum state which is almost similar to a classical harmonic oscillator. The coherent state of a cavity field means that the cavity field will be in an equilibrium position where if the cavity field fluctuates away from the equilibrium point, it will eventually restore to the equilibrium position. Equation (2.19) shows that the annihilation operator is on the left side of the coherent state. The annihilation operator is also the eigenvalue of the coherent state, shown in equation (2.20). Equation (2.19) also tells that the coherent state is not influenced by the annihilation operator, which means that the coherent state will remain unchanged compared to the quantum state. Hence, detecting back the quantum state will no longer be possible.

$$a^t|\alpha\rangle = \alpha|\alpha\rangle \tag{2.19}$$

$$\alpha = |\alpha|exp(i\varphi), \ |\alpha\rangle = \sum_{n=0}^{\infty} Q_n \, exp(in\varphi)|n\rangle \tag{2.20}$$

The coherent state of the cavity field represented by equation (2.21).

$$Q_n = exp\left(-\frac{\bar{n}}{2}\right)\frac{\bar{n}^{n/2}}{\sqrt{n!}} \tag{2.21}$$

$$\bar{n} = |\alpha|^2$$

- **Lorentzian Spectral Density**

Lorentzian spectral density is a model for a cavity field based on a Lorentzian function. This model is a realistic cavity field where a photon will be able to be leaked out (An et

28

al., 2011). Equation (2.22) represents Lorentzian spectral density. Γ represents half maximum of the value where the positive half will be considered. Figure 2.3 shows an example of Lorentzian spectral density was applied to the model and the entanglement measurement showed that the LBC started from 0 to the maximum value of 1. The equation was influenced by the atom-cavity coupling strength and will be useful in determining the Markovian and non-Markovian environment.

$$J(\omega) = \frac{R^2}{\pi} \frac{\Gamma}{(\omega - \omega_c)^2 + \Gamma^2} \qquad (2.22)$$
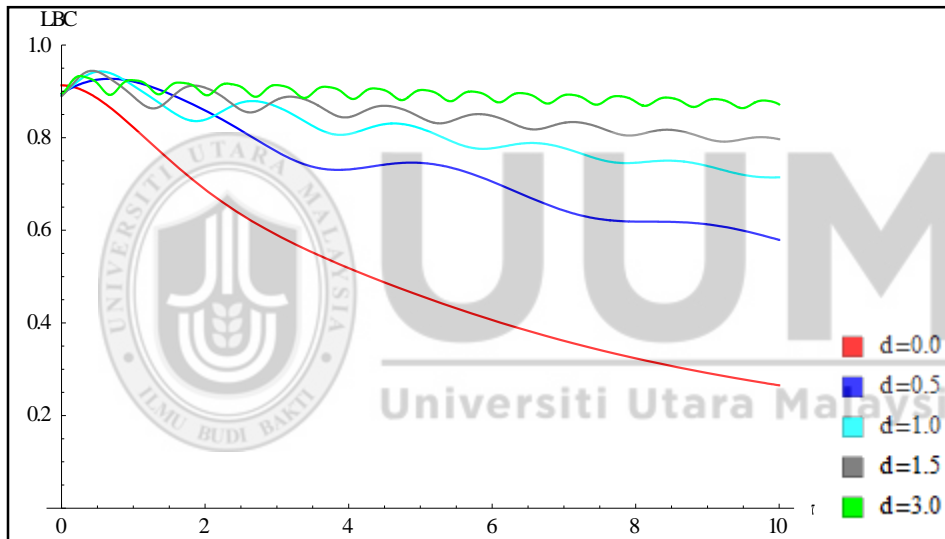
Figure 2.3. Entanglement measurement for Lorentzian spectral density with function of time under Markovian environment

2.3.2.3 Quantum System of Jaynes Cummings Model

Initially the quantum system was in a separate state with no interaction between each other, as shown in equation (2.23).

29

$$|\Psi(0)\rangle = |1\rangle \otimes |\alpha\rangle$$

$$= \sum_n Q_n \, exp(in\varphi)|e,n\rangle \qquad (2.23)$$

When the quantum state, the cavity field and the Kerr-like medium coupling start to interact with each other as shown in Equation (2.18) for t>0, the quantum will start to act differently. Equation (2.18) will become the model to represent the quantum behaviour when the interaction occurs, equation (2.24) (Gantsog et al., 1996).

$$|\Psi(t)\rangle = \sum_{n=0}^{\infty} Q_n e^{in\varphi} \, exp(-i\chi tn^2)[C_n(t)|0,n+1\rangle + D_n(t)|1,n\rangle] \qquad (2.24)$$

with,

$$C_n(t) = -i \sin 2\beta_n \sin \Omega_n t \,, \; D_n(t) = \cos \Omega_n t - i \cos 2\beta_n \cos \Omega_n t$$

$$\sin 2\beta_n = \frac{g\sqrt{\dfrac{(n+1)!}{n!}}}{\Omega_n}, \quad \cos 2\beta_n = \frac{\Delta/2 + \chi n}{\Omega_n}$$

$$\Omega_n^2 = \left(\frac{\Delta}{2} + \chi n\right)^2 + g^2(n+1)$$

2.3.3 Markovian and Non-Markovian

A Markovian environment is also called a memoryless environment because in this environment information lost will not return (Breuer et al., 2009). This is based on Markov property where the future state of a system only depends on the present state (Terhal et al., 2005). This is a kind of a stochastic process and for a quantum system interaction it is common to use a Markovian environment. The Markovian environment will also occur when the qubit and cavity field is in weak coupling.

This study considers both Markovian and non-Markovian environment where for non-Markovian, this environment information will flow back to the quantum system. This means that the future state is not only based on the current state but it also considers other conditions, such as the past event of the quantum state that is going to change the quantum state. A strong coupling between the qubit and cavity field will lead to a non-Markovian environment.

A Markovian and a non-Markovian environment are determined by the strength of the coupling between a qubit and the cavity field represented in equation (2.25). If $T_c > T_q$ this means that the quantum system is in a non-Markovian environment, which also indicates that the coupling strength is strong and vice versa. R represent the coupling strength between quantum state and cavity field, α is the dimentionless constant value to represent the qubit, T_q is the qubit relaxation time and T_c is the cavity correlation time.

$$G = \frac{2R\alpha}{\Gamma} \qquad\qquad\qquad (2.25)$$

$$\alpha = \sqrt{\sum_{n=1}^{3} \alpha_n^2}$$

$$T_q = 2R\sqrt{\alpha_n^2}$$

$$T_c = \Gamma$$

2.4 Characteristics of a Three-Qubit Quantum System

In this section, properties of a three-qubit quantum entanglement are discussed. The manner in which the entanglement of a three-qubit quantum system occurs is discussed as well.

Stochastic local operations and classical communication have also been used to study the entanglement of a three-qubit quantum system (Dür et al., 2000). The study (Dür et al., 2000) used the invertible local operator to relate the states, and then used stochastic local operations and communication to obtain and analyse the quantum entanglement. The results showed that a three-qubit entanglement contained two classes, which were GHZ and W, where W class was more robust than GHZ class in terms of a bipartite entanglement. Equations (2.26) and (2.27) show the state of the GHZ and W classes, respectively.

$$|GHZ\rangle = \frac{1}{\sqrt{2}}\left(|000\rangle + |111\rangle\right)$$

<div align="right">(2.26)</div>

$$|W\rangle = \frac{1}{\sqrt{3}}\left(|001\rangle + |010\rangle + |100\rangle\right)$$

<div align="right">(2.27)</div>

The properties of a three-qubit quantum system is similar to W class in that a three-qubit entanglement was more robust than the bipartite entanglement (Coffman et al., 2000). The difference is that stochastic local operations and classical communication were not used to build the model, but instead the model was built by defining the tangle itself using the spin-flipped density matrix. Tangle would be the entanglement of the states.

Another similar three-qubit quantum entanglement in W class is a three-qubit entanglement whereby each three-qubit entanglement was separated by a biseparable state in a positive partially transpose mixture (Jungnitsch et al., 2011). Entanglement occurred when the biseparable state no longer existed. Although the research showed that GHZ class had higher white noise tolerance than W class, the white tolerance for W class was still not optimal compared to GHZ class.

W class was also used for a tripartite entanglement on perfect quantum teleportation and superdense coding (Agrawal et al., 2006). Equation (2.26) is not suitable for quantum teleportation and superdense coding. Later it has found that W class was suitable for quantum teleportation, as shown in equation (2.28), which was used as the initial state to study a three-qubit entanglement.

$$|W\rangle = \frac{1}{2}\Big(|100\rangle + |010\rangle + \sqrt{2}|001\rangle\Big) \qquad\qquad (2.28)$$

2.5 Entanglement Measurement and Phase Properties

This section discusses quantum entanglement and phase properties to be used in this study. As quantum states interact with the measurement apparatus, decoherence will occur because the quantum system will change into a classical system because it had lost the quantum properties, as explained in the introduction (Paz, 2001). Hence, to reduce decoherence it is important for this study to use suitable measurement techniques. However, while past researchers have used several measurement techniques, this section discusses the ones to be applied in the current study. Before introducing different measurement techniques, the condition for a good entanglement is explained first, followed by an explanation about concurrence which will be used for a three-qubit quantum measurement and the Pegg-Barnett formalism which will be used to measure multi-photon transition phase properties.

2.5.1 Entanglement Measure Condition

A quantum entanglement is divided into a pure state entanglement and a mixed state entanglement. A pure state entanglement contains only a pure state in a system, while a mixed state consists of several pure states in a system that entangle with each other. The pure state entanglement can be quantified using the Von Nuemann entropy which cannot

be applied fully to the mixed state entanglement. The measurement of a mixed state entanglement can be different in different situations, further explained in a later section. A pure state is represented by the Hilbert space of a quantum system which is the state vector shown in equation (2.29). Equation (2.30) shows an example of a pure state for a two-qubit quantum system.

$$H1 = H1_1 \otimes H1_2 \otimes ... \otimes H1_n \tag{2.29}$$

$$\left| \Phi \right\rangle = \sum_{i=1}^{n} c_i \left| \Phi_i^A \right\rangle \otimes \left| \Phi_i^B \right\rangle \tag{2.30}$$

A mixed state consists of multiple pure states and is denoted by:

$$\rho = \sum_i p_i \left| \psi_i \right\rangle \left\langle \psi_i \right|$$

$$p_i \geq 0 \text{ and } \sum_i p_i = 1$$
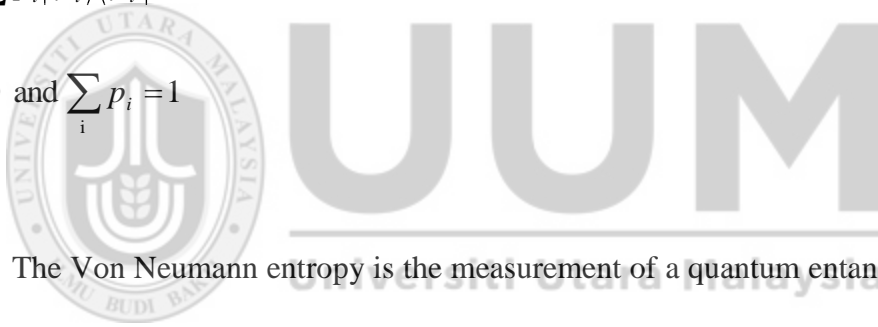
The Von Neumann entropy is the measurement of a quantum entanglement which is continuous probability. Equation (2.31) shows the Von Nenmann entropy measurement of a quantum entanglement with a function of density matrix. A fully entangled pure state will be a pure state which means that $S_v(\rho)$ is equal to 1 and vice versa for a separable state.

35

$$S_v(\rho) = -Tr(\rho \, log_2 \, \rho)$$
$$= -\sum p \, log_2 \, p \tag{2.31}$$

For example, based on equation (2.31) a quantum entanglement for a pure state can be measured. Equation (2.32) shows the entanglement measurement of a two-qubit quantum system for the pure state.

$$\rho_{Q1} = Tr_{Q2}\left(\left|\Phi^+\right\rangle\left\langle\Phi^+\right|\right) = \frac{|0\rangle\langle0| + |1\rangle\langle1|}{2} \tag{2.32}$$

For a mixed state, there is no unique method to measure the quantum entanglement. The Von Neumann entropy is unable to fully quantify the quantum entanglement for the mixed state. For example,

$$\rho_A = \frac{1}{2}\left(|01\rangle\langle01| + |01\rangle\langle10| + |10\rangle\langle01| + |10\rangle\langle10|\right) = \left|\Psi^+\right\rangle\left\langle\Psi^+\right| \tag{2.33}$$

$$\rho_B = \frac{1}{2}\left(|01\rangle\langle01| + |10\rangle\langle10|\right) = \frac{1}{2}\left(\left|\Psi^+\right\rangle\left\langle\Psi^+\right| + \left|\Psi^-\right\rangle\left\langle\Psi^-\right|\right) \tag{2.34}$$

Equation (2.34) shows a maximally entangled state. However, equation (2.34) does not. Although it has two maximally entangled states, the Von Neumann entropy is considered a separable state.

The measurement of a quantum entanglement is considered good when it is able to fulfil the following criteria (Ho, 2008):

- Entanglement is the mapping of positive real numbers from a density operator for bipartite systems.

36

- If a quantum state is separable, then the entanglement measurement will have a zero value which means that the quantum state in the quantum system does not have any entanglement properties.

- Unitary transformation will not change the quantity of entanglement,

$$E(\rho) = E\left(U_A \otimes U_B \rho U_A^t \otimes U_B^t\right)$$

- The expected entanglement will not increase under a local operation and classical communication is used to distinguish a quantum correlation from a quantum state and classical correlation.

- Entanglement measure will reduce the entropy of the entanglement of pure states.

2.5.2 Entanglement of Formation and Concurrence

Entanglement of formation has been used to measure a bipartite entanglement of quantum states. Entanglement of formation was used to measure the entanglement of a two-qubit state (Li et al., 2006). Another piece of study by (Coffman et al.,2000) was regarding how a three-qubit entanglement could be formed under a maximum entanglement. Study also used entanglement of formation to measure the three-qubit entanglement where it is stated that entanglement of formation was unable to perform a three-qubit mix state measure accurately (Eisert & Plenio, 1999). Hence, concurrence was used to calculate the mixed state entanglement of entanglement formation as it was simpler. Concurrence is defined as the maximum of square root of eigenvalues of product matrix, shown in equation (2.35) . The eigenvalues are in a decreasing order.

$$C(\rho) = max\left(0, \lambda_1 - \lambda_2 - \lambda_3 - \lambda_4\right)$$
(2.35)

In the measurement of a mixed state, entanglement of formation will take the infimum of all the pure state decomposition of ρ, (Wootters, 2001).

$$E_f = inf \sum_j p_j E(\Phi_j)$$
(2.36)

$$E(\Phi_j) = S_v(\rho_i)$$
(2.37)

Taking infimum of a pure state to measure the entanglement of a mixed state will result in a lot of work as an infinite pure state needs to be measured. Equation (2.36) is the reduced density matrix of one of the two-qubit quantum system. Based on equation (2.37), the entanglement formation also means that by producing infinite of quantum state for the measurement of the quantum entanglement.

2.5.3 Pegg-Barnett Formalism

Besides measuring the quantum entanglement, the measurement of a quantum state is also one of the important features to consider before measuring the quantum entanglement. A quantum state can be measured via representation of a linear Hermitian operator. A Hermitian operator is a self-adjoint operator and is restricted to *(s+1)*-dimensional quantum state space spanned by the first number states (Obada et al., 1998). This measurement uses the state of a well-defined phase as a starting point.

38

$$|\theta_m\rangle \equiv \frac{1}{\sqrt{s+1}}\sum_{n=0}^{s}exp(in\theta_m)|n\rangle \tag{2.38}$$

where,

$$\theta_m \equiv \theta_0 + \frac{2\pi m}{s+1}$$

m 0, 1, ..., s

$$\hat{\phi}_\theta \equiv \sum_{m=0}^{s}\theta_m|\theta_m\rangle\langle\theta_m| \tag{2.39}$$

The value of   represents the arbitrary of a particular basic set of *(s+1)* which is a mutual

orthogonal phase state. Equation (2.38) is the orthogonal phase state which is the eigenstate

of the Hermitian operators, shown in equation (2.39). Using these operators will enable us

to obtain the expectation value and the variance which will be able to explain the quantum

phase state behaviour.

In evaluating the phase properties in the Jaynes-Cummings model, the Pegg-

Barnett Hermitian phase operator formalism is used. This formalism introduces a finite

(s+1)-dimensional space spanned by the number of states (Gantsog et al., 1996). The

expectation value in equation (2.38) will be calculated and the value of *s* will reach infinity.

Equation (2.40) shows the complete orthonormal basis of *(s+1)* states.

$$|\theta_m\rangle \equiv \frac{1}{\sqrt{s+1}}\sum_{n=0}^{s}exp(in\theta_m)|n\rangle \tag{2.40}$$

The value of θ_0 represents the arbitrary of a particular basic set of *(s+1)* which is a mutual

orthogonal phase state. The Hermitian phase operator shown in equation (2.39). θ is the

dependence on the choice of θ_0. Equation (2.40) is the eigenstates for the phase operator in equation (2.39) with eigenvalues which lie between θ_0 and $\theta_0 + 2\pi$. Hence, the expectation value will be in a state described by the density operator, as shown in equation (2.41).

$$\left\langle \hat{\phi}_\theta^k \right\rangle = Tr\left\{\rho\hat{\phi}_\theta^k\right\} = \sum_{m=0}^{s} \theta_m^k \left\langle \theta_m \left| \rho \right| \theta_m \right\rangle \tag{2.41}$$

$\left\langle \theta_m \left| \rho \right| \theta_m \right\rangle$ is probability in a phase state $\left| \theta_m \right\rangle$. Based on equation (2.41), as s tends to reach infinity with a density phase states, the equation can be rewritten as

$$\left\langle \hat{\phi}_\theta^k \right\rangle = \int_{\theta_0}^{\theta_0 + 2\pi} \theta^k P(\theta) d\theta$$

and a continuum phase distribution can be introduced.

$$P(\theta) = \lim_{s \to \infty} \frac{s+1}{2\pi} \left\langle \theta_m \left| \rho \right| \theta_m \right\rangle$$
$$= \frac{1}{2\pi} \sum_{n,n'=0}^{\infty} \rho(n,n') exp[-i(n-n')\theta]$$

The continuous phase variable θ replacing θ_m and $\rho(n,n')$ are the matrix elements of the density operator in a number state basis.

2.6 Conclusion

This study mainly focuses on the Jaynes-Cummings model with coupling to a Kerr-like medium where it is derived from the Hamiltonian rotating wave approximation. Then the Schrondiger equation is used to produce a time dependent model to observe a quantum system evolution through time. This study is divided into two areas, the models of which

40

are shown in Table 2.2. One area studies the quantum behaviour of a multi-photon Jaynes-Cummings model coupling with a Kerr-like medium and the second studies a three-qubit Jaynes-Cummings model coupling with a Kerr-like medium.

A study on a quantum behaviour will use only a single qubit Jaynes-Cummings model that interacts with a coherent cavity field. This study focuses on the change of a quantum behaviour under a multi-photon transition coupling with a Kerr-like medium. This study focuses up to six-photon transition because the result starts to show similarity in the pattern of the quantum behaviour which will be further explained in Chapter 3.

Next is the study of a quantum entanglement for a three-qubit Jaynes-Cummings model coupling with a Kerr-like medium. The cavity used in this case is the multi-mode leaky cavity field. This study only has a single photon transition which mainly focuses on a three-qubit quantum entanglement.

Table 2.2

Two different types of Jaynes-Cummings model and measurement techniques used in this study.

	Study of quantum behaviour	Study of three-qubit quantum entanglement
Number of qubit	One	Three
Number of photon transition	Up to six	One
Kerr-like medium coupling	Yes	Yes
Cavity field	Coherent field	Lorentzian spectral density for Markovian and non-Markovian representation.
Measurement techniques	Pegg-Barnett Formalism	Lower bound concurrence

CHAPTER THREE

MULTI-PHOTON TRANSITION FOR JAYNES-CUMMINGS MODEL WITH KERR-LIKE MEDIUM

In this chapter, a model of multi-photon transition is developed based on the Jaynes-Cummings model. This study only considers a single atom or a one-qubit quantum state interacting with a cavity field with the purpose to observe the phase properties of a quantum system interacting with the cavity field.

Section 3.1 presents the development of the Jaynes-Cummings model. Then, Section 3.2 discusses the Pegg-Barnett Formalism in measuring the phase properties of the Jaynes-Cummings model under different Kerr-like medium coupling strength and different number photon transition. The analysis of the quantum behaviour will be provided in Section 3.3. Finally, Section 3.4 summarizes the findings of the presented algorithm.

3.1 Jaynes-Cummings Model with Kerr-Like Medium

The Hamiltonian with rotating-wave approximation is used as the fundamental equation to develop a multi-photon transition of the Jaynes-Cummings model with a Kerr-like medium (Qing et al., 2010). These models will be separated into two parts, which is a cavity field and a model for a quantum state (Huai et al., 2000). Then both the cavity field and a two-level atoms will consider the time evolution of the quantum system when the cavity field and the atoms interact which each other. This interaction will be represented by the Schrodinger equation (Yu et al., 2010).

43

Based on the interaction with the Hamiltonian rotating wave approximation of equation (2.15), the model will be enhanced to include a multi-photon transition (see equation (3.1)), in which the Jaynes-Cummings model will be completed with the interaction between the atom and cavity field. As a multi-photon transition will produce k-photon, the annihilation and the creation operator will be the power of k. This means that the annihilation and the creation operator will be used to increase and decrease the number of photons in the cavity field. With the power of k this will lead to a multi-photon transition.

$$H = \omega a^t a + \omega_0 \sigma_z + g\left(\sigma^+ a^k + \sigma^- a^{tk}\right) + \chi a^{t2} a^2 \tag{3.1}$$

$$H_0 = \omega_0\left(a^t a + 2\sigma_z\right) \tag{3.2}$$

$$H_I = \frac{\Delta}{2}\sigma_z + g\left(\sigma^+ a^k + \sigma^- a^{tk}\right) + \chi a^{t2} a^2 \tag{3.3}$$

Hamiltonian is divided into two sections, which is free Hamiltonian and interaction Hamiltonian, as shown in equation (3.2) and (3.3), respectively. H_I will be considered while H_0 will be ignored in this study as the focus is on the phase properties when the interaction between qubit, cavity field, and Kerr-like medium takes place. In the Hamitonian equation, ω and ω_0 are the field frequency and atomic transition frequency, respectively. a^t and a are the annihilation and the creation operator, respectively. σ_z, σ^+ and σ^- are inverse operator, raising operator, and lowering operator, respectively. Lastly, χ is a Kerr-like medium coupling, g the coupling strength between cavity field and qubit, and $\Delta = \omega - k\omega_0$. k will be added to the field frequency for Δ due to k photon will be

44

released into the cavity field when a multi-photon transition happens. Based on the commutation relation in equation (3.4) and the creation and the annihilation operator relation in equation (3.5), the Kerr-like medium term will be shown in equation (3.6),

$$[a, a^t] = 1, [N, a^t] = a^t, [a, N] = -a \tag{3.4}$$

$$a^t a = N \tag{3.5}$$

$$H_1 = \frac{\Delta}{2}\sigma_z + g(\sigma^+ a^k + \sigma^- a^{tk}) + \chi N^2 - \chi N \tag{3.6}$$

The matrix form of H_1 is as shown in equation (3.7).

$$H_1 = \begin{pmatrix} \frac{\Delta}{2} & 0 \\ 0 & -\frac{\Delta}{2} \end{pmatrix} + \begin{pmatrix} 0 & ga^k \\ 0 & 0 \end{pmatrix} + \begin{pmatrix} 0 & 0 \\ ga^{tk} & 0 \end{pmatrix} + \begin{pmatrix} -\chi N & 0 \\ 0 & -\chi N \end{pmatrix} + \chi N^2 \tag{3.7}$$

The initial state of the system is shown in equation (3.8). Initially the system is prepared in the excited state, $|1\rangle$ and initially no photon is released with the existing n-photon in the cavity field. When a qubit undergoes a transition from the excited state to the ground state, it will release a photon to the field, which will add to $(n+1)$-photon. This process will happen repeatedly to produce more $(n+k)$-photon to the cavity field. The cavity field is initially prepared in a coherent state with no coupling with a Kerr-like medium. Equation (3.8) also shows that initially the system, $|\Psi(0)\rangle$ is separable where there is no interaction between the cavity field and the qubit with $|\alpha\rangle$ is the cavity field

45

state, n the number of photon, and φ the phase angle. The average photon number is represented by $\bar{n} = |\alpha|^2$ (Gantsog et al., 1996).

$$|\Psi(0)\rangle = |1\rangle \otimes |\alpha\rangle = \sum_{n=0}^{\infty} Q_n \, exp(in\varphi)|1,n\rangle \tag{3.8}$$

$$Q_n = exp(-\bar{n}/2)\frac{\bar{n}^{n/2}}{\sqrt{n!}}$$

Equation (3.9) is multi-transition photon for a cavity field where initially no photon is available in the field (Gantsog et al., 1996).

$$|n\rangle = \frac{\left(a^t\right)^n}{\sqrt{(n)!}}|0\rangle \tag{3.9}$$

For existing n-photon in the cavity field, the multi-photon transition is shown in equation (3.10). This is acquired using factorial series shown in equation (3.11) where series of photon transition are formulated. Then based on the series, in equation (3.11) can be generalized to be equation (3.10) for a multi-photon transition developed in this study. Equation (3.10) is applied to the Jaynes-Cummings model for a multi-photon transition.

$$a^{tk}|n\rangle = \sqrt{\frac{(n+k)!}{n!}}|n+k\rangle \tag{3.10}$$

$$
\begin{aligned}
a^t|n\rangle &= \sqrt{n+1}|n+1\rangle \\
a^{t2}|n\rangle &= \sqrt{n+1}\sqrt{n+2}|n+2\rangle \\
a^{t3}|n\rangle &= \sqrt{n+1}\sqrt{n+2}\sqrt{n+3}|n+3\rangle \\
&= \sqrt{(n+1)(n+2)(n+3)}|n+3\rangle \\
&= \sqrt{\frac{(n+3)!}{n!}}|n+3\rangle
\end{aligned}
\tag{3.11}
$$

46

In the Schrodinger equation, as times past, the result of the interaction between a qubit and a cavity field with coupling with a Kerr-like medium is shown in equation (3.12) where $C_n(t)$ and $D_n(t)$ are the observables. In the end a quantum system will have two states. One state will be the excited state with n-photon in the cavity field. Another state will be the ground state with $(n+k)$-photon in the cavity field,

$$|\Psi(t)\rangle = \sum_{n=0}^{\infty} Q_n e^{in\varphi}\left[C_n(t)|0,n+k\rangle + D_n(t)|1,n\rangle\right] \tag{3.12}$$

For a Kerr-like medium coupling term, $\chi(N^2 - N)$ the N will convert to another form as shown in equation (3.14) and (3.15) based on equation (3.13),

$$N|n\rangle = n|n\rangle \tag{3.13}$$

$$\left(N^2 - N\right)|n\rangle = \left(n^2 - n\right)|n\rangle \tag{3.14}$$

$$\begin{aligned}\left(N^2 - N\right)|n+k\rangle &= \left((n+k)^2 - (n+k)\right)|n+k\rangle \\ &= \left(n^2 + 2nk + k^2 - (n+k)\right)|n+k\rangle\end{aligned} \tag{3.15}$$

Due to a multi-photon transition, a new model is needed, as shown in equation (3.15). The term k is added to indicate a multi-photon transition, so equations (3.14) and (3.15) will be simplified to equations (3.16) and (3.17), respectively. This simplification is to balance between both cavity states $|n\rangle$ and $|n+k\rangle$ needed in the later Jaynes-Cummings model.

$$\left(N_k^2 - N_k\right)|n\rangle \tag{3.16}$$

$$\left(N_k^2 - N_k\right)|n+k\rangle \tag{3.17}$$

with

$$N_k^2 = n^2 + (k-1)\left(n + \frac{k}{2}\right)$$

$$N_k = \frac{k}{2}(1 - 2n - k)$$

In order to obtain a model for a multi-photon transition, a quantum system which changes over time, and the Schrodinger equation (see equation (2.17)) are used (Gantsog et al., 1996). Base on equation (3.6) as explained previously, only the interaction Hamiltonian is used for the observation of the phase properties. In this study the Schrodinger equation is shown in equation (3.18),

$$\begin{aligned} |\Psi(t)\rangle &= \exp(iH_1 t)|\Psi(0)\rangle \\ &= \exp\left(i\left(\frac{\Delta}{2}\sigma_z + g(\sigma^+ a^k + \sigma^- a^{tk}) + \chi N^2 - \chi N\right)t\right)\sum_{n=0}^{\infty} Q_n \exp(in\varphi)|1,n\rangle \end{aligned}$$

(3.18)

the equation is further simplified as showed below,

$$|\Psi(t)\rangle = \exp(iAt)\sum_{n=0}^{\infty} Q_n \exp(in\varphi)\exp\left(it\chi N_k^2\right)|1,n\rangle$$

with,

$$A = \frac{\Delta}{2}\sigma_z + g(\sigma^+ a^k + \sigma^- a^{tk}) - \chi N$$

By using equation (3.7), let A as shown in equation (3.19). A^2 and A^{2n+1} be shown below. In equation (3.19), the Kerr-like medium term, one of the term in the matrix will be converted to be positive to provide a diagonal Hamiltonian equation (Klimov et al., 2002).

$$A = \begin{pmatrix} \left(\frac{\Delta}{2} - \chi N_k\right) & ga^k \\ ga^{tk} & \left(-\frac{\Delta}{2} + \chi N_k\right) \end{pmatrix}$$

(3.19)

48

$$
A^2 = \begin{pmatrix} \left(\dfrac{\Delta}{2} - \chi N_k\right) & ga^k \\ ga^{tk} & \left(-\dfrac{\Delta}{2} + \chi N_k\right) \end{pmatrix} \begin{pmatrix} \left(\dfrac{\Delta}{2} - \chi N_k\right) & ga^k \\ ga^{tk} & \left(-\dfrac{\Delta}{2} + \chi N_k\right) \end{pmatrix}
$$

$$
= \begin{pmatrix} \left(\dfrac{\Delta}{2} - \chi N_k\right)^2 + g^2 a^k a^{tk} & 0 \\ 0 & \left(-\dfrac{\Delta}{2} + \chi N_k\right)^2 + g^2 a^{tk} a^k \end{pmatrix} \tag{3.20}
$$

With the substitution of the annihilation and the creation operator to a photon transition, term A^2 forms,

$$
A^2 = \begin{pmatrix} \left(\dfrac{\Delta}{2} - \chi N_k\right)^2 + g^2 \dfrac{(n+k)!}{n!} & 0 \\ 0 & \left(-\dfrac{\Delta}{2} + \chi N_k\right)^2 + g^2 \dfrac{(n)!}{(n-k)!} \end{pmatrix} \tag{3.21}
$$

Equation (3.21) is a diagonal matrix where power of n will produce the same diagonal matrix with the array to be power of n as well. This is as shown in equation (3.22). Hence, the equation for A^{2n+1} is as shown in equation (3.23).

$$
A^{2n+1} = \begin{pmatrix} \left(\left(\dfrac{\Delta}{2} - \chi N_k\right)^2 + g^2 \dfrac{(n+k)!}{n!}\right)^n & 0 \\ 0 & \left(\left(-\dfrac{\Delta}{2} + \chi N_k\right)^2 + g^2 \dfrac{(n)!}{(n-k)!}\right)^n \end{pmatrix} \times
$$

$$
\begin{pmatrix} \left(\dfrac{\Delta}{2} - \chi N_k\right) & ga^k \\ ga^{tk} & \left(-\dfrac{\Delta}{2} + \chi N_k\right) \end{pmatrix} \tag{3.22}
$$

$$A^{2n+1} = \begin{pmatrix} \left[\left(\dfrac{\varDelta}{2} - \chi N_k \right)^2 + g^2 \dfrac{(n+k)!}{n!} \right]^n \left(\dfrac{\varDelta}{2} - \chi N_k \right) & \left[\left(\dfrac{\varDelta}{2} - \chi N_k \right)^2 + g^2 \dfrac{(n+k)!}{n!} \right]^n ga^2 \\ \left[\left(-\dfrac{\varDelta}{2} + \chi N_k \right)^2 + g^2 \dfrac{n!}{(n-k)!} \right]^n ga^{t2} & \left[\left(-\dfrac{\varDelta}{2} + \chi N_k \right)^2 + g^2 \dfrac{n!}{(n-k)!} \right]^n \left(-\dfrac{\varDelta}{2} + \chi N_k \right) \end{pmatrix} \tag{3.23}$$

The exponential for the term $exp[-itA]$ is shown in equation (3.24). The exponential function is expanded by using the trigonometry role of $exp(ix) = cosx - i\,sinx$. Then it is converted into power series,

$$\exp[-itA] = \sum_{n=0}^{\infty} \frac{(-t)^n}{(2n)!} A^{2n} - i\sum_{n=0}^{\infty} \frac{(-t)^n}{(2n+1)!} A^{2n+1} \tag{3.24}$$

Equation (3.24) will then be solved by separating the equation into two sections. The first section will be $\sum_{n=0}^{\infty} \frac{(-t)^n}{(2n)!} A^{2n}$ and the secong section will be $-i\sum_{n=0}^{\infty} \frac{(-t)^n}{(2n+1)!} A^{2n+1}$. The respective A^{2n} and A^{2n+1} will be converted into matrix form. Then using the Taylor series both equations will then be converted into trigonometry function.

50

$$\sum_{n=0}^{\infty}\frac{(-it)^n}{(2n)!}A^{2n}=\sum_{n=0}^{\infty}\frac{(-t)^n}{(2n)!}\begin{pmatrix}\left(\left(\frac{\Delta}{2}-\chi N_k\right)^2+g^2\frac{(n+k)!}{n!}\right)^n & 0\\[3ex] 0 & \left(\left(-\frac{\Delta}{2}+\chi N_k\right)^2+g^2\frac{(n)!}{(n-k)!}\right)^n\end{pmatrix}$$

$$=\begin{pmatrix}\cos t\sqrt{\left(\frac{\Delta}{2}-\chi N_k\right)^2+g^2\frac{(n+k)!}{n!}} & 0\\[3ex] 0 & \cos t\sqrt{\left(-\frac{\Delta}{2}+\chi N_k\right)^2+g^2\frac{(n)!}{(n-k)!}}\end{pmatrix}$$

$$-i\sum_{n=0}^{\infty}\frac{(-t)^n}{(2n+1)!}A^{2n+1}$$

$$=-i\sum_{n=0}^{\infty}\frac{(-t)^n}{(2n+1)!}\begin{pmatrix}\left(\left(\frac{\Delta}{2}-\chi N_k\right)^2+g^2\frac{(n+k)!}{n!}\right)^n\times\left(\frac{\Delta}{2}-\chi N_k\right) & \left(\left(\frac{\Delta}{2}-\chi N_k\right)^2+g^2\frac{(n+k)!}{n!}\right)^n ga^2\\[4ex] \left(\left(-\frac{\Delta}{2}+\chi N_k\right)^2+g^2\frac{(n)!}{(n-k)!}\right)^n\times ga^{t2} & \left(\left(-\frac{\Delta}{2}+\chi N_k\right)^2+g^2\frac{(n)!}{(n-k)!}\right)^n\left(-\frac{\Delta}{2}+\chi N_k\right)\end{pmatrix}$$

$$=-i\begin{pmatrix}\dfrac{\sin\left[t\sqrt{\left(\frac{\Delta}{2}-\chi N_k\right)^2+g^2\sqrt{\frac{(n+k)!}{n!}}}\right]\left(\frac{\Delta}{2}-\chi N_k\right)}{\sqrt{\left(\frac{\Delta}{2}-\chi N_k\right)^2+g^2\sqrt{\frac{(n+k)!}{n!}}}} & \dfrac{\sin\left[t\sqrt{\left(\frac{\Delta}{2}-\chi N_k\right)^2+g^2\sqrt{\frac{(n+k)!}{n!}}}\right]}{\sqrt{\left(\frac{\Delta}{2}-\chi N_k\right)^2+g^2\sqrt{\frac{(n+k)!}{n!}}}}ga^2\\[6ex] \dfrac{\sin\left[t\sqrt{\left(-\frac{\Delta}{2}+\chi N_k\right)^2+g^2\sqrt{\frac{(n)!}{(n-k)!}}}\right]}{\sqrt{\left(-\frac{\Delta}{2}+\chi N_k\right)^2+g^2\sqrt{\frac{(n)!}{(n-k)!}}}}ga^{t2} & \dfrac{\sin\left[t\sqrt{\left(-\frac{\Delta}{2}+\chi N_k\right)^2+g^2\sqrt{\frac{(n)!}{(n-k)!}}}\right]}{\sqrt{\left(-\frac{\Delta}{2}+\chi N_k\right)^2+g^2\sqrt{\frac{(n)!}{(n-k)!}}}}\left(-\frac{\Delta}{2}+\chi N_k\right)\end{pmatrix}$$

51

For simplification, Ω_n and Ω_n^- will be introduced as showed in equation (3.25) and (3.26).

These equation will then be substituted to equation (3.24) and form equation (3.27).

$$\Omega_n = \sqrt{\left(\frac{\Delta}{2} - \chi N_k\right)^2 + g^2\sqrt{\frac{(n+k)!}{n!}}} \qquad (3.25)$$

$$\Omega_n^- = \sqrt{\left(-\frac{\Delta}{2} + \chi N_k\right)^2 + g^2\sqrt{\frac{(n)!}{(n-k)!}}} \qquad (3.26)$$

$$\exp[-itA] = \begin{pmatrix} \cos(\Omega_n t) & 0 \\ 0 & \cos(\Omega_n^- t) \end{pmatrix} - i \begin{pmatrix} \dfrac{\sin(\Omega_n t)\left(\dfrac{\Delta}{2} - \chi N_k\right)}{\Omega_n} & \dfrac{\sin(\Omega_n t)}{\Omega_n} g a^k \\ \dfrac{\sin(\Omega_n^- t)}{\Omega_n^-} g a^{tk} & \dfrac{\sin(\Omega_n^- t)}{\Omega_n^-}\left(-\dfrac{\Delta}{2} + \chi N_k\right) \end{pmatrix}$$

$$(3.27)$$

Using the role $af(a^t a) = f(a^t a + 1)a$ and $a^t f(aa^t) = a^t f(a^t a + 1)$ (Huai et al., 2000), Ω_n^- can be converted into Ω_n , $\dfrac{\sin(\Omega_n^- t)}{\Omega_n^-} a^{t2} = a^{t2} \dfrac{\sin(\Omega_n t)}{\Omega_n}$.

$$\exp[-itA] = \begin{pmatrix} \cos(\Omega_n t) - i\,\dfrac{\sin(\Omega_n t)\left(\dfrac{\Delta}{2} - \chi N_k\right)}{\Omega_n} & -i\,\dfrac{\sin(\Omega_n t)}{\Omega_n} g a^k \\ g a^{tk}\,\dfrac{\sin(\Omega_n t)}{\Omega_n} & \cos(\Omega_n^- t) - i\,\dfrac{\sin(\Omega_n^- t)}{\Omega_n^-}\left(-\dfrac{\Delta}{2} + \chi N_k\right) \end{pmatrix}$$

$$(3.28)$$

The value of $exp[-itA]$ will be substituted to the Schrodinger equation and yield the following,

52

$$\left|\Psi(t,\chi,k)\right\rangle = \sum_{n=0}^{\infty} Q_n \exp(i\varphi n)\exp(i\chi N_k^2 t)\times$$

$$\begin{pmatrix} \cos(\Omega_n t)-i\dfrac{\sin(\Omega_n^+ t)\left(\dfrac{\Delta}{2}-\chi N_k\right)}{\Omega_n^+} & -i\dfrac{\sin(\Omega_n t)}{\Omega_n}ga^2 \\[3ex] ga^{t2}\dfrac{\sin(\Omega_n t)}{\Omega_n} & \cos t\Omega_n^- -i\dfrac{\sin(\Omega_n^- t)}{\Omega_n^-}\left(-\dfrac{\Delta}{2}+\chi N_k\right) \end{pmatrix}\begin{pmatrix}|n\rangle \\ 0 \end{pmatrix}$$

$$\left|\Psi(t,\chi,k)\right\rangle = \sum_{n=0}^{\infty} Q_n \exp(in\varphi)\exp(it\chi N_k^2)\begin{pmatrix} \cos t\Omega_n -i\dfrac{\sin t\Omega_n\left(\dfrac{\Delta}{2}-\chi N_k\right)}{\Omega_n}|n\rangle \\[3ex] ga^{tk}\dfrac{\sin t\Omega_n}{\Omega_n}|n\rangle \end{pmatrix}$$

$$(3.29)$$

Using equation (3.11), equation (3.29) $a^{tk}|n\rangle$ and $a^k|n\rangle$ will be converted into equation (3.30),

$$\left|\Psi(t,\chi,k)\right\rangle = \sum_{n=0}^{\infty} Q_n \exp(in\varphi)\exp(it\chi N_k^2)\begin{pmatrix} \cos t\Omega_n -i\dfrac{\sin t\Omega_n\left(\dfrac{\Delta}{2}-\chi N\right)}{\Omega_n}|n\rangle + \\[3ex] g\dfrac{\sin t\Omega_n}{\Omega_n}\dfrac{\sqrt{(n+k)!}}{\sqrt{n!}}|n+k\rangle \end{pmatrix}$$

$$(3.30)$$

Equation (3.30) then convert into non-matrix form as showed in equation (3.31).

53

$$|\Psi(t,\chi,k)\rangle = \sum_{n=0}^{\infty} Q_n \, exp(in\varphi) exp(it\chi N_k^2) \left[\begin{array}{c} \left(g\, \dfrac{sint\Omega_n}{\Omega_n} \dfrac{\sqrt{(n+k)!}}{\sqrt{n!}} |n+k\rangle \right) + \\[2em] \left(cos\,t\Omega_n - i\, \dfrac{sint\Omega_n \left(\dfrac{\Delta}{2} - \chi N \right)}{\Omega_n} |n\rangle \right) \end{array} \right]$$

(3.31)

Hence, the developed Jaynes-Cummings model for a multi-photon transition coupling with a Kerr-like medium in this study is shown in equation (3.32).

$$|\Psi(t,\chi,k)\rangle = \sum_{n=0}^{\infty} \left[\begin{array}{c} Q_n e^{in\varphi} \, exp\left(-i\chi t\left(n^2 + (k-1)\left(n+\dfrac{k}{2}\right) \right) \right) \times \\[1em] [C_n(t)|0,n+k\rangle + D_n(t)|1,n\rangle] \end{array} \right]$$

(3.32)

$$C_n(t) = -isi(n2\beta_n)sin(\Omega_n t)$$

$$D_n(t) = cos(\Omega_n t) - i\,cos(2\beta_n)cos(\Omega_n t)$$

$$sin(2\beta_n) = \frac{g\sqrt{\dfrac{(n+k)!}{n!}}}{\Omega_n}$$

$$cos(2\beta_n) = \frac{\Delta/2 + k\chi/2(1-2n-k)}{\Omega_n}$$

$$\Omega_n^2 = \left(\frac{\Delta}{2} + k\chi/2(1-2n-k) \right)^2 + g^2 \frac{(n+k)!}{n!}$$

It is shown that the quantum phase state will mainly be influenced by the change of time, the Kerr-like medium, and the number of photon transition. In this study the purpose is to observe the influence of the Kerr-like medium coupling and the number of photon

transition on the phase properties, so the time and also the phase angle will be set to a certain range to enable for comparison between the change of number of photon transition and the Kerr-like medium coupling strength.

3.2 Measuring Quantum Phase State

In measuring the quantum phase state, the Pegg-Barnett Formalism is used. The Pegg-Barnett Formalism uses the phase probability to indicate the behaviour of the quantum phase state. As explained in Chapter 2, the Pegg-Barnett Formalism is an introduction of finite *(s+1)*-dimensional space, ψ (Lahti et al., 2002). The phase probability is used to understand the quantum phase behaviour under the effect of a Kerr-like medium and the number of photon transition.
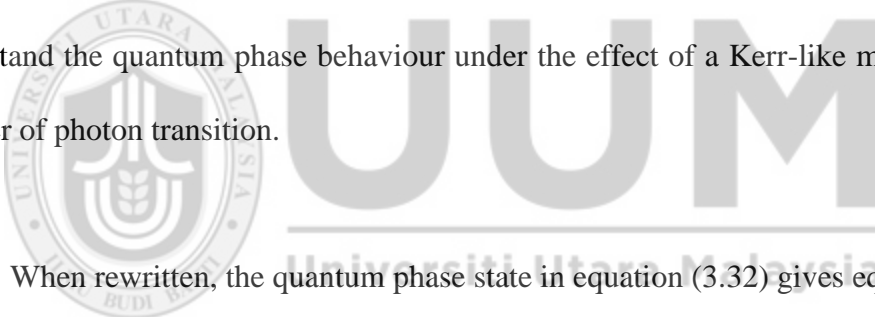
When rewritten, the quantum phase state in equation (3.32) gives equation (3.33),

$$\left|\psi(t)\right\rangle = \left|\psi_g(t)\right\rangle|g\rangle + \left|\psi_e(t)\right\rangle|e\rangle \tag{3.33}$$

where

$$\left|\Psi_g(t)\right\rangle = -i\sum_{n=0} Q_n e^{in\varphi} exp\left(-i\chi t\left(n^2 + (k-1)\left(n+\frac{k}{2}\right)\right)\right) sin(2\beta_n) sin(\Omega_n t)|n+k\rangle$$

$$\left|\Psi_e(t)\right\rangle = \sum_{n=0} Q_n e^{in\varphi} exp\left(-i\chi t\left(n^2 + (k-1)\left(n+\frac{k}{2}\right)\right)\right) sin(2\beta_n) sin(\Omega_n t)|n\rangle$$

By tracing over the atomic variables, $\left|\Psi_g(t)\right\rangle$ and $\left|\Psi_e(t)\right\rangle$, the reduced density operator will be as shown in equation (3.34)

55

$$\rho(t) = \text{Tr}_A |\psi(t)\rangle\langle\psi(t)| = |\psi_g(t)\rangle\langle\psi_g(t)| + |\psi_e(t)\rangle\langle\psi_e(t)| \qquad (3.34)$$

Using the continuum phase distribution of the Pegg-Barnett Formalism, the phase probability distribution in function of time, t and phase state, θ is written as shown in equation (3.35)

$$P(\theta,t) = \frac{1}{2\pi}\left(\begin{array}{l} 1 + 2\sum_{m>n} Q_n Q_m A_{nm}(t)cos\{(m-n)\theta + \chi t(\gamma_{mn})\} \\ + 2\sum_{m>n} Q_n Q_m B_{nm}(t)sin\{(m-n)\theta + \chi t(\gamma_{mn})\} \end{array} \right) \qquad (3.35)$$

where

$$A_{mn}(t) = cos(\Omega_m t)cos(\Omega_n t) + cos[2(\beta_m - \beta_n)]sin(\Omega_m t)sin(\Omega_n t)$$
$$B_{mn}(t) = cos(2\beta_n)cos(\Omega_m t)sin(\Omega_n t) - cos(2\beta_k)cos(\Omega_n t)sin(\Omega_m t)$$
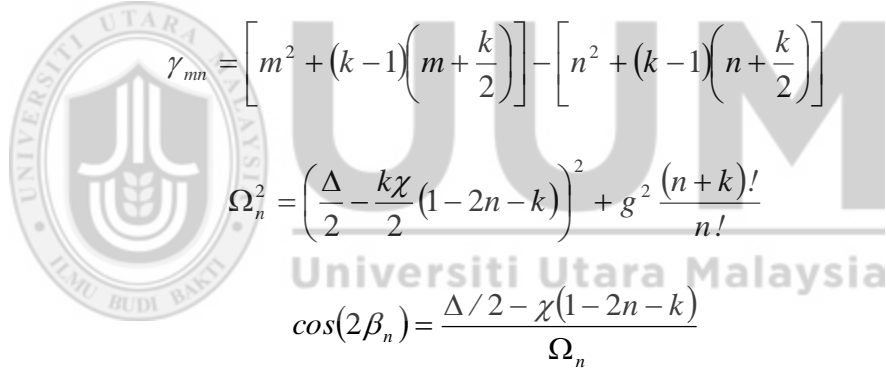
$$\gamma_{mn} = \left[m^2 + (k-1)\left(m + \frac{k}{2}\right)\right] - \left[n^2 + (k-1)\left(n + \frac{k}{2}\right)\right]$$

$$\Omega_n^2 = \left(\frac{\Delta}{2} - \frac{k\chi}{2}(1 - 2n - k)\right)^2 + g^2 \frac{(n+k)!}{n!}$$

$$cos(2\beta_n) = \frac{\Delta/2 - \chi(1 - 2n - k)}{\Omega_n}$$

$$sin(2\beta_n) = \frac{g\sqrt{\dfrac{(n+k)!}{n!}}}{\Omega_n}$$

The number of photon transition is considered until six because when it reaches a six-photon transition the quantum phase state shows the same behaviour like the previous number of photon transition, which will be explained later. For variable Ω_n^2, $cos(2\beta_n)$ and $sin(2\beta_n)$, refer to section, 3.1.

56

As shown from equation (3.35), the value of γ_{mn} increases when the photon number transition increases. This indicates that a higher photon transition will lead to more fluctuations on the function. For example, for a number photon transition $k = 5$ and $m = n - 1 = 3$, the first case and second case are $k = 4$ and $m = n - 1 = 3$.

First case k 5 and m $n - 1$ 3

$$\gamma_{mn} = \left[m^2 + 4\left(m + \frac{5}{2} \right) \right] - \left[n^2 + 4\left(n + \frac{5}{2} \right) \right]$$
$$= \left[16 + 4\left(4 + \frac{5}{2} \right) \right] - \left[9 + 4\left(3 + \frac{5}{2} \right) \right] = 11$$

Second case k 4 and m $n - 1$ 3

$$\gamma_{mn} = \left[m^2 + 3(m + 2) \right] - \left[n^2 + 3(n + 2) \right]$$
$$= \left[16 + 3(4 + 2) \right] - \left[9 + 3(3 + 2) \right] = 10$$

This is only a part of the function. The next section explains further how the quantum phase state behaves.

3.3 Analysis of Quantum Phase State

This section discusses the phase properties of the quantum phase state for different number of photon transition and also a Kerr-like medium coupling. The result is produced via Mathematica software and programming language, as shown in Appendix A.

57

The phase properties are analyzed from a single till a six-photon transition scenarios. The mean photon number is set at $|\alpha^2| = 10$ as further increase in the mean photon number will not impact on the results and the detuning change is set at $\frac{\Delta}{g} = 0$ for a resonance transition of a qubit state. The variable is $\frac{\chi}{g}$ to see the changes on the phase properties when there is an increase in the Kerr-like medium. The values $\frac{\chi}{g}$ are 0, 0.01 and 0.1 to observe the quantum behaviour when the coupling strength of the Kerr-like medium is higher. The phase properties are observed with the range of time, gt and also the phase state, θ. Figure 3.1 until 3.6 illustrate the phase properties of a single to a six-photon transition, respectively, where a, b, and c represent different Kerr-like medium coupling strength of 0, 0.01, and 0.1.
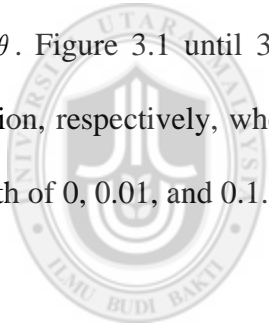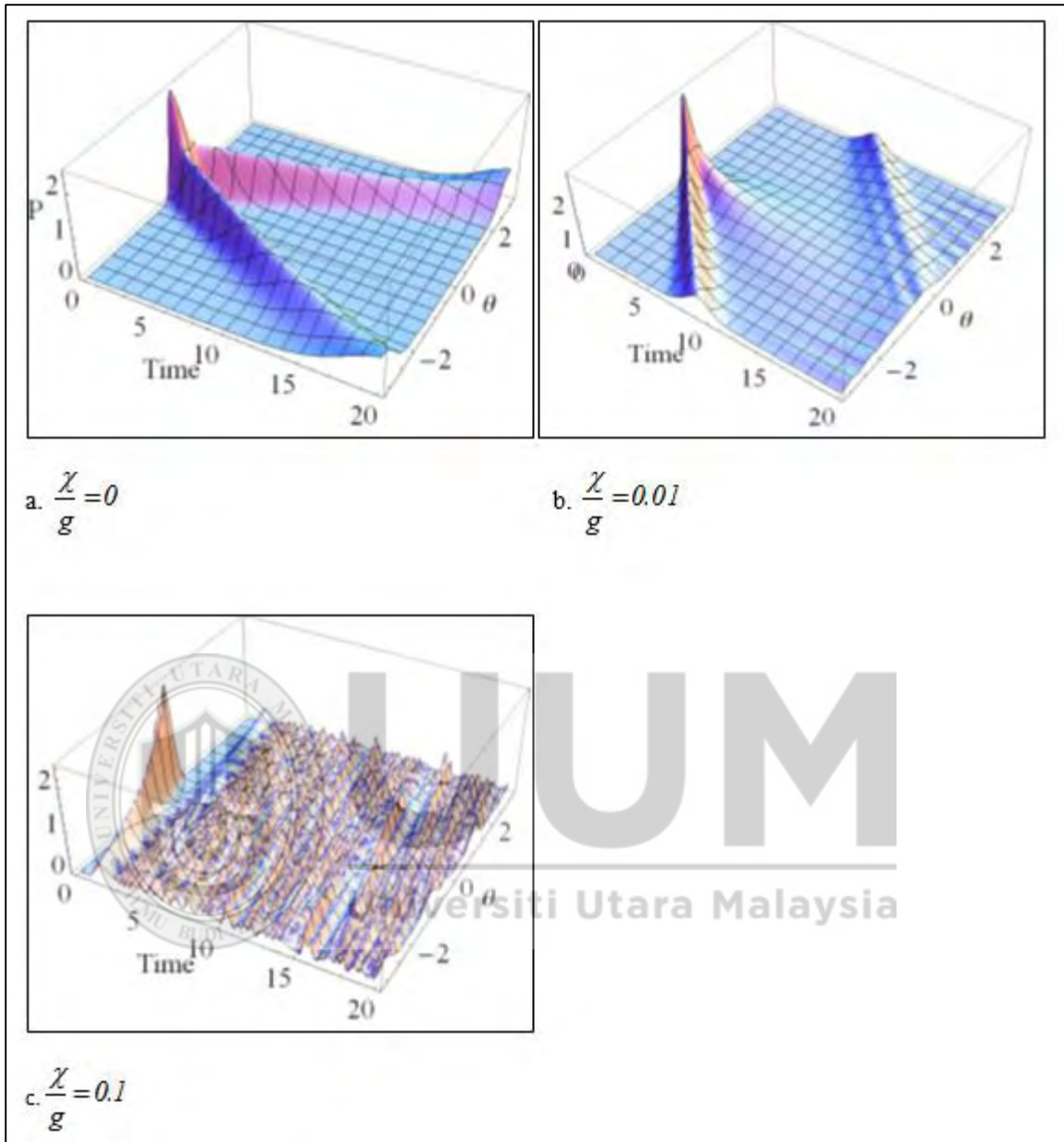
Figure 3.1. Phase probability distribution for $k = 1$, scale time $0 \leq gt \leq 20$, and phase probability $0 \leq P(\theta, t) \leq 2.5$

Figure 3.1 shows that with an increase in the Kerr-like medium, the collapse and revival increase and the amplitude of phase probability is reduced (Obada et al., 1998).

When there is an increase in Kerr-like medium coupling strength, the pattern changes (compare Figure 3.1a with Figure 3.2b). The peak is still maintained for different coupling strength where for the value $\theta = 0$ the phase probability is at $P(\theta,t) \approx 2.0$. When $\frac{\chi}{g} = 0.1$, Figure 3c shows that the wave like pattern disappears, which is replaced by a small amplitude with $P(\theta,t) \approx 0.22$ of collapse and revivals.

Figure 3.2 shows the phase probability of a two-photon transition. Figure 3.2a shows a wave pattern which disappears when $\frac{\chi}{g}$ increases. Figure 3.2b shows that a slight increase in $\frac{\chi}{g}$ reduces the wave pattern at $gt \approx 2.5$. An increase in $\frac{\chi}{g}$ also increases the collapses and revivals, as shown in Figure 3.2c where the increase in the collapses and revivals $P(\theta,t) \approx 0.16$. Similar to Figure 3.1, there is a peak at $\theta = 0$ with $P(\theta,t) \approx 2.0$ (Gantsog et al., 1996).

Figure 3.2 shows that when the photon transition increases to two photon, the collapse and revival also increase. Figure 3.2a shows that the wave of the phase probability increases (compare it with Figure 3.1a), which shows an increase in the collapse and revival activity. Figure 3.2 also shows that the collapse and revival increase with amplitude when the coupling strength of Kerr medium increases (compare Figure 3.2b and 3.2c with Figure 3.1b and 3.1c). However, in Figure 3.1c there are more small peaks (average phase probability of 0.16) with lesser amplitude (average phase probability of 0.17), whereas

Figure 3.2c contains a big wave along the time. This is because the two-photon transition plays a role in the phase properties along with the increase in Kerr-like medium coupling strength.
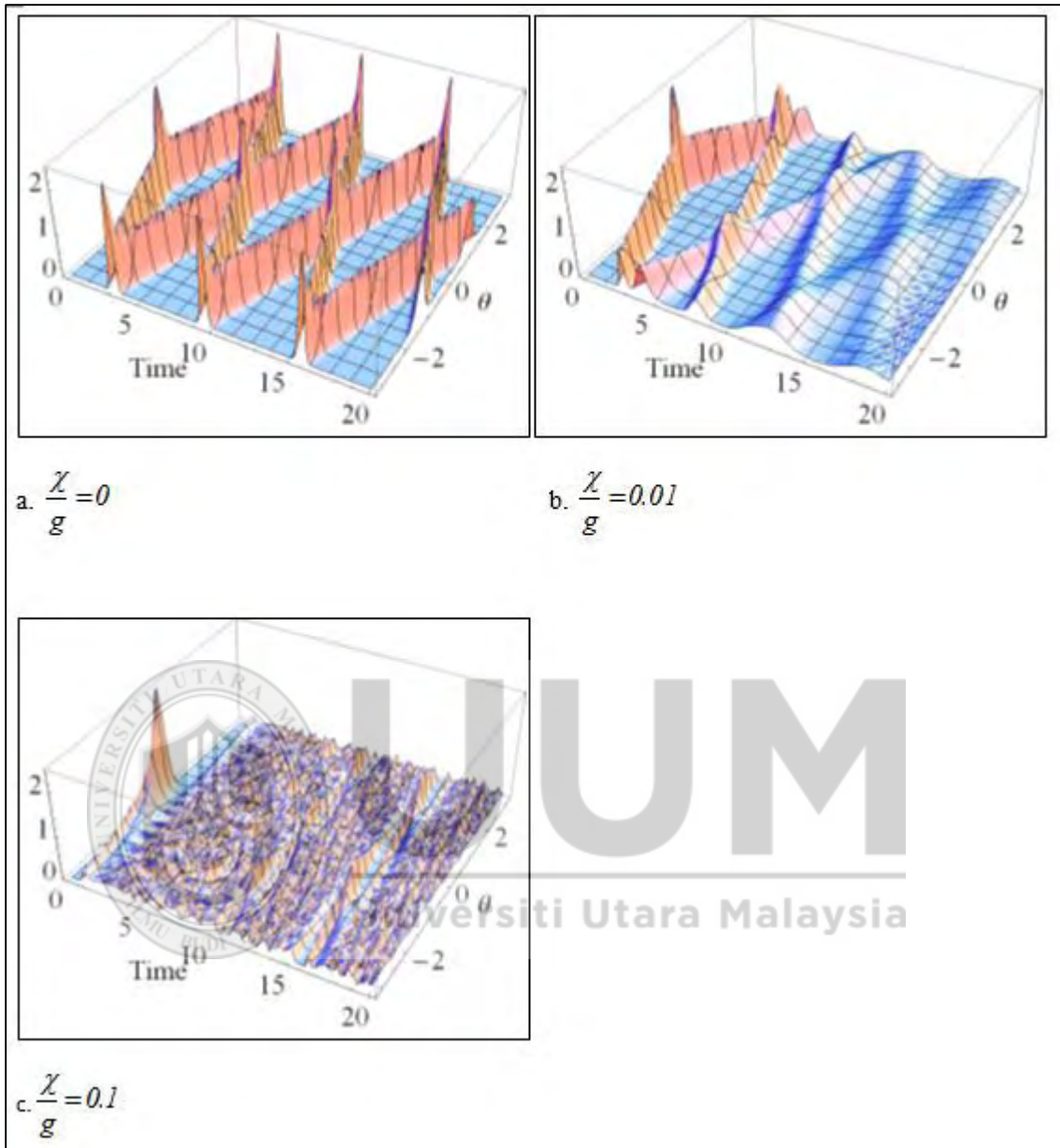
Figure 3.2. Phase probability distribution for $k = 2$ scale time $0 \le gt \le 20$ and phase
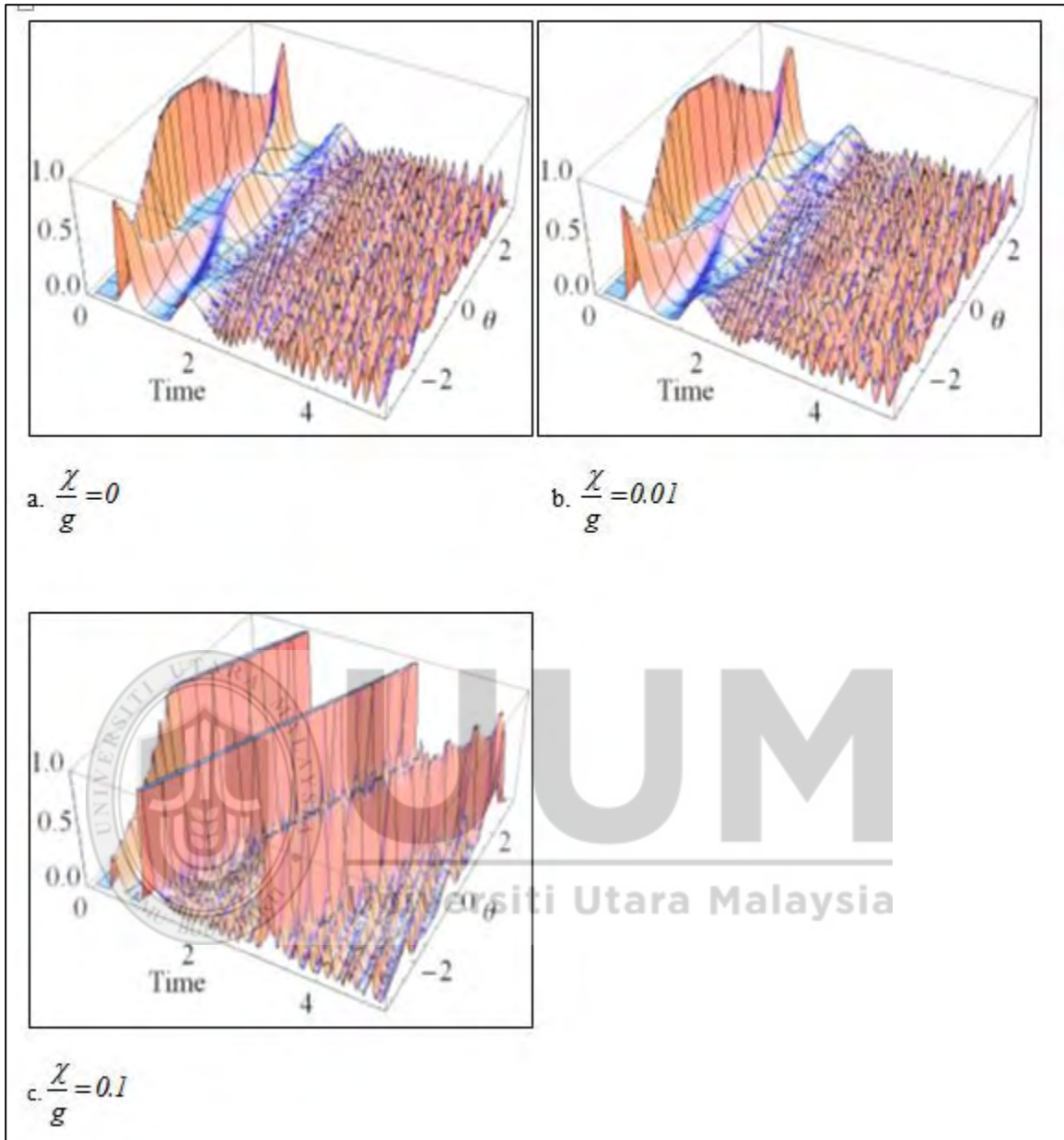
probability $0 \le P(\theta,t) \le 2.5$

Figure 3.3. Phase probability distribution for $k = 3$ scale time $0 \le gt \le 5$ and phase probability $0 \le P(\theta,t) \le 1.0$

Figure 3.3 shows the phase properties of a three-photon transition. Figure 3.3a and 3.3b show the same phase properties, which tell us that at this number of photon transition,

weak Kerr-like medium coupling will not have any impact on the phase properties. Both Figure 3.3a and 3.3b show a peak at $\theta = 0$ and then gradually decreases when $\theta \neq 0$ and together with time. There is also another peaks at the end of both sides. This shows that there is a collapse and revival within this. As compared to Figure 3.3c there exist a big wave with small collapse and revival in between of the wave. It also showed that the amplitude of the wave is high with more than one.

Compared to a single and a two-photon transition, a three-photon transition has a shorter wave for weak Kerr-like medium coupling. When the Kerr-like medium coupling becomes stronger, in overall there is wave with the phase properties showed more small fluctuations compared to the lesser photon transition.

Next is the four-photon transition. Figure 3.4 shows that the wave like pattern no longer appears and peaks only appear at the beginning, then they become smaller for all the Kerr-like medium coupling strength. Then at $gt \approx 3.1$ there is a sudden high peak or revival with showing the highest peak (see Figure 3.4a). The sudden peak also appears in Figure 3.4b but with lesser amplitude.
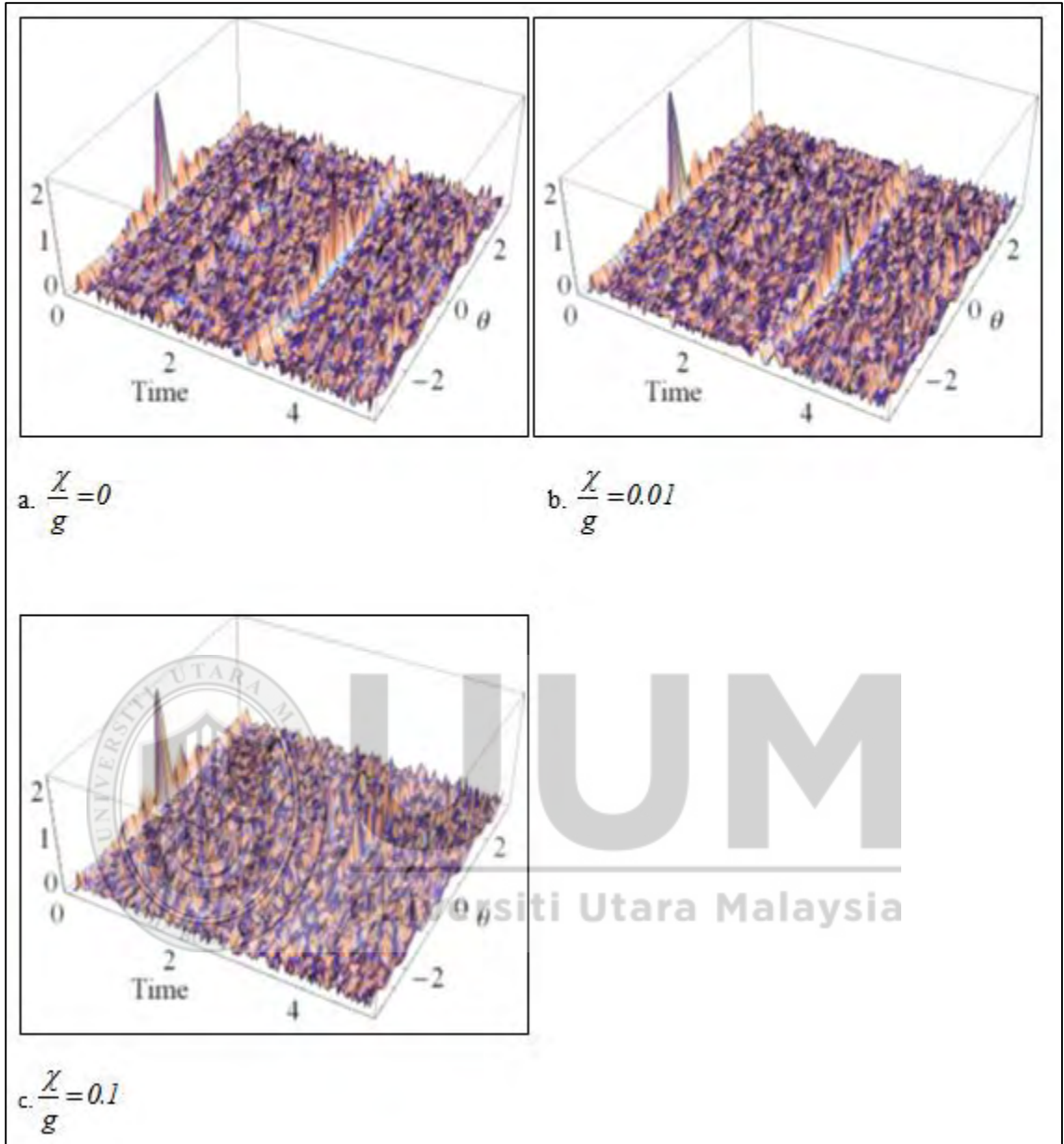
Figure 3.4. Phase probability distribution for $k = 4$ scale time $0 \leq gt \leq 5$ and phase probability $0 \leq P(\theta,t) \leq 2.5$

A further increase in photon transition destroys the wave pattern of the phase properties which become more active with collapses and revivals (see Figure 3.4). In

comparison to Figure 3.4a, the wave pattern only exists at $gt \approx 0.1$. Figure 3.4a and 3.4b

show a sudden peak at $gt \approx 3.2$ which does not occur in a lesser photon transition with a

maximum phase probability at $\theta = 0$ of $P(\theta,t) \approx 6.14$ and average $P(\theta,t) \approx 1.62$ for $\theta \neq 0$

. Figure 3.4a and 3.4b show that at $gt \approx 3.2$ till $gt \approx 4.0$ there is a huge wave. An increase

in a photon transition has reduced the wave into a small sudden peak in a short time. For a

four-photon transition, when the Kerr-like medium coupling is strong, Figure 3.4c shows

that the wave pattern is diminished with a small fluctuation. An increase in the number of

photon transition has reduced the big wave (see Figure 3.1c, Figure 3.2c, and Figure 3.3c).

Figure 3.4 and 3.5 show the results when the photon transition increases to four and

five. Higher photon transitions has caused the initial spread and the wave like pattern to

disappear, which are found in a single, two-, and three-photon transitions. The four-photon

transition in Figure 3.4a shows that there are some large peaks at $gt \approx 3.2$ but they

disappear in a five-photon transition (see Figure 3.5a). In the five-photon transition, the

wave pattern totally disappears and is being totally substituted by uncertain collapses and

revivals. The amplitude of the phase probability amplitude is lesser than the four-photon

transition. For example, at $gt = 3.0$ for $\dfrac{\chi}{g} = 0.1$, the average is $P(\theta,t) \approx 0.19$ for the four-

photon transition, while for the five-photon transition the average is $P(\theta,t) \approx 0.17$. For the

five-photon transition, it can be seen that an increase in $\dfrac{\chi}{g}$ does not form any wave like

pattern. This has increased uncertainty. As shown in Table 3.1, the average is $P(\theta,t)$ for

different values of $\dfrac{\chi}{g}$. It seems that for $\dfrac{\chi}{g} = 0$, $P(\theta,t)$ is lesser than for $\dfrac{\chi}{g} = 0.01$ but

higher than $\dfrac{\chi}{g} = 0.1$. $\dfrac{\chi}{g} = 0.1$ shows the least $P(\theta,t)$ among the other Kerr-like medium

coupling strength.

Table 3.1

Average of $P(\theta,t)$ for different θ.2

χ / g	0	0.01	0.1
$P(\theta,t)$	0.1575	0.1614	0.1556
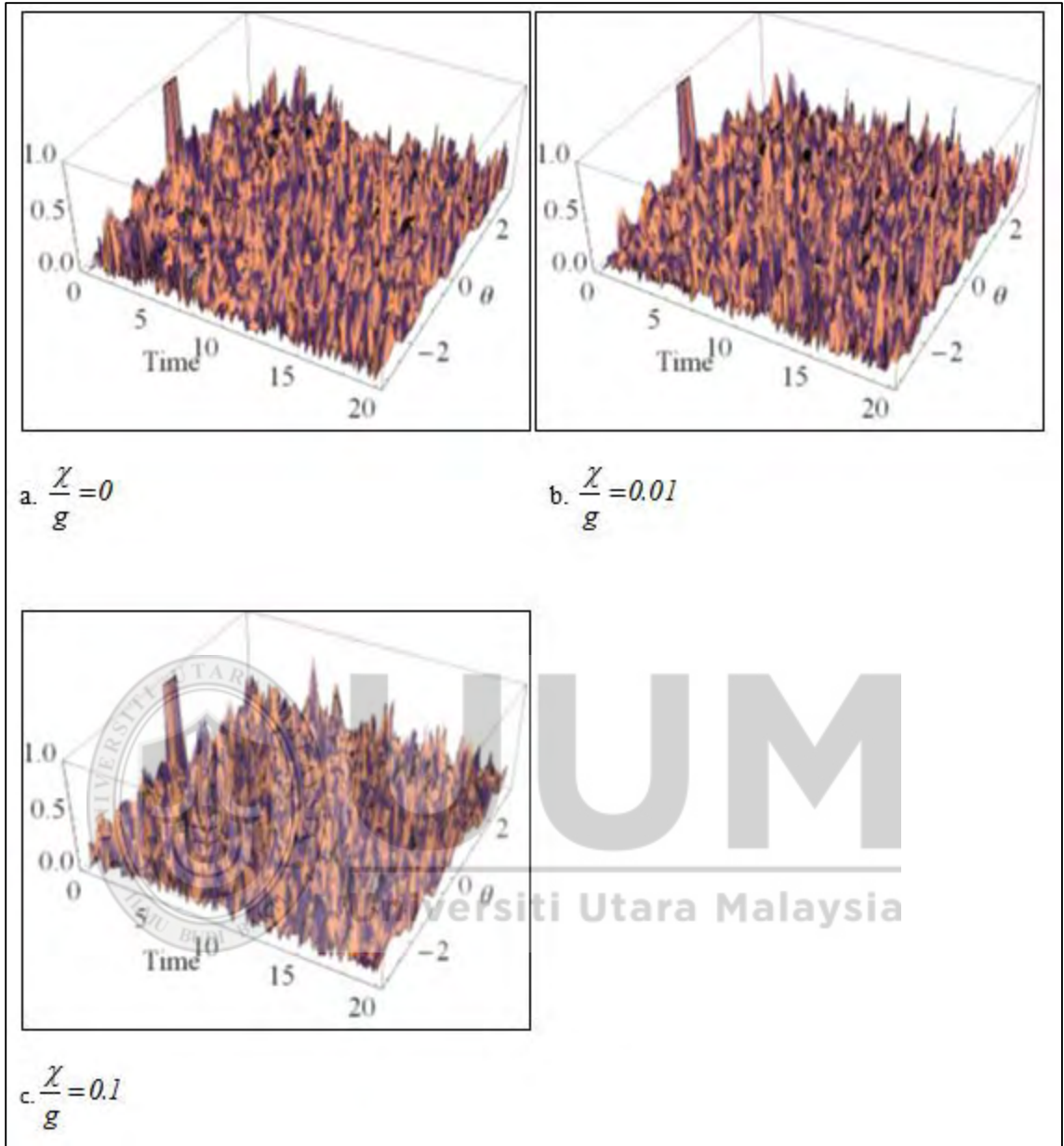
Figure 3.5. Phase probability distribution for $k = 5$ scale time $0 \leq gt \leq 20$ and phase probability $0 \leq P(\theta, t) \leq 1.0$
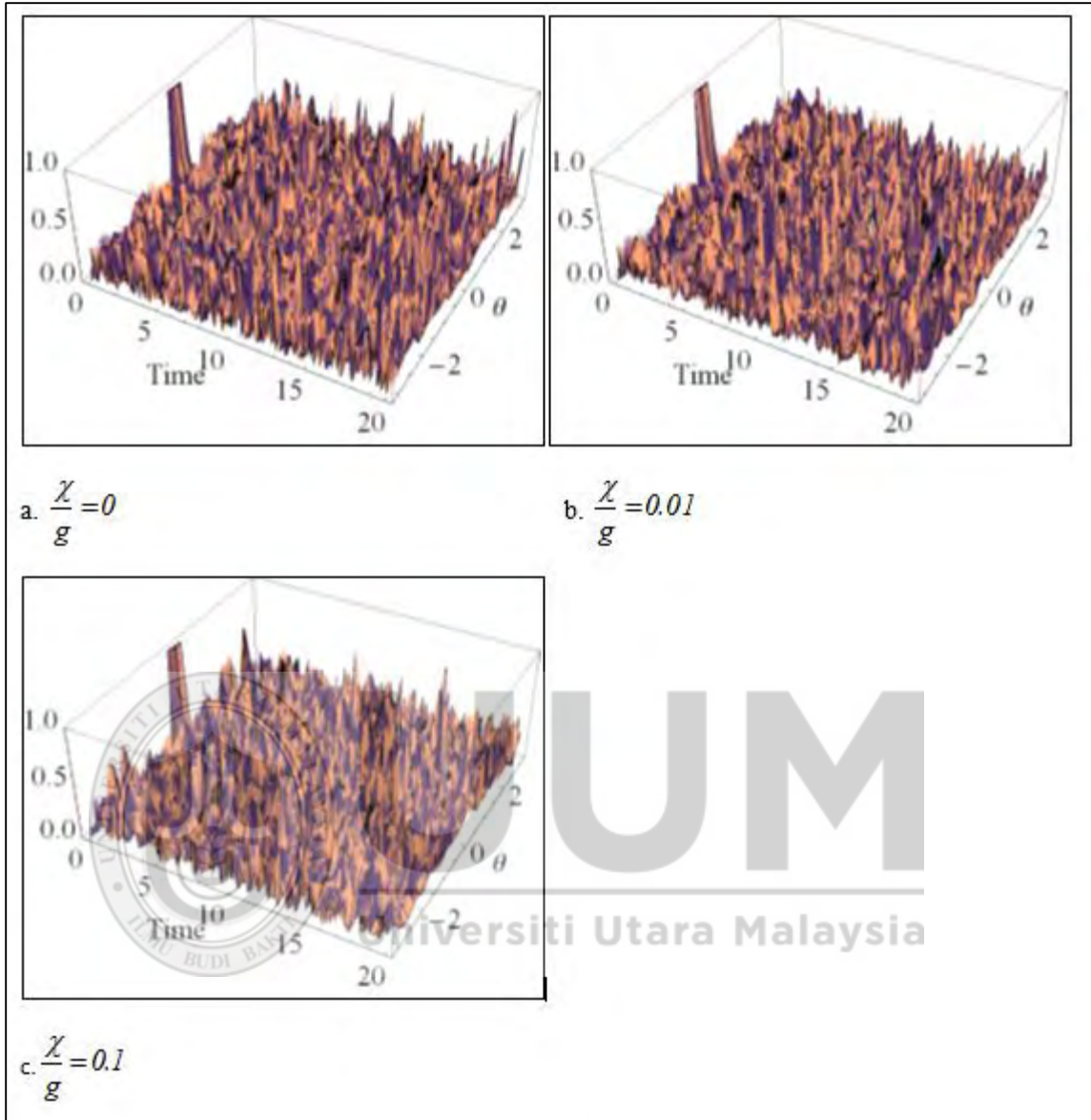
Figure 3.6. Phase probability distribution for $k = 6$ scale time $0 \leq gt \leq 20$ and phase probability $0 \leq P(\theta,t) \leq 1.0$

As the number of photon transition increases, the phase properties show the same pattern. Figure 3.4 and Figure 3.5 show that the phase properties of a quantum system fluctuate in an uncertain way where the wave like pattern no longer appears. The changes

are lesser (see Figure 3.6) and they become similar (see Figure 3.5) with differences in amplitude. Hence, this study considers only a six-photon transition as no changes are observed when the number of photon increases beyond this point (see Figure 3.6). These scenarios tell us that at a high number of photon transition, the behaviour of the quantum system becomes more uncertain.

3.4 Conclusion

Under the Pegg-Barnett Formalism there exists a wave shaped pattern for a single and a two-photon transition. However, such pattern disappears at higher photon transitions resulting in a more frequent fluctuation on the collapse and revival. As the number of photon transition increases, the Kerr-like medium coupling becomes less influential on the phase properties. Initially, the Kerr-like medium coupling had a big influence on the phase properties but when it reaches a five-photon transition, the impact on the phase properties becomes less where the pattern of the fluctuation becomes similar with only a slight change in amplitude.

CHAPTER FOUR

QUANTUM SYSTEM ENTANGLEMENT WITH KERR-LIKE MEDIUM

4.1 Introduction

After the phase state is derived for the Jaynes-Cummings model with the interaction between the cavity field and the atoms, this chapter considers the interaction between the atoms for the case of a three-qubit W-state. In this case focus is on the quantum entanglement behaviour with coupling of a Kerr-like medium, so the Jaynes-Cummings model will have only a single photon transition number.

This chapter is divided into three sections. Section 4.2 is the development of the Jaynes-Cummings model with the integration of a three-qubit quantum system and a Kerr-like medium coupling. Section 4.3 discusses the measurement of a quantum entanglement. The discussion on the quantum entanglement based on the measurement results is included in the Section 4.4. Lastly, Section 4.5 concludes this chapter.

4.2 Three-Qubit Jaynes-Cummings with Kerr-Like Medium

This section discusses the development of a three-qubit Jaynes-Cummings model coupling with a Kerr-like medium. Section 4.2.1 describes the Hamiltonian equation which include the Kerr-like medium coupling. Section 4.2.2 describes the quantum system for a three-

qubit quantum state coupling with a cavity field and the Kerr-like medium. Section 4.2.3 discusses the Hamitonian model and the quantum system to find the time-dependent coefficient of the quantum system needed to determine the quantum entanglement behaviour. Time coefficient will be the observables of the quantum system used to measure the robustness of the quantum entanglement.

4.2.1 Hamiltonian system for Three-Qubit Quantum System

The Hamiltonian equation considers a three-qubit quantum state in a quantum system with coupling with a Kerr-like medium. This model represents the three-qubit quantum state interacting with the cavity field in the presence of the Kerr-like medium. Besides, a leaky multimode cavity field is considered as well, where it is modelled using Lorentzian spectral density (An et al., 2011). Hence, another factor considered in this case is the non-Markovian and Markovian approximation, which represent the cavity field that will regain the part of the information or energy loss and the cavity field which is unable to regain the information lost, respectively.

Based on equation (3.1) in Chapter 3, H_2 is added to represent the interaction between the three-qubit quantum state (An et al., 2011). After the modification of equation (3.1), the Hamiltonian rotating wave approximation of the total quantum system is shown in equation (4.1)-(4.4) (Flores & Galapon, 2015).

$$H = H_0 + H_1 + H_2 \tag{4.1}$$

$$H_0 = \sum_{n=1}^{3} \omega_0 \sigma_n^+ \sigma_n^- + \sum_j \omega_j a_j^t a_j \qquad (4.2)$$

$$H_1 = \sum_{n=1}^{3} \sum_j \alpha_n \left(g_j \sigma_n^+ a_j + g_j^* \sigma_n^- a_j^t \right) + \sum_j \chi_j a_j^{t2} a_j^2 \qquad (4.3)$$

$$H_2 = D_1 \left(\sigma_2^+ \sigma_3^- + \sigma_3^+ \sigma_2^- \right) + D_2 \left(\sigma_3^+ \sigma_1^- + \sigma_1^+ \sigma_3^- \right) + D_3 \left(\sigma_1^+ \sigma_2^- + \sigma_2^+ \sigma_1^- \right) \qquad (4.4)$$

j : Mode of photon.

ω_j: Cavity frequency for cavity mode of j photon.

For the interaction Hamiltonian between the atom and the cavity field, H_1 additional parameter introduced to individualize the atom (An et al., 2011). This parameter is the dimensionless real constant, α_n. The coupling strength between the qubit and the cavity field is represented by $\alpha_n |g_j|$. D_l with $l \in \{1,2,3\}$ is introduced to represent the dipole-dipole interaction between the qubit with $D_l = \left[d.d - 3 (d.r_{mn})(d.r_{mn}) / r_{mn}^2 \right] / r_{mn}^3$. The qubit's electric dipole moment is represented by d and r_{mn} represents a two qubit separation (An et al., 2011). This study includes Kerr-like medium coupling strength represented by $\sum_j \chi_j a_j^{t2} a_j^2$ term in equation (4.3).

4.2.2 Quantum System for Three-Qubit

This section discusses the development of a time-dependent quantum system under the Schrodinger equation. The quantum system changes over time and this model represents the quantum system behaviour in the specific time. A three-qubit state is represented by a

73

W state generalization as a W state is more robust than a GHZ state (Vidal et al., 2000). The W state is able to maintain a bipartite entanglement after one of the atoms is being traced out, as explained in Chapter 2.

The initial state of the W state is shown in equation (4.5) for an empty cavity field, that is, $|\overline{0}\rangle$. $a_l(0)$ with $l = 1,2,3$ being the time-dependent coefficients.

$$|W(0)\rangle = a_1(0)|100\rangle_{123} + a_2(0)|010\rangle_{123} + a_3(0)|001\rangle_{123}$$
$$\sum_{n=1}^{3} |a_n(0)|^2 = 1 \tag{4.5}$$

The total quantum system when the atom interacts with the cavity field,

$$|\psi(0)\rangle = |W(0)\rangle|\overline{0}\rangle \tag{4.6}$$

$$|\psi(t)\rangle = e^{-it\omega_0}\left[a_1(t)|100\rangle_{123} + a_2(t)|010\rangle_{123} + a_3(t)|001\rangle_{123}\right]|\overline{0}\rangle$$
$$+ \sum_j b_j(t)e^{-it(\omega_j+\chi_j)}|000\rangle_{123}|1_j\rangle_c \tag{4.7}$$

where $|\overline{0}\rangle$ is the cavity field state with zero photon on mode j and $|1_j\rangle_c$ is the cavity field mode when for one photon with mode j.

Equation (4.6) is the initial total quantum system and equation (4.7) is the state of the total system when $t > 0$. In equation (4.7) a Kerr-like medium is included only in the second term $\sum_j b_j(t)e^{-it(\omega_j+\chi_j)}|000\rangle_{123}|1_j\rangle_c$ which is the development done in this study. Initially when the cavity was zero, there will not be any Kerr-like medium until there is one photon in the cavity. Hence, the first term of equation (4.7) shows that the W state is

acting on the transition frequency. This also means that only a single photon transition will be considered in this study.

4.2.3 Time Dependent Coefficients

Time-dependent coefficients are observables measured to study the quantum behaviour. In other words, time-dependent coefficients explain the robustness of a quantum entanglement when measured. This section will solve the time-dependent coefficients to obtain an equation. The derived model in Section 4.2.1 and 4.2.2 is used to determine the time-dependent coefficient, $a_i(t)$ and $b_j(t)$, $\dfrac{id|\psi(t)\rangle}{dt} = (H_1 + H_2)|\Psi(t)\rangle$, which is the Schrodinger equation of motion, which will also be used. Next, the Schrodinger equation is divided into two portions, H_1 and H_2 for simplicity in solving the Schrodinger equation.

Equation (4.9) shows H_1 term acting on the quantum system. Using the commutation relation for the annihilation and creation operator in Chapter 2 and,

$$\sigma^+|1\rangle = 0, \ \sigma^+|0\rangle = |1\rangle, \sigma^-|1\rangle = |0\rangle, \sigma^-|0\rangle = 0 \tag{4.8}$$

$$H_1 \left\{ \begin{array}{l} e^{-it\omega_0}\big[a_1(t)|100\rangle_{123} + a_2(t)|010\rangle_{123} + a_3(t)|001\rangle_{123}\big]|\bar{0}\rangle + \\ \sum_j b_j(t)e^{-it(\omega_j+\chi_j)}|000\rangle_{123}|1_j\rangle_c \end{array} \right\} \tag{4.9}$$

75

n is the number of photon released to the cavity field. For $|\bar{0}\rangle$, $n = 0$ and $|1_j\rangle_c$, $n = 1$ because there is no photon that exists for the quantum state $|\bar{0}\rangle$ while one photon is released to the cavity field for the quantum state $|1_j\rangle_c$. Substituting the respective n into the cavity field state, equation (4.9) will result in equation (4.10).

$$\left[\sum_{n=1}^{3}\sum_{j}\begin{pmatrix}\alpha_n\left(g_j\sigma_n^+ a_j + g_j^*\sigma_n^- a_j^t\right)\\+\chi_j n\end{pmatrix}\right]\left\{\begin{aligned}&e^{-it\omega_0}\left[a_1(t)|100\rangle_{123} + a_2(t)|010\rangle_{123} + a_3(t)|001\rangle_{123}\right]|\bar{0}\rangle\\&+\sum_j b_j(t)e^{-it(\omega_j+\chi_j)}|000\rangle_{123}|1_j\rangle_c\end{aligned}\right\}$$

$$=\left[\sum_{n=1}^{3}\sum_{j}\begin{pmatrix}\alpha_n\left(g_j\sigma_n^+ a_j + g_j^*\sigma_n^- a_j^t\right)\\+\chi_j n\end{pmatrix}\right]e^{-it\omega_0}\left[\begin{aligned}&a_1(t)|100\rangle_{123} + a_2(t)|010\rangle_{123} +\\&a_3(t)|001\rangle_{123}\end{aligned}\right]|\bar{0}\rangle +$$

$$\left[\sum_{n=1}^{3}\sum_{j}\left(\alpha_n\left(g_j\sigma_n^+ a_j + g_j^*\sigma_n^- a_j^t\right)+\chi_j n\right)\right]\sum_j b_j(t)e^{-it(\omega_j+\chi_j)}|000\rangle_{123}|1_j\rangle_c$$

Term $g_j\sigma_n^+ a_j$ acting on $\left[\begin{aligned}&a_1(t)|100\rangle_{123} + a_2(t)|010\rangle_{123} +\\&a_3(t)|001\rangle_{123}\end{aligned}\right]|\bar{0}\rangle$ will lead to zero due to the annihilation operator. Then using equation (4.8), the term $g_j^*\sigma_n^- a_j^t$ acting on in equation (4.10) will become zero which can be ignored. In the end, equation (4.10) evolves, as shown in equation (4.11).

$$\left[\sum_{n=1}^{3}\sum_{j}\left(\alpha_n\left(g_j\sigma_n^+ a_j + g_j^*\sigma_n^- a_j^t\right)\right)\right]e^{-it\omega_0}\left[\begin{aligned}&a_1(t)|100\rangle_{123} + a_2(t)|010\rangle_{123} +\\&a_3(t)|001\rangle_{123}\end{aligned}\right]|\bar{0}\rangle +$$

$$\left[\sum_{n=1}^{3}\sum_{j}\left(\alpha_n\left(g_j\sigma_n^+ a_j + g_j^*\sigma_n^- a_j^t\right)+\chi_j\right)\right]\sum_j b_j(t)e^{-it(\omega_j+\chi_j)}|000\rangle_{123}|1_j\rangle_c$$

(4.10)

$$\left[\alpha_n g_j^*\sum_{n=1}^{3}a_n(t)+\sum_j\chi_j b_j(t)e^{-it(\omega_j+\chi_j)}\right]|000\rangle_{123}|1_j\rangle_c +$$

$$\sum_j g_j b_j(t)e^{-it(\omega_j+\chi_j)}\left(\alpha_1|100\rangle_{123} + \alpha_2|010\rangle_{123} + \alpha_3|001\rangle_{123}\right)|\bar{0}\rangle$$

(4.11)

Next will be the term for the three-qubit quantum state acting on the phase state. In this case term $\sum_j b_j(t)e^{-it(\omega_j+\chi_j)}|000\rangle_{123}|1_j\rangle_c$ will be zero since no W state exists, as shown in equation (4.14). Using equation (4.8) to expand equation (4.12), (4.13), and (4.14), this results in equation (4.15).

$$
e^{-it\omega_0}H_2|W(0)\rangle = \left[D_1\left(\sigma_2^+\sigma_3^- + \sigma_3^+\sigma_2^-\right) + D_2\left(\sigma_3^+\sigma_1^- + \sigma_1^+\sigma_3^-\right) + D_3\left(\sigma_1^+\sigma_2^- + \sigma_2^+\sigma_1^-\right)\right]\times
$$
$$
\left\{e^{-it\omega_0}\left[a_1(t)|100\rangle_{123} + a_2(t)|010\rangle_{123} + a_3(t)|001\rangle_{123}\right]|\bar{0}\rangle\right\} \tag{4.12}
$$

$$
e^{-it\omega_0}H_2|W(0)\rangle = e^{-it\omega_0}\begin{pmatrix} a_1(t)D_2|001\rangle_{123} + a_1(t)D_3|010\rangle_{123} + a_2(t)D_1|001\rangle_{123} + \\ a_2(t)D_3|100\rangle_{123} + a_3(t)D_1|010\rangle_{123} + a_3(t)D_2|100\rangle_{123} \end{pmatrix}|\bar{0}\rangle \tag{4.13}
$$

$$
H_2|\Psi(t)\rangle = e^{-it\omega_0}H_2|W(0)\rangle + \begin{bmatrix} D_1\left(\sigma_2^+\sigma_3^- + \sigma_3^+\sigma_2^-\right) + D_2\left(\sigma_3^+\sigma_1^- + \sigma_1^+\sigma_3^-\right) + \\ D_3\left(\sigma_1^+\sigma_2^- + \sigma_2^+\sigma_1^-\right) \end{bmatrix}\times
$$
$$
\left(\sum_j b_j(t)\exp(-i\omega_j t)|000\rangle\right)|1_j\rangle_c \tag{4.14}
$$

$$
H_2|\Psi(t)\rangle = e^{-it\omega_0}\begin{pmatrix} a_1(t)D_2|001\rangle_{123} + a_1(t)D_3|010\rangle_{123} + a_2(t)D_1|001\rangle_{123} + \\ a_2(t)D_3|100\rangle_{123} + a_3(t)D_1|010\rangle_{123} + a_3(t)D_2|100\rangle_{123} \end{pmatrix}|\bar{0}\rangle \tag{4.15}
$$

With equation (4.11) and (4.15), the Schrodinger equation for the respective time coefficient becomes equation (4.16), (4.17), (4.18), and (4.19).

$$
e^{-i\omega_0 t}\frac{ida_1(t)}{dt} = \sum_j e^{-it(\omega_j+\chi_j)}\alpha_1 g_j b_j(t) + e^{-i\omega_0 t}D_3 a_2(t) + e^{-i\omega_0 t}D_2 a_3(t)
$$
$$
\frac{ida_1(t)}{dt} = \sum_j e^{-i(\omega_j-\omega_0+\chi_j)t}\alpha_1 g_j b_j(t) + D_3 a_2(t) + D_2 a_3(t)
$$

$$
\frac{ida_1(t)}{dt} = \alpha_1\sum_j e^{-i(\omega_j-\omega_0+\chi_j)t} g_j b_j(t) + D_3 a_2(t) + D_2 a_3(t) \tag{4.16}
$$

$$
\frac{ida_2(t)}{dt} = \alpha_2\sum_j e^{-i(\omega_j-\omega_0+\chi_j)t} g_j b_j(t) + D_3 a_1(t) + D_1 a_3(t) \tag{4.17}
$$

$$\frac{ida_3(t)}{dt} = \alpha_3 \sum_j e^{-i(\omega_j - \omega_0 + \chi_j)t} g_j b_j(t) + D_2 a_1(t) + D_1 a_2(t) \tag{4.18}$$

When t becomes large, $e^{-i\omega_j t}$ the term $\sum_j \chi_j b_j(t) e^{-i\omega_j t}$ becomes smaller. The value

of this term asymptotically goes to zero. Hence, equation (4.19) will become zero which

will be substituted into equation (4.20),

$$e^{-i(\omega_j + \chi)t} \frac{idb_j(t)}{dt} = e^{-i\omega_0 t} \alpha_n g_j^* \sum_{n=1}^{3} a_n(t) + \sum_j \chi_j b_j(t) e^{-i\omega_j t}$$

$$\sum_j \chi_j b_j(t) e^{-i\omega_j t} = 0 \tag{4.19}$$

$$\frac{idb_j(t)}{dt} = e^{-i(\omega_0 - \omega_j - \chi)t} \alpha_n g_j^* \sum_{n=1}^{3} a_n(t) + \sum_j \chi_j b_j(t) e^{-i\chi t} \tag{4.20}$$

Integrating $b_j(t)$ in equation (4.20) with the initial condition of $b_j(t) = 0$ will produce,

$$b_j(t) = -i \int_0^t e^{-i(\omega_0 - \omega_j - \chi)t'} g_j^* \sum_{n=1}^{3} \alpha_n a_n(t) dt' \tag{4.21}$$

Substituting equation (4.21) into equation (4.16)-(4.18) gives,

$$\frac{da_1(t)}{dt} = -\alpha_1 \int_0^t dt' \left[\sum_j |g_j|^2 e^{-i[(\omega_j - \omega_0)(t - t') + \chi(t' - t)]} \times \sum_{n=1}^{3} \alpha_n a_n(t') \right] - iD_3 a_1(t) - iD_1 a_3(t) \tag{4.22}$$

$$\frac{da_2(t)}{dt} = -\alpha_2 \int_0^t dt' \left[\sum_j |g_j|^2 e^{-i[(\omega_j - \omega_0)(t - t') + \chi(t' - t)]} \times \sum_{n=1}^{3} \alpha_n a_n(t') \right] - iD_3 a_1(t) - iD_1 a_3(t) \tag{4.23}$$

$$\frac{da_3(t)}{dt} = -\alpha_3 \int_0^t dt' \left[\sum_j |g_j|^2 e^{-i[(\omega_j - \omega_0)(t - t') + \chi(t' - t)]} \times \sum_{n=1}^{3} \alpha_n a_n(t') \right] - iD_2 a_1(t) - iD_1 a_2(t) \tag{4.24}$$

78

$\sum_j \left| g_j \right|^2 e^{-i\left[(\omega_j - \omega_0)(t-t') + \chi(t'-t) \right]}$ will be substituted and become $\int d\omega J(\omega) e^{-i\left[(\omega_j - \omega_0)(t-t') + \chi(t'-t) \right]}$

where $J(\omega)$ is the spectral density of a cavity structure. Substituting this into equation (4.22)-(4.24) will get,

$$\frac{da_1(t)}{dt} = -\alpha_1 \int_0^t dt' \left[\left(\sum_{n=1}^3 \alpha_n a_n(t') \int d\omega J(\omega) e^{-i\left[(\omega_j - \omega_0)(t-t') + \chi(t'-t) \right]} \right) \right] - iD_3 a_2(t) - iD_2 a_3(t) \quad (4.25)$$

$$\frac{da_2(t)}{dt} = -\alpha_2 \int_0^t dt' \left[\left(\sum_{n=1}^3 \alpha_n a_n(t') \int d\omega J(\omega) e^{-i\left[(\omega_j - \omega_0)(t-t') + \chi(t'-t) \right]} \right) \right] - iD_3 a_1(t) - iD_1 a_3(t) \quad (4.26)$$

$$\frac{da_3(t)}{dt} = -\alpha_3 \int_0^t dt' \left[\left(\sum_{n=1}^3 \alpha_n a_n(t') \int d\omega J(\omega) e^{-i\left[(\omega_j - \omega_0)(t-t') + \chi(t'-t) \right]} \right) \right] - iD_2 a_1(t) - iD_1 a_2(t) \quad (4.27)$$

From the spectral density of cavity field which used to represent the photon leak to the environment shown in equation (4.28). This equation is called Lorentzian broadening (Weisstein, 2002).

$$J(\omega) = \frac{R^2}{\pi} \frac{\Gamma}{(\omega - \omega_c)^2 + \Gamma^2} \quad (4.28)$$

A cavity supported mode is represented by ω_c and Γ is the half width at half height of the field spectrum profile inside the cavity. Besides, R is the atom-cavity coupling strength and T_c is the cavity correlation time with $T_c = \Gamma^{-1}$. Other than cavity correlation time, the qubit relaxation time will be $T_q = \left(2R\sqrt{\alpha_1^2 + \alpha_2^2 + \alpha_3^2} \right)^{-1}$. The cavity correlation time and the qubit relaxation time are used to determine whether the environment is a Markovian or non-Markorian, which represents a weak and strong environment, respectively. A

Markovian mean is when $T_c < T_q$ while a non-Markovian is when $T_c > T_q$ (Breuer et al., 2009).

Next, based on equations (4.25)-(4.27) the Laplace transformation is taken from both sides of the equations to produce a set of equations for $\{\tilde{a}_n = (z); n = 1,2,3\}$. The Laplace transformation will transform the equations into a complex argument of z where z represents a pole in Lorenztian broadening. The notation is $\tilde{f}(z) = L[f(\tau)] = \int_0^\infty f(\tau)e^{-z\tau}d\tau$ (Douglas et al., 2012). The set of equation is as follows:

$$\tilde{a}_n(z) = \frac{\sum_{m=1}^{3} A_{nm}(z)a_m(0)}{\sum_{m=0}^{4} B_m z^m} \tag{4.29}$$

where $l,m,n \in \{1,2,3\}$ with condition $l \neq m \neq n \neq l$

$$A_{nn}(z) = \left(z^2 + d_n^2\right)\left(z + 1 + i(\delta - K)\right) + \frac{G^2}{4}\left[\left(1 - r_n^2\right)z - 2id_n r_l r_m\right]$$

$$A_{nm}(z) = A_{mn}(z) = -\left(z + 1 + i(\delta - K)\right)\left(d_m d_n + izd_l\right) + \frac{iG^2}{4}\left[d_m r_m + d_n r_n - d_l r_l - ir_m r_n z\right]$$

and

$$B_0 = \frac{G_2}{4}\left[d_1^2 r_1^2 + d_2^2 r_2^2 + d_3^2 r_3^2 - 2\left(d_1 d_2 r_1 r_2 + d_1 d_3 r_1 r_3 + d_2 d_3 r_2 r_3\right)\right] -$$

$$2id_1 d_2 d_3\left(1 + i(\delta - K)\right)$$

$$B_1 = -\frac{iG_2}{4}\left(d_1 r_1 r_2 + d_2 r_3 r_1 + d_3 r_2 r_1\right) + \left(d_1^2 + d_2^2 + d_3^2\right)\left(1 + i(\delta - K)\right) - 2id_1 d_2 d_3$$

$$B_2 = -\frac{G_2}{4} + d_1^2 + d_2^2 + d_3^2, B_3 = 1 + i(\delta - K), B_4 = 1$$

For convenience, dimensionless quantities are introduced based on above equation,

$$d_l = \frac{D_l}{\Gamma} , \; \delta = \frac{\omega_c - \omega_0}{\Gamma} , \; \beta = \sqrt{\sum_{n=1}^{3} \alpha_n^2} , \; r_n = \frac{\alpha_n}{\alpha} , \; G = \frac{2R\alpha}{\Gamma} , K = \frac{\chi}{\Gamma} \qquad (4.30)$$

by definition $\sum_{n=1}^{3} r_n^2 = 1$. Applying the inverse Laplace transform will get the time-dependent coefficient.

$$a_n(\tau) = \sum_j \lim_{z \to z_j} (z - z_j) \tilde{a}_n(z) e^{z_j \tau} \qquad (4.31)$$

$\tau = \Gamma t$ and z_j are a pole of $\tilde{a}_n(z)$. Using the residue theory let $\sum_{m=0}^{4} B_m z^m = 0$, which will produce a value of z_j which is needed for the measurement of the quantum entanglement.

A single-photon collective normalized state of the cavity field is represented as

$$\left| \overline{1} \right\rangle = \frac{e^{i\omega_c \chi t}}{b(\tau)} \sum_j b_j(\tau) e^{-i\omega_j \chi t} \left| 1_j \right\rangle_c ,$$

for

$$b(\tau) = \sqrt{1 - \sum_{n=1}^{3} |a_n(\tau)|^2} \qquad (4.32)$$

The total state of the system developed in this study after obtaining the time-dependent coefficient will be

$$\left| \psi(\tau) \right\rangle = e^{-i(\overline{\omega}_0 + K)\tau} \left[a_1(\tau) \left| 100 \right\rangle_{123} + a_2(\tau) \left| 010 \right\rangle_{123} + a_3(\tau) \left| 001 \right\rangle_{123} \right] \left| \overline{0} \right\rangle + e^{-i(\overline{\omega}_c + K)\tau} b(\tau) \left| 000 \right\rangle_{123} \left| \overline{1} \right\rangle \qquad (4.33)$$

with $\overline{\omega}_0 = \frac{\omega_0}{\Gamma}$ and $\overline{\omega}_c = \frac{\omega_c}{\Gamma}$.

4.3 Measurement for Three-Qubit System

After the development of a three-qubit quantum system model with coupling to a Kerr-like medium, this section measures the time-dependent coefficients to study the quantum entanglement. The time-dependent coefficients in equation (4.31) are used to measure the tripartite entanglement of the quantum system. In measuring the entanglement there are a few conditions that need to be met, which were explained in Section 2.5.1. The quantification of the quantum system needs to be done to measure the entanglement.

Initially the quantum system was in a separable state between the qubit, $|W(0)\rangle$ and the empty field. The coefficient, $a_n(0)$ of the qubit is a non-zero value, which means that initially the entanglement already existed. Then, over time the qubit and the cavity field will be interacting with each other which will change the entanglement properties. This change is also transforming the quantum state from the pure to the mixed state. In measuring the entanglement and its changes, a concurrence of a three-qubit quantum state is used, which was explained in Chapter 2.

When the qubit and the cavity field start to interact with each other the quantum state of the qubit will change from the pure state to the mixed state, explained in the previous paragraph. This is shown in equation (4.34) and (4.35) (An et al., 2011).

$$|W(0)\rangle \Rightarrow \rho(\tau) = Tr_{cavity} |\psi(\tau)\rangle\langle\psi(\tau)| \tag{4.34}$$

$$\rho(\tau) = |W(\tau)\rangle_{123123}\langle W(\tau)| + |b(\tau)|^2 |000\rangle_{123123}\langle 000| \tag{4.35}$$

In this case the concurrence will be included to the mixed state by using the convex roof construction (Li et. al, 2008),

$$C_3 = \min_{[p_j, \Psi_j]} \sum_j p_j C_3\left(|\Psi_j\rangle\right) \tag{4.36}$$

where $|\Psi_j\rangle$ is the quantum state of the qubit which includes both the mixed and the pure state and p_j is the probability of the quantum state with $p_j > 0$ and $\sum_j p_j = 1$. Besides that, $C_3\left(|\Psi_j\rangle\right)$ is the concurrence for all possible decomposition density matrices, $\rho = \sum_i p_i |\psi_i\rangle\langle\psi_i|$.

In this study the concurrence used is the lower bound concurrence which is on linear entropy. A lower bound concurrence (LBC) uses a bipartite entanglement to calculate the overall entanglement. A bipartite entanglement consists of two qubits being entangled, with one qubit entangling with another qubit, as explained in Chapter 2's two partial positive transpose. The expression for the LBC is

$$\underline{C}_3(\rho) = \sqrt{\frac{1}{3}\sum_{j=1}^{6}\left\{\left[C_j^{12|3}(\rho)\right]^2 + \left[C_j^{23|1}(\rho)\right]^2 + \left[C_j^{31|2}(\rho)\right]^2\right\}} \tag{4.37}$$

for

$$C_j^{mn|l}(\rho) = max\left\{0, \sqrt{\lambda_{j,1}^{mn|l}} - \sum_{q>1}\sqrt{\lambda_{j,q}^{mn|l}}\right\} \qquad (4.38)$$

where $\lambda_{j,1}^{mn|l}$ is the eigenvalues in a decreasing order for matrix

$$\tilde{\rho} = \rho\left(L_j^{mn} \otimes \sigma_y^l\right)\rho^*\left(L_j^{mn} \otimes \sigma_y^l\right),$$

L_j^{mn} for $j = 1,2,...,6$ is the generator of orthogonal group $SO(4)$ which acts on qubits m, n, and σ_y^l. $SO(4)$ is the rotation about a fixed point in four-dimensional Euclidean space.

σ_y^l is the Pauli matrix acting on qubit l (An et al., 2011). A concurrence measurement indicates the higher the value of concurrence, $\underline{C}_3(\rho) > 0$. The stronger the entanglement will be when the concurrence approaches zero. In this case the quantum system model represents rank 4, which coincides between LBC and the convex roof for rank less than 4. The LBC is shown in equation (4.39).

$$\underline{C}_3(\rho(\tau)) = \sqrt{\frac{8}{3}\sum_{m,n;m<n}^{3}\left|a_m(\tau)a_n(\tau)\right|^2} \qquad (4.39)$$

4.4 Quantum System Entanglement in Kerr-like Medium

A quantum entanglement is discussed in this section. The value of the LBC is produced by using Mathematica software based on the measurement equation (4.39) and the programming language used is shown in Appendix B. This section is divided into two areas: the first one will be the study of a tripartite entanglement, and the second one is the study of quantum entanglement between a cavity field and a three-qubit quantum state. Different values in the dipole-dipole interaction and Kerr-like medium coupling are

considered to observe the quantum entanglement robustness. The cavity field environment will be divided into a non-Markovian and Markavian environment.

4.4.1 Three-Qubit Entanglment

This section analyzes the entanglement of a three-qubit quantum system in influencing the Kerr-like medium under the environment of non-Markovian, $G = 8.0$ and Markovian, $G = 0.8$. The quantum entanglement is measured via LBC with $\delta = -1$, $r_1 = \dfrac{1}{\sqrt{2}}$, $r_2 = \dfrac{1}{\sqrt{3}}$, $r_3 = \dfrac{1}{\sqrt{6}}$, $a_1(0) = a_2(0) = \dfrac{1}{2}$ and $a_3(0) = \dfrac{1}{\sqrt{2}}$. LBC will have a value from zero to one, with one having the most robust quantum entanglement and vice versa. The value of r_n is chosen with a combination of value $a_n(0)$ to achieve a robust entanglement (An et al., 2011), while the value of $a_n(0)$ is used based on the quantum state in quantum teleportation (Agrawal et al., 2006). For a dipole-dipole interaction, d will vary as shown in Figure 4.1e and Figure 4.2e and several Kerr-like medium coupling strength is used to analyze the effect of the quantum entanglement of the three-qubit quantum system. The value of pole, z_j will vary according to the different values of the Kerr-like medium and the dipole-dipole interaction which contain three negative real numbers and a complex value, shown in Appendix C and D, except for a zero dipole-dipole interaction where z_j consists of only two poles, as shown in Table 4.1 and 4.2. Both Table 4.1 and Table 4.2 are extracted from Appendix C and D.

85

Table 4.1

Values of Poles for No Dipole-dipole Interaction, $d = 0$ and $G = 0.8$ with Different

Kerr-like Medium Coupling Strength

K	z_j
0.000	*0.000*
0.000	*-0.0728 -0.0852 i*
0.000	*-0.9272 + 1.0852 i*
0.0100	*0.000*
0.0100	*-0.0721 -0.0850 i*
0.0100	*-0.9279 + 1.0950 i*
0.1000	*0.000*
0.1000	*-0.0658 -0.0833 i*
0.1000	*-0.9342 + 1.1833 i*
2.5000	*0.000*
2.5000	*-0.0117 -0.0419 i*
2.5000	*-0.9883 + 3.5419 i*
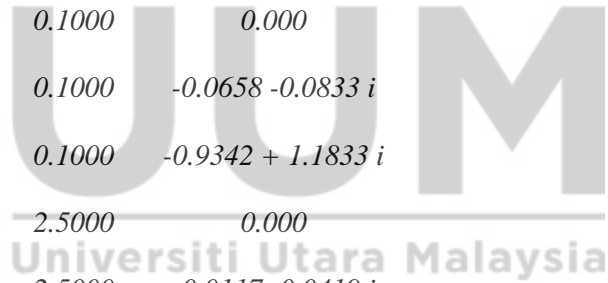
Table 4.2

Values of Poles for No Dipole-dipole Interaction, $d = 0$ and $G = 8.0$ with Different

Kerr-like Medium Coupling Strength

K	z_j
0.000	0.000
0.000	-0.4375 -3.5005 i
0.000	-0.5625 + 4.5005 i
0.010	0.000
0.010	-0.4369 -3.4961 i
0.010	-0.5631 + 4.5061 i
1.000	0.000
1.000	-0.3779 -3.0945 i
1.000	-0.6221 + 5.0945 i
3.000	0.000
3.000	-0.2753 -2.4498 i
3.000	-0.7247 + 6.4498 i
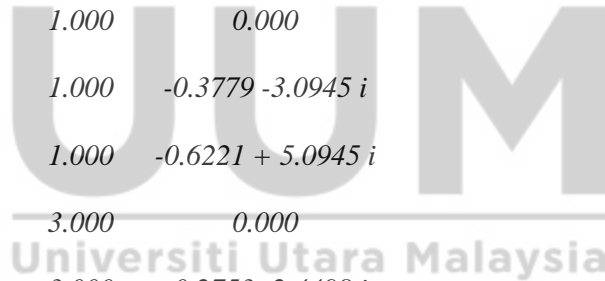
Figure 4.1 shows the entanglement strength for various dipole-dipole interactions and different Kerr-like medium coupling strength. Figure 4.1a shows that when there is no Kerr-like medium coupling, *d* increases the quantum entanglement, which becomes more robust and stable (An et al., 2011).

87

The quantum entanglement is shown in Figure 4.1b and 4.1c when the Kerr-like medium coupling strength is weak and the LBC shows that quantum entanglement is identical to each other. A slight increase in Kerr-like medium coupling does not seem to influence the quantum entanglement. For example, under $d = 0.5$ the value for one of the poles is shown in Table 4.3. It seems that the change of the poles is less than *0.0006* on average for the real and the imaginary part. The small change has caused the LBC to be identical.

Table 4.3

Values of Poles for $G = 0.8$, $d = 0.5$ and Different Values of K
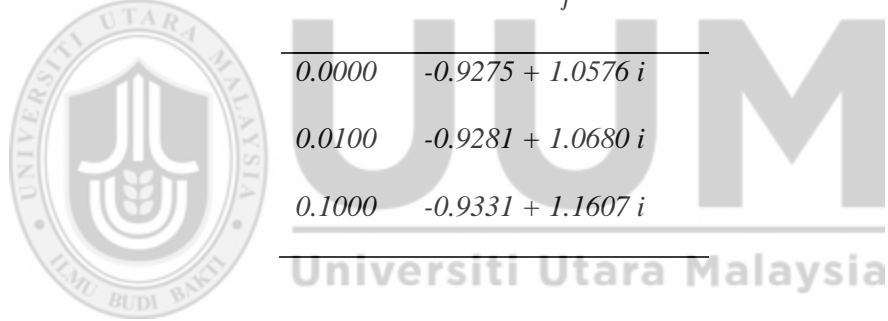
K	z_j
0.0000	-0.9275 + 1.0576 i
0.0100	-0.9281 + 1.0680 i
0.1000	-0.9331 + 1.1607 i

However, when there is strong Kerr-like medium coupling, a change in the quantum entanglement is observed (see Figure 4.1d). In the beginning when there is a dipole-dipole interaction the quantum entanglement strength is in the same range except for *d=0.5* where it seems to be above the other dipole-dipole interaction strength around. As usual for *d=0.0* the LBC is at the lowest in comparison with other *d*. As the time goes further decoherence occurs. It is also showed that a strong dipole-dipole interaction decay slower compared to other lower *d*.
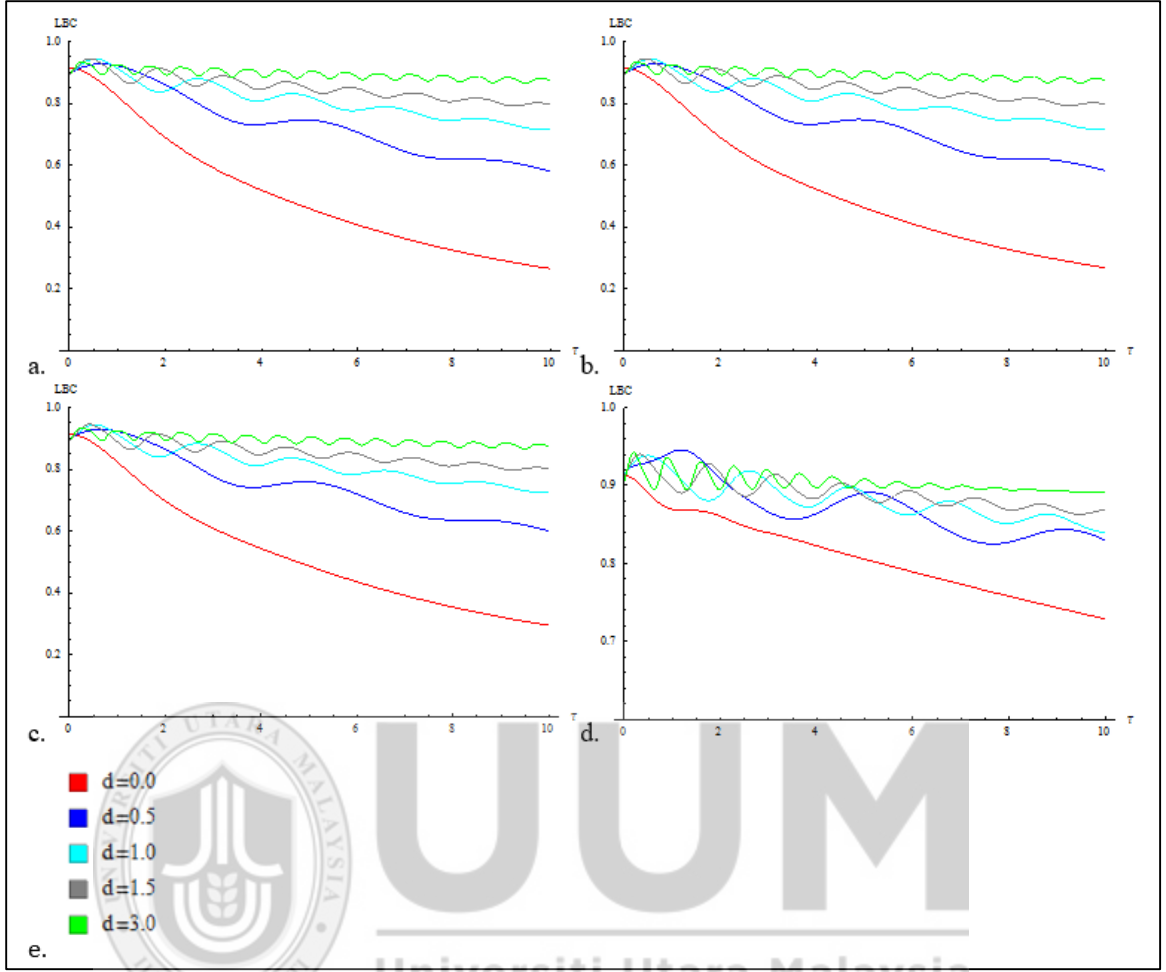
Figure 4.1. Lower Bound Concurrence (LBC) $G = 0.8$, various d as shown in e. and a. $K = 0.00$, b. $K = 0.01$, c. $K = 0.10$, d. $K = 2.50$. Time scale, $1 \leq \tau \leq 10$

When comparing the various Kerr-like medium coupling strength, the quantum entanglement for $d = 0$ and strong Kerr-like medium coupling, it is showed that the decoherence increases at $\tau > 2$. When Figure 4.1a, Figure 4.1b, and Figure 4.1c are compared with Figure 4.1d, the decoherence rate is slower, which produces a more robust quantum entanglement. This is also true for other dipole-dipole interactions except for $d = 3.0$. $d = 3.0$ shows that the decoherence rate is faster (compare Figure 4.1d with Figure

4.1a, Figure 4.1b, and Figure 4.1c). Besides, the fluctuation in Figure 4.1d is reduced when

τ increases and then decreases linearly (compare with Figure 4.1a, Figure 4.1b, and Figure

4.1c). This tells us that an increase in the Kerr-like medium reduces the quantum

entanglement robustness for a strong dipole-dipole interaction, $d = 3.0$. At the right d and

strong K the decoherence rate is reduced, which shows a robust quantum entanglement (An

et al., 2011).

Figure 4.2 shows the quantum entanglement robustness for various Kerr-like

medium coupling and dipole-dipole interactions in a non-Markovian environment. Figure

4.2a shows that where no Kerr-like medium coupling exists, a stronger dipole-dipole

interaction leads to a robust quantum entanglement. The fluctuation, which is a small wave

like pattern, also increases for strong a dipole-dipole interaction. The wave like pattern

fluctuates in the same manner for $d = 15.0$ and in the least decoherence rate. Hence, the

quantum entanglement is most robust at the strong dipole-dipole interaction.

As the Kerr-like medium coupling slightly increases to $K = 0.01$ (see Figure 4.2b),

the quantum entanglement behaviour still shows an identical pattern as in Figure 4.2a.

When the Kerr-like medium coupling strength further increases to become $K = 1.00$,

Figure 4.2c shows this has caused slight changes in $d = 9.0$ where at $\tau < 0.5$ there is a drop

in the LBC before it increases back. This means that the quantum entanglement shows

decoherence due to the effect of the Kerr-like medium coupling, but at $\tau \approx 0.55$ the LBC

increases back which is identical to Figure 4.2a and 4.2b. For a strong Kerr-like medium

coupling, $K = 3.00$, some changes are shown in Figure 4.2d where the minimum level of

the LBC increases in comparison when $K < 3.00$. For example, for $d = 3.0$ and $K = 1.00$ (see Figure 4.2c) and $d = 3.0$ and $K = 3.00$ (see Figure 4.2d) at $\tau \approx 0.5$, there is a drop in the LBC, which leads to an increase in decoherence. When these two are compared, the drop in Figure 4.2d is lesser than that in Figure 4.2c, which tells us that the Kerr-like medium coupling is able to increase the quantum entanglement robustness. However, as d becomes stronger, the fluctuation pattern becomes the same, except when $\tau < 0.5$ and $d = 0$. In this case, some differences in the fluctuation pattern can be observed. Hence, in the non-Markovian environment, only when $K > 0.01$ the impact on the quantum entanglement is strong when the Kerr-like medium reduces the decoherence rate under $d < 9.0$. For $d = 15.0$ the LBC is the same for all where Figure 4.2 shows the highest quantum entanglement robustness. Overall, a strong dipole-dipole interaction reduces the impact of the Kerr-like medium on the quantum entanglement.
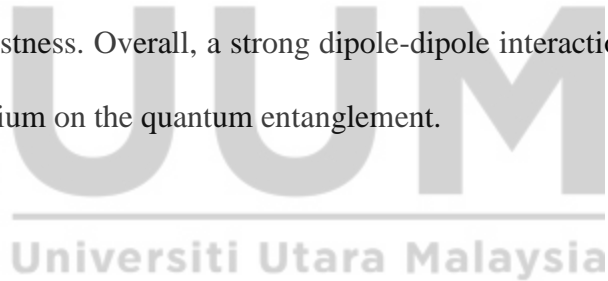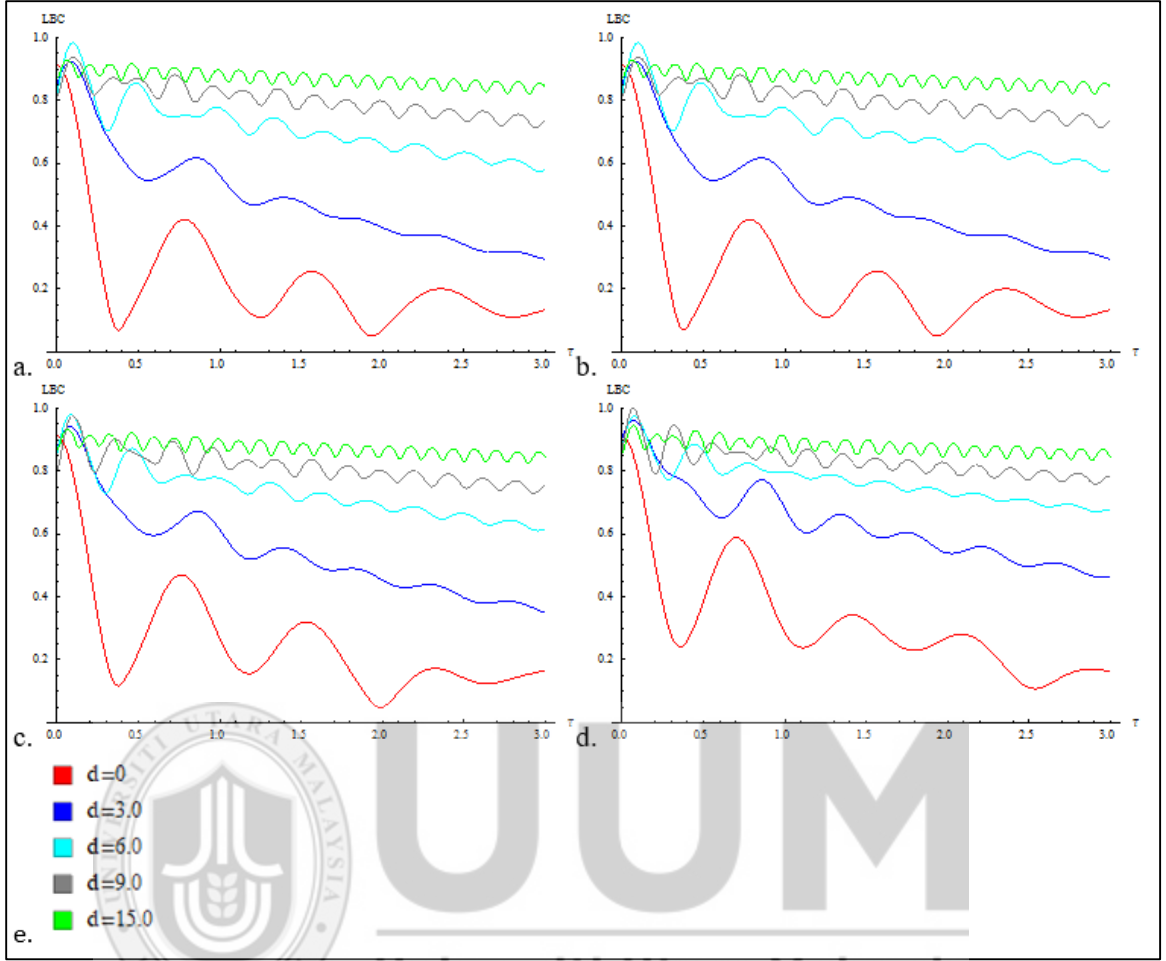
Figure 4.2. Lower Bound Concurrence (LBC) for $G = 8.0$, various d as shown in e. and a. $K = 0.00$, b. $K = 0.01$, c. $K = 1.00$, d. $K = 3.00$. Time scale, $1 \leq \tau \leq 3$

Hence, a strong Kerr-like medium coupling will only change the quantum entanglement strength of three qubits. Besides, the quantum entanglement robustness is shown to have been less influenced by the Kerr-like medium in the Markovian environment and also when the dipole-dipole interaction is strong. When compared to the non-Markovian environment, there is a huge change in the quantum entanglement robustness when the Kerr-like medium coupling is strong enough. However, quantum entanglement

92

showed the same results where the strong dipole-dipole coupling reduces the influence of the quantum entanglement by the Kerr-like medium. The Markovian environment contains a more robust quantum entanglement than the non-Markovian environment because the coupling between the qubits and the cavity field has disrupted the tripartite quantum entanglement system.

4.4.2 Positive Detuning Frequency

This section discusses the quantum entanglement when detuning frequency is positive. The value for different parameters under positive detuning is displayed in Appendix E and F. Positive detuning has shown a different behaviour on the quantum entanglement behaviour from Section 4.4.2 where an in increase in the dipole-dipole interaction no longer produces a robust quantum entanglement.
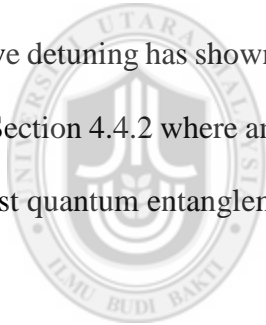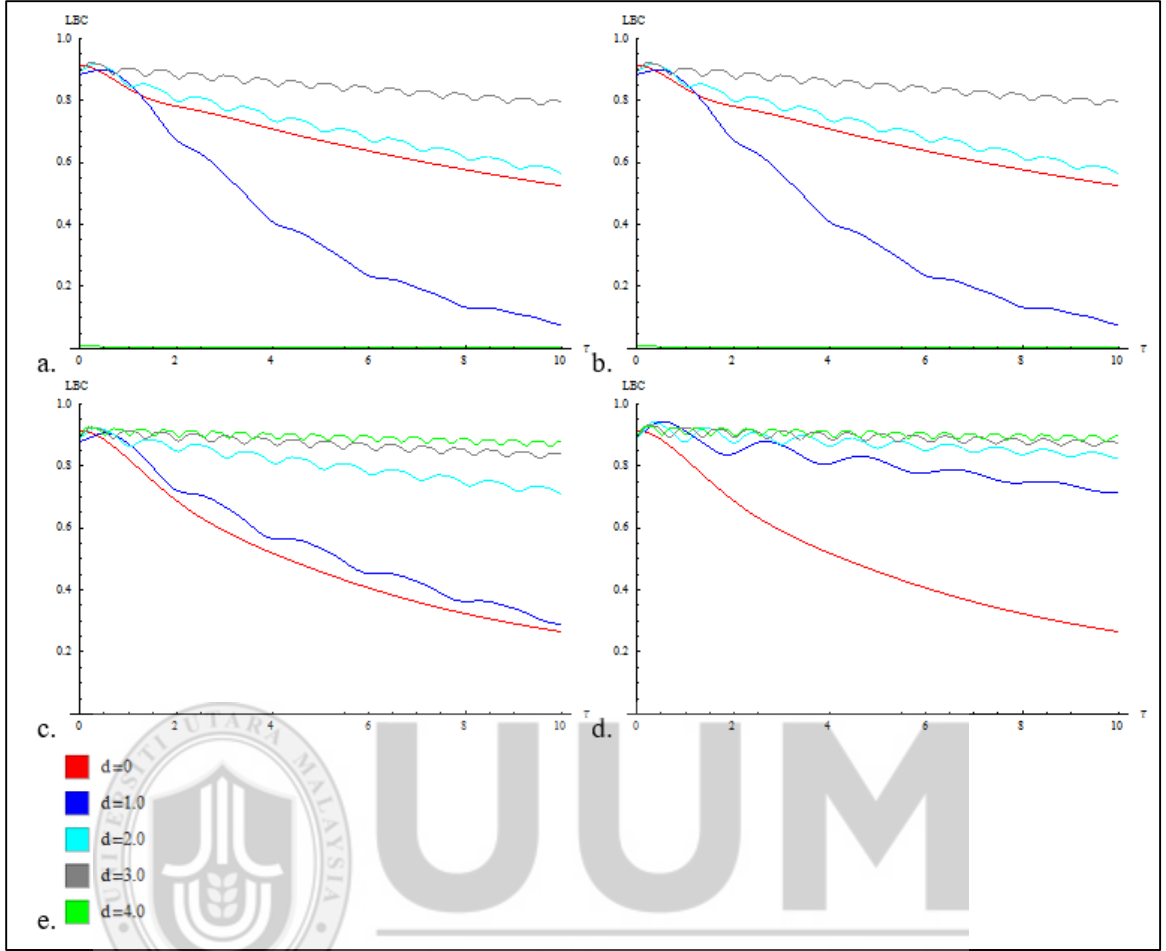
Figure 4.3. Lower Bound Concurrence (LBC) for $\delta = 2.0$ and $G = 0.8$, various d as shown in e. and a. $K = 0.00$, b. $K = 0.01$, c. $K = 1.00$, d. $K = 3.00$. Time scale, $1 \leq \tau \leq 10$

Figure 4.3 shows the LBC in the Markovian environment with a different value of d and K. In Figure 4.3a and 4.3b, the pattern is no longer observed where a stronger d leads to a robust quantum entanglement, as shown in Section 4.2.1. Instead, the LBC shows that the decoherence rate is random for the strong and weak dipole-dipole interaction. After the change of $\delta = 2.0$, the initial increase in $d = 1.0$ reduced the robustness of the quantum

entanglement, but once $4.0 > d \geq 1.0$ the robustness increases back in a lesser rate of decoherence. Then when $d = 4.0$ the quantum state is close to the separable state with the LBC near zero, with an average LBC value of *0.0058 for both $K = 0.00$ and $K = 0.01$,* respectively (see Table 4.4).

Table 4.4

Value of LBC for Different K and τ

τ	$K > 0.01$	$K = 0.01$
0	0.0068	0.0068
1	0.0066	0.0066
2	0.0063	0.0063
3	0.0062	0.0062
4	0.0060	0.0060
5	0.0058	0.0058
6	0.0056	0.0056
7	0.0055	0.0055
8	0.0053	0.0053
9	0.0052	0.0052
10	0.0050	0.0050

Both Figure 4.3a and Figure 4.3b produce the same pattern of output and quantum entanglement strength, which tells us that a weak Kerr-like medium coupling does not have

a big influence on the entanglement. As shown in Table 4.5 the poles changes only in a small value when K increases from *0.00 to 0.01*.

Table 4.5

Value of Poles Changes Slightly for Weak Kerr-like Medium

K	d	z_j
0.0000	1.0000	- 0.8600 + 2.0096 i
0.0000	1.0000	- 0.1390 + 1.9985 i
0.0000	1.0000	-0.0209 + 1.1285 i
0.0100	1.0000	- 0.8600 + 1.9977 i
0.0100	1.0000	- 0.1390 + 2.0004 i
0.0100	1.0000	-0.0210 + 1.1287 i

when $K > 0.01$, Figure 4.3c and 4.3d indicate that the entanglement shows a pattern where an increase in d leads to an increase in the quantum entanglement robustness. An increase in the Kerr-like medium coupling from $K = 1.00$ to $K = 3.00$ increases the robustness for $d > 0.0$. Initially at $d = 0.0$ the same rate of decoherence was observed (see Figure 4.3c and Figure 4.3d). However, when $d > 0.0$ there is an increase in the entanglement robustness with a lesser decoherence rate (compare Figure 4.3d with Figure 4.3c). Figure 4.3d shows that for $d > 0.0$ the line is getting closer together. Figure 4.3d also shows a more robust quantum entanglement than $K < 0.01$.

96
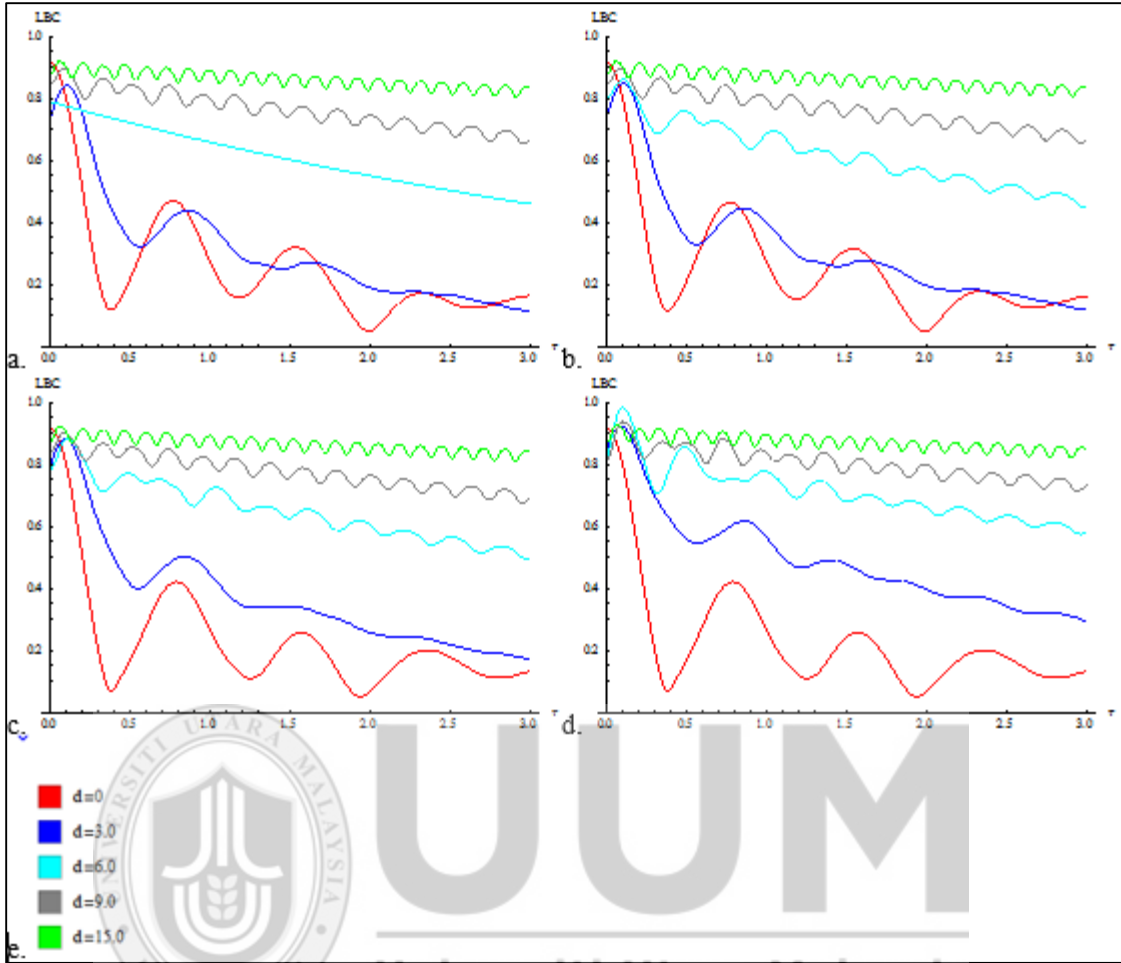
Figure 4.4. Lower Bound Concurrence (LBC) for $\delta = 2.0$ and $G = 8.0$, various d as shown in e. and a. $K = 0.00$, b. $K = 0.10$, c. $K = 1.00$, d. $K = 3.00$. Time scale, $1 \leq \tau \leq 3.0$

Figure 4.4 shows the LBC in the function of τ, which in this case will be in the non-Markovian environment. The result showed that there are 6 points where the LBC for $d = 0.0$ and $d = 3.0$ crossed with each other (see Figure 4.4a and 4.4b). The result also showed that an increase from $K = 0.0$ to $K = 0.1$ increases the amplitude with an average difference of *0.063* from $d = 0.0$ to $d = 3.0$. An increase in the Kerr-like medium coupling

97

helps improve the quantum entanglement and reduces the random affect of positive detuning in this case. When $d > 6.0$, Figure 4.4a and Figure 4.4b show that the quantum entanglement is more robust with a huge increase, but Figure 4.4b has more waves than Figure 4.4a for $d = 6.0$, which indicates some instability to the entanglement. When K is further increased the cross, as shown in Figure 4.4c and 4.4d, disappears and it is followed by an increase in the quantum entanglement robustness with an increase in d, as shown in Figure 4.4c and Figure 4.4d. For $d = 0.0$, both Figure 4.4c and Figure 4.4d show the same pattern and the difference is close to zero. Table 4.6 shows that the value of z_j is the same for both $K = 1.00$ and $K = 3.00$ for $d = 0.0$. Then, when $d > 0.0$, the quantum entanglement becomes stronger for $K = 3.00$ than for $K \leq 1.00$. When d reaches 9.0 the differences between Figure 4.4c and 4.4d become lesser with an average deviation of 0.01 for $d = 15.0$.
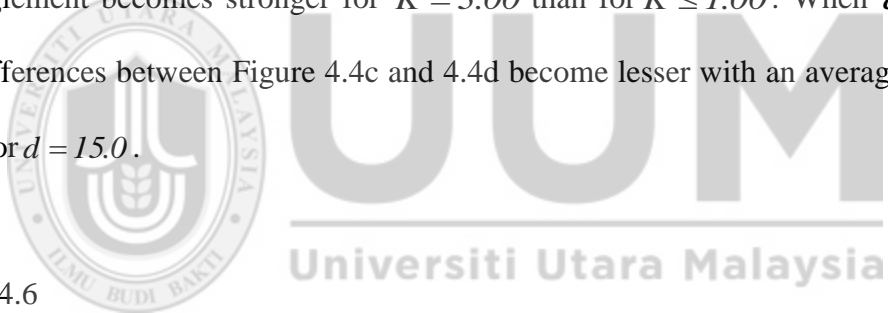
Table 4.6

Value of Poles for K 3.000 and K 1.000 under d 0.000

K	z_j
1.00	- 0.5625 + 4.5005 i
1.00	-0.4375 + 3.5005 i
1.00	0.0000
3.00	0.0000
3.00	-0.5625 + 4.5005 i
3.00	- 0.4375 + 3.5005 i

Next, δ is increased to *10.0,* which shows a random LBC for a different value of d (see Figure 4.5). When compared with Figure 4.3 where the randomness only applies to low K, Figure 4.5 shows that the strength of K only improves the entanglement robustness for certain dipole-dipole interaction strength. As usual, a weak Kerr-like medium coupling (see Figure 4.5a and 4.5b) shows a similar fluctuation pattern with pairs of $d = 0.0$ and $d = 9.0$, $d = 3.0$ and $d = 6.0$ fluctuating close to each other. These two pairs become closer to each other when there is a further increase in $K = 1.00$ (see Figure 4.5c). Lastly, when K is increased to 3.00, the LBC changes with the close fluctuation does no longer exist and the quantum entanglement is seen to be more robust except for $d = 0$ and $d = 3.0$, which show a higher decoherence rate.
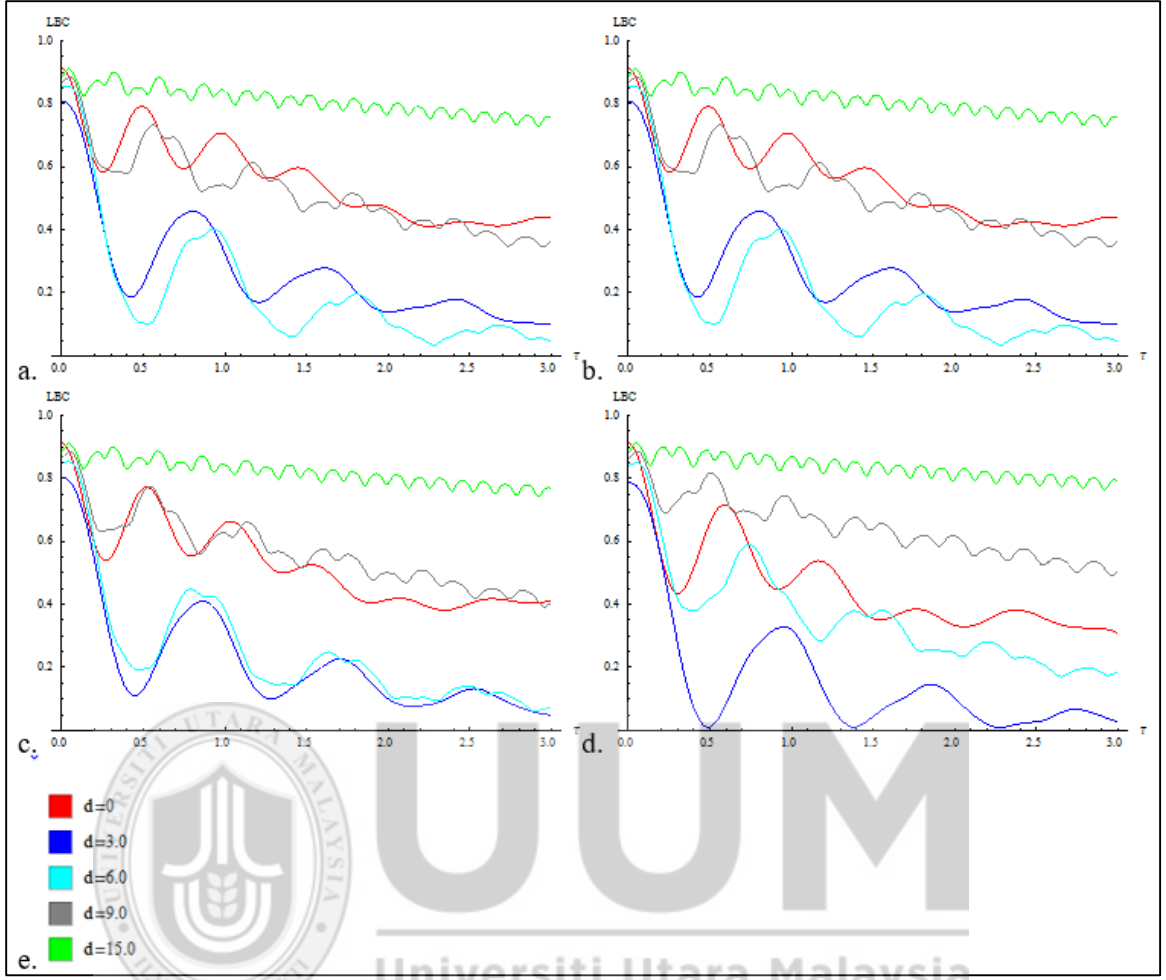
Figure 4.5. Lower Bound Concurrence (LBC) for $\delta = 10.0$ and $G = 8.0$, various d as shown in e. and a. $K = 0.00$, b. $K = 0.10$, c. $K = 1.00$, d. $K = 3.00$. Time scale, $1 \leq \tau \leq 3.0$

Between the Markovian and the non-Markovian environment, the latter environment shows better quantum entanglement strength because of the energy that was lost will flow back to the quantum system. The Kerr-like medium coupling also influences the quantum entanglement where it reduces the decoherence rate. However, in the non-

Markovian environment with $\delta = 10.0$, the Kerr-like medium does not have enough influence on the entanglement.

4.4.3 Conclusion

Different parameters are observed and studied for the robustness quantum entanglement. Overall, a weak Kerr-like medium coupling does not influence much the quantum entanglement in all environments and also dipole-dipole interactions. Further enhancement of the Kerr-like medium coupling changes the quantum entanglement with different parameters of dipole-dipole interaction, environment or detuning frequency. Besides, a strong dipole-dipole interaction also reduces the influence of the Kerr-like medium coupling.

For negative detuning frequency, the quantum entanglement becomes more robust with an increase in the dipole-dipole interaction and the strong Kerr-like medium coupling is able to increase the entanglement robustness. However, a higher decoherence occurs for the strong dipole-dipole interaction with the strong Kerr-like medium coupling in the Markovian environment. In the non-Markovian environment the quantum entanglement becomes more robust with an increase in the dipole-dipole interaction. This impact is reduced when the dipole-dipole interaction is getting stronger.

For positive detuning frequency, the quantum entanglement robustness no longer increases with the dipole-dipole interaction. This happens in both the Markovian and non-

Markovian environments where the entanglement robustness is in random when the dipole-dipole interaction changes. With the appearance of the Kerr-like medium coupling, the random behaviour reduces and eventually reverts back to the same trend as negative detuning frequency for Markovian behaviour. The difference is that the quantum entanglement is more robust with a strong Kerr-like medium. In the non-Markovian environment, a strong Kerr-like medium produces a robust quantum entanglement and eliminates the randomness. However, for higher detuning frequency, $\delta = 10.0$, the randomness still exists for a strong Kerr-like medium coupling where a certain dipole-dipole coupling showed a more robust quantum entanglement, while the other showed a less robust entanglement when the Kerr-like medium coupling was weak.

CHAPTER FIVE

CONCLUSON

A study on the Jaynes-Cummings model under influence of a Kerr-like medium is presented in this thesis. From this model new features of quantum behaviour and the major influence of quantum behaviour are produced. Specifically, this model presents the new features of a quantum entanglement of a three-qubit quantum state under the influence of the Kerr-like medium.

This chapter discusses the contribution of this study and offers recommendations for future study.

5.1 Contribution of the Study

This study developed the Jaynes-Cummings model for a multi-photon transition coupling with a Kerr-like medium and a three-qubit quantum state coupling with a Kerr-like medium. Using these two models, measurement was conducted to study the quantum behaviour and the quantum entanglement properties.

A multi-photon transition of the Jaynes-Cummings model coupling with the Kerr-like medium shows more collapses and revivals with the presence of both photons and the Kerr-like medium. With the increase in the number of photons, the influence of the Kerr-like medium becomes lesser. Besides, the increase in the multi-photon transition increases

103

the collapses and revivals where the fluctuation becomes more frequent and random. This tells us that the increase in the multi-photon transition leads to an increase in the activity of the quantum behaviour.

Another study of quantum entanglement shows that the Kerr-like medium coupling plays an important role with a three-qubit Jaynes-Cummings model. An increase in the Kerr-like medium coupling strength increases the entanglement robustness. However, the influence is reduced when a dipole-dipole coupling increases.

As explained earlier, these two studies provide a good understanding of quantum system behaviour which will be useful in the future study of quantum entanglement under the coupling of a Kerr-like medium. Better understanding of the quantum entanglement will allow researchers to be able to optimize maximum robustness of the application. In this study, it was found that the Kerr-like medium will improve the quantum entanglement robustness especially with strong dipole-dipole coupling. This allows us to utilize the condition under which the influence on the quantum behaviour is likely to optimally robust. Hence, the application of quantum information can improve stability under a robust quantum entanglement. For example, quantum teleportation is the transmission of information from one place to another place using a quantum entanglement of qubit. The robustness of the quantum entanglement will ensure that quality information is able to be transferred with a high success rate.

5.2 Suggestion of Future Research

A higher number of qubit in the Jaynes-Cummings model can be considered for future study. This will further increase the understanding of quantum behaviour. A three-qubit quantum state is the basic state of a multi-photon quantum state as the three-qubit quantum state contains more complex quantum entanglement, as explained in Section 1.3. A higher qubit quantum state will contain even more complex quantum entanglement which needs to be understood.

Based on the Jaynes-Cummings model, more atom transition level could be considered as well. In reality atoms contain more than two levels. Further study on a higher qubit level, such as three, four or more will offer a better understanding of quantum behaviour.
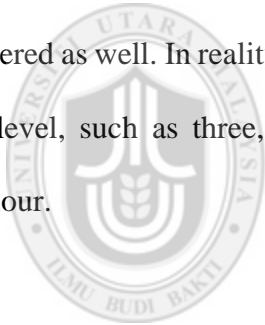
REFERENCES

Abdalla, M. S., Khalil, E. M., Obada, A. F., Peřina, J., & Křepelka, J. (2015). Quantum statistical characteristics of the interaction between two two-level atoms and radiation field. *The European Physical Journal Plus*, *130*(11), 1-19. doi: 10.1140/epjp/i2015-15227-9

Abdel-Aty, M., & Everitt, M. J. (2010). Delayed creation of entanglement in superconducting qubits interacting with a microwave field. *The European Physical Journal B-Condensed Matter and Complex Systems*, *74*(1), 81-89. doi: 10.1140/epjb/e2010-00056-y

Abdel-Aty, M., Larson, J., & Eleuch, H. (2010). Decoherent many-body dynamics of a nano-mechanical resonator coupled to charge qubits. *Physic E* 43, 1625-1640. doi: 10.1016/j.physe.2011.05.010

Abdel-Aty, M., Abdalla, M. S., & Sanders, B. C. (2009). Tripartite entanglement dynamics for an atom interacting with nonlinear couplers. *Physics Letters A*, *373*(3), 315-319. doi: 10.1016/j.physleta.2008.11.036

Agrawal, P., & Pati, A. (2006). Perfect teleportation and superdense coding with W states. *Physical Review A*, *74*(6), 062320-062328.
doi : http://dx.doi.org/10.1103/PhysRevA.74.062320

An, N. B., Kim, J., & Kim, K. (2011). Entanglement dynamics of three interacting two-level atoms within a common structured environment. *Physical Review A*, *84*(2), 022329.
doi: http://dx.doi.org/10.1103/PhysRevA.84.022329

Atteberry, J. (n.d.). *Discovery*. Retrieved from 10 Real-world Applications of Quantum Mechanics:http://dsc.discovery.com/tv-shows/curiosity/topics/10-real-world-applications-of-quantum-mechanics.htm

Baghshahi, H. R., Tavassoly, M. K., & Faghihi, M. J. (2014). Entanglement analysis of a two-atom nonlinear Jaynes–Cummings model with nondegenerate two-photon transition, Kerr nonlinearity, and two-mode Stark shift. *Laser Physics*, *24*(12), 125203-125215.
Retrieved from http://iopscience.iop.org/article/10.1088/1054-

660X/24/12/125203/meta;jsessionid0C000089415FA94F94EE23EE3672D084.c3.iopscience.cld.iop.org

Breuer, H. P., Laine, E. M., & Piilo, J. (2009). Measure for the degree of non-Markovian behaviour of quantum processes in open systems. *Physical Review Letters*, *103*(21), 210401-210405.
doi: http://dx.doi.org/10.1103/PhysRevLett.103.210401

Behrman, E. C., & Steck, J. E. (2013). A quantum neural network computes its own relative phase. In *Swarm Intelligence (SIS), 2013 IEEE Symposium on* (pp. 119-124).
doi: 10.1109/SIS.2013.6615168

Buchleitner, A., Viviescas, C., & Tiersch, M. (Eds.). (2008). *Entanglement and decoherence: Foundations and modern trends* (Vol. 768). Place: Springer. Retrieved from http://hdl.handle.net/961944/100255

Chen, X. Y., Jiang, L. Z., Yu, P., & Tian, M. (2012). Total and genuine entanglement of three qubit GHZ diagonal states. *arXiv preprint arXiv:1204.5511*. Retrieve from http://arxiv.org/abs/1204.5511

Chia, C. Y., & Ibrahim, H (2014). Phase Properties of a Multi-Photon Jaynes-Cummings Model. Quant. Inf. Rev. 2, No. 2, 21-25.
doi : 10.12785/qir/020201

Coffman, V., Kundu, J., & Wootters, W. K. (2000). Distributed entanglement. *Physical Review A*, *61*(5), 052306-052318.
doi : http://dx.doi.org/10.1103/PhysRevA.61.052306

Dür, W., Vidal, G., & Cirac, J. I. (2000). Three qubits can be entangled in two inequivalent ways. *Physical Review A*, *62*(6), 062314-062325.
doi: http://dx.doi.org/10.1103/PhysRevA.62.062314

Eisert, J., & Plenio, M. B. (1999). A comparison of entanglement measures. *Journal of Modern Optics, 46*(1), 145-154.
doi: 10.1080/09500349908231260

Flores, M. M., & Galapon, E. A. (2015). Two qubit entanglement preservation through the addition of qubits. *Annals of Physics*, *354*, 21-30.
doi:10.1016/j.aop.2014.11.011

Gantsog, T., Joshi, A., & Tanas, R. (1996). Phase properties of one-and two-photon Jaynes-Cummings models with a Kerr medium. *Quantum and Semiclassical Optics: Journal of the European Optical Society Part B*, *8*(3), 445-456.

Heo, J., Hong, C. H., Lim, J. I., & Yang, H. J. (2015). Simultaneous quantum transmission and teleportation of unknown photons using intra-and inter-particle entanglement controlled-not gates via cross-Kerr nonlinearity and P-homodyne measurements. *International Journal of Theoretical Physics*, 1-17. doi: 10.1007/s10773-014-2448-3

Ho-Chih, L. (2008). *Local approach to quantum entanglement* (Doctoral dissertation, University of London), 36-37.
Retrieved from http://discovery.ucl.ac.uk/1446283/

Huai-Xin, L. U., & Xiao-Qin, W. (2000). Multiphoton Jaynes-Cummings model solved via supersymmetric unitary transformation. *Chinese Physics*, *9*(8), 568-571.
doi: http://dx.doi.org/10.1088/1009-1963/9/8/003

Ithier, G., Collin, E., Joyez, P., Meeson, P. J., Vion, D., Esteve, D., ... & Schön, G. (2005). Decoherence in a superconducting quantum bit circuit. *Physical Review B*, *72*(13),134519-134584.
doi:http://dx.doi.org/10.1103/PhysRevB.72.134519

Jungnitsch, B., Moroder, T., & Gühne, O. (2011). Taming multiparticle entanglement. *Physical Review Letters*, *106*(19), 190502-190514.
doi: http://dx.doi.org/10.1103/PhysRevLett.106.190502

Klimov, A. B., Romero, J. L., Delgado, J., & Sanchez-Soto, L. L. (2002). Master equations for effective Hamiltonians. *Journal of Optics B: Quantum and Semiclassical Optics*, *5*(1), 34-43.
doi : http://dx.doi.org/10.1088/1464-4266/5/1/304

Lahti, P., & Pellonpää, J. P. (2002). The Pegg-Barnett formalism and covariant phase observables. *Physica Scripta*, *66*(1), 66-75.
doi: http://dx.doi.org/10.1238/Physica.Regular.066a00066

Langer, C., Ozeri, R., Jost, J. D., Chiaverini, J., DeMarco, B., Ben-Kish, A., ... & Leibfried, D. (2005). Long-lived qubit memory using atomic ions. *Physical review letters*, *95*(6), 060502-060506.
Doi : http://dx.doi.org/10.1103/PhysRevLett.95.060502

108

Li, P., Gu, Y., Wang, L., & Gong, Q. (2008). Fifth-order nonlinearity and 3-qubit phase gate in a five-level tripod atomic system. *JOSA B*, *25*(4), 504-512. doi : 10.1364/JOSAB.25.000504

Li, Y., Hang, C., Ma, L., & Huang, G. (2006). Controllable entanglement of lights in a five-level system. *Physics Letters A*, *354*(1), 1-7. Retrieved from http://arxiv.org/pdf/quant-ph/0511027

Makhlin, Y., Schön, G., & Shnirman, A. (2001). Quantum-state engineering with Josephson-junction devices. *Reviews of Modern Physics*, *73*(2), 357-402. doi: http://dx.doi.org/10.1103/RevModPhys.73.357

Mooij, J. E., Orlando, T. P., Levitov, L., Tian, L., Van der Wal, C. H., & Lloyd, S. (1999). Josephson persistent-current qubit. *Science*, *285*(5430), 1036-1039. doi: 10.1126/science.285.5430.1036

Nakamura, Y., Pashkin, Y. A., Yamamoto, T., & Tsai, J. S. (2002). Charge echo in a Cooper-pair box. *Physical Review Letters*, *88*(4), 47901-47904. doi: http://dx.doi.org/10.1103/PhysRevLett.88.047901

Negele, J. W., & Orland, H. (1988). *Quantum many-particle systems* (Vol. 200). New York: Addison-Wesley.

Nielsen, M. A., & Chuang, I. L. (2010). *Quantum computation and quantum information*. New York: Cambridge university press. Retrieved from http://www.idt.mdh.se/~gdc/work/ARTICLES/2014/3-CiE-journal/Background/QUANTUMINFO-book-nielsen-and-chuang-toc-and-chapter1-nov00-acro5.pdf

Obada, A. S., Abdel-Hafez, A. M., & Abdelaty, M. (1998). Phase properties of a Jaynes-Cummings model with Stark shift and Kerr medium. *The European Physical Journal D-Atomic, Molecular, Optical and Plasma Physics*, *3*(3), 289-294. doi: 10.1007/s100530050176

Paz, J. P., & Zurek, W. H. (2001). Environment-induced decoherence and the transition from quantum to classical. In *Coherent atomic matter waves* (pp. 533-614). Springer Berlin Heidelberg. doi: 10.1007/3-540-45338-5_8

109

Plenio, M. B., & Virmani, S. S. (2014). An Introduction to Entanglement Theory. In *Quantum Information and Coherence* (pp. 173-209). Springer International Publishing. doi: 10.1007/978-3-319-04063-9_8

Qing-Hong, L., Ahmad, M. A., Yue-Yuan, W. A. N. G., & Shu-Tian, L. (2010). Properties of Linear Entropy in k-Photon Jaynes–Cummings Model with Stark Shift and Kerr-Like Medium. *Communications in Theoretical Physics*, *53*(5), 931-935. doi : 0253-6102-53-5-27

Rui-Tong, Z., Qi, G., Liu-Yong, C., Li-Li, S., Hong-Fu, W., & Shou, Z. (2013). Two-qubit and three-qubit controlled gates with cross-Kerr nonlinearity. *Chinese Physics B*,*22*(3),030313-030320. doi: http://dx.doi.org/10.1088/1674-1056/22/3/030313

Ruiz, A. M., Frank, A., & Urrutia, L. F. (2013). Jaynes-Cummings model in a finite Kerr medium, 1-16. Retrieved from http://arxiv.org/abs/1302.0588

Spiller, T. P. (1996). Quantum information processing: cryptography, computation, and teleportation. *Proceedings of the IEEE*, *84*(12), 1719-1746. doi: 10.1109/5.546399

Tanaś, R., & Kielich, S. (1983). Self-squeezing of light propagating through nonlinear optically isotropic media. *Optics Communications*, *45*(5), 351-356. Retrieved from

http://www.sciencedirect.com/science/article/pii/003040188390264X#

Tahir, M., & MacKinnon, A. (2010). Current noise of a resonant tunnel junction coupled to a nanomechanical oscillator. *arXiv preprint arXiv:1005.3713*. Retrieved from http://arxiv.org/abs/1005.3713

Terhal, B. M., & Burkard, G. (2005). Fault-tolerant quantum computation for local non-Markovian noise. *Physical Review A*, *71*(1), 012336-012355. doi: http://dx.doi.org/10.1103/PhysRevA.71.012336

Trung Dung, H., Tanaś, R., & Shumovsky, A. S. (1990). Collapses, revivals, and phase properties of the field in Jaynes-Cummings type models. *Optics Communications*,

110

79(6),462-468.
doi:10.1016/0030-4018(90)90483-A

Verstraete, F., Audenaert, K., Dehaene, J., & De Moor, B. (2001). A comparison of the entanglement measures negativity and concurrence. *Journal of Physics A: Mathematical and General, 34*(47), 10327-10331. doi: http://dx.doi.org/10.1088/0305-4470/34/47/329

Weisstein, Eric W.(2002). "Lorentzian Function." Retrieved from http://mathworld.wolfram.com/LorentzianFunction.html

Wigner, E. (1932). On the quantum correction for thermodynamic equilibrium. *Physical Review*,*40*(5),749-759.
doi: http://dx.doi.org/10.1103/PhysRev.40.749

Wootters, W. K. (2001). Entanglement of formation and concurrence. *Quantum Information & Computation*, *1*(1), 27-44.
Retrieved from http://www.rintonpress.com/journals/qic-1-1/eof2.pdf

Yu-Qing, Z., Lei, T., Zhong-Hua, Z., Zu-Zhou, X., & Li-Wei, L. (2010). Partial entropy change and entanglement in the mixed state for a Jaynes–Cummings model with Kerr medium. *Chinese Physics B*, *19*(2), 024210-024218.
doi: http://dx.doi.org/10.1088/1674-1056/19/2/024210

Yu, X. Y., & Li, J. H. (2013). The effect of dipole-dipole interactions on the single-photon transmission spectrum. *The European Physical Journal D*, *67*(8), 1-6.
doi: 10.1140/epjd/e2013-40012-y

Zhang, Z. M., Xu, L., Li, F. L., & Chai, J. L. (1991). Long-time behaviour of field fluctuation in the M-photon Jaynes-Cummings model. *Zeitschrift für Physik B Condensed Matter*, *84*(2), 329-331.
doi: 10.1007/BF01313556